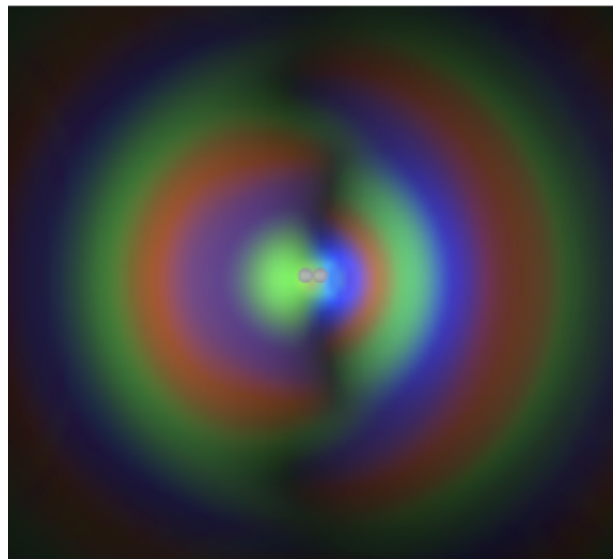# Combining electronic and nuclear motion in strong and high-energy fields with MCTDHF

Daniel J. Haxton,

AMO theory group, Chemical Sciences; Ultrafast X-Ray Science Laboratory LBNL

LCLS-II Scientific Opportunities Workshop Feb 13 2015

"The Multiconfiguration Time Dependent Hartree Fock method for interactions of molecules with strong, ultrafast, high energy pulses"

DOE Funded FY2013 through FY 2017

<u>Atomic, Molecular, and Optical theory group LBNL</u>

MULTICONFIGURATION TIME DEPENDENT HARTREE-FOCK

IS NOT HARTREE-FOCK

ON THE CONTRARY

IT IS MULTICONFIGURATION

Follows very successful implementation
of MCTDH (no asymmetry of wave function)
for nuclear dynamics – quantum reactive
scattering, Photodissociation, etc. by
HD Meyer, G Worth, A Jackle, M Beck et al,
University of Heidelberg, Germany
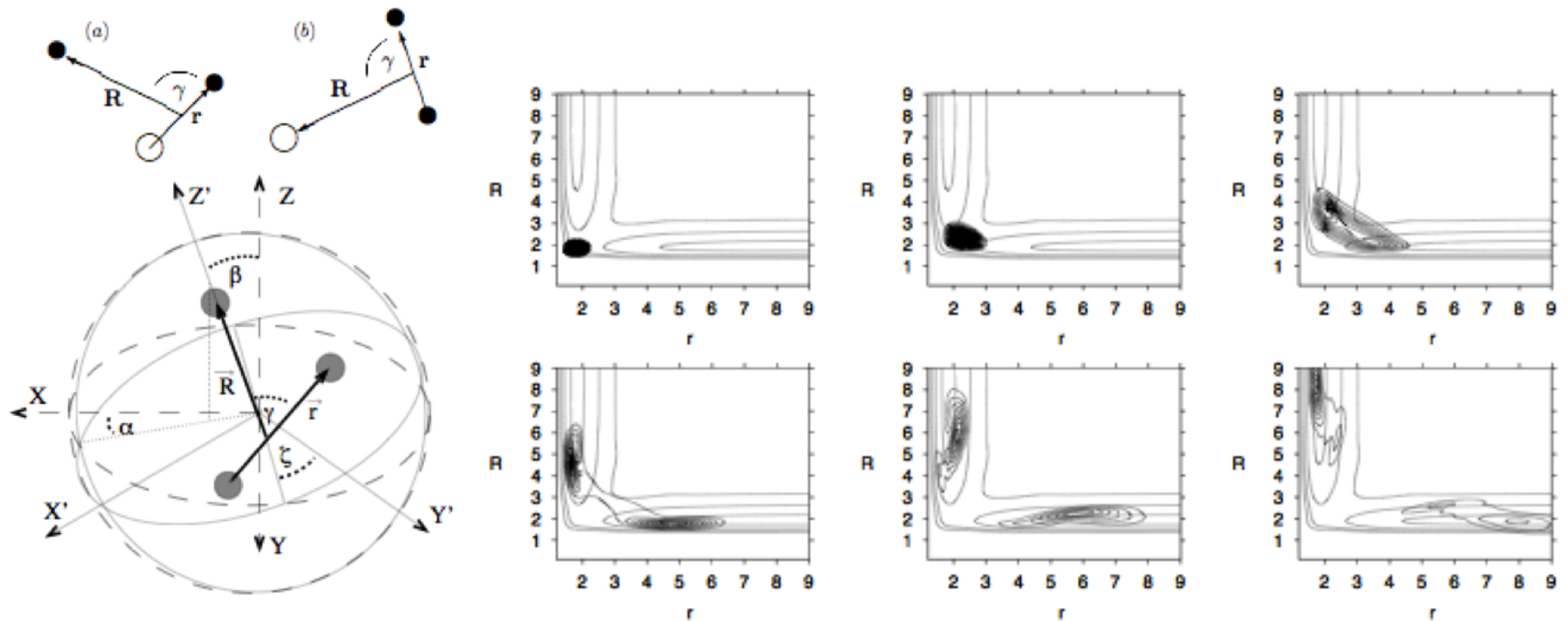
The Heidelberg MCTDH Package

Version 8

Release 4   Revision 10

What's new

• User's Manual

- ○ **Installation and Compilation**
- ○ **User's Guide (PDF)**
- ○ **Troubleshooting**
- ○ The MCTDH Program
  - ▪ **Capabilities and Usage**
  - ▪ **Input Documentation**
  - ▪ **Output Documentation**
  - ▪ **Hamiltonian Documentation**
  - ▪ **Optimal Control Documentation**
- ○ The Potfit Program
  - ▪ **Program Documentation**
  - ▪ **Input Documentation**
  - ▪ **Output Documentation**
  - ▪ **The Projection Program**
  - ▪ **Monte-Carlo Potfit**
- ○ **Cluster-Expansion**
- ○ **The Analyse Programs**

• Developer's Manual

- ○ **Guidelines for Developers**
- ○ **Automatic Program Test** *(Elk Test)*
- ○ **Code Description**
- ○ **Operator Details**
- ○ **Libraries Description**
- ○ **Developing New Analysis Programs**
- ○ **The MCTDH backup utility**

Ofir Alon
MCTDHB

Bosons
(cold atoms mostly)

Physics Department
Technion - Israel Institute of Technology

http://www.pci.uni-heidelberg.de/tc/usr/mctdhb/people.html

HEIDELBERG UNIVERSITY

MCTDHB Home >

People

MCTDHB founders

Lorenz S. Cederbaum E-mail, Homepage
Ofir E. Alon E-mail, Homepage
Alexej I. Streltsov E-mail, Homepage

MCTDHB Package developers

Alexej I. Streltsov (Project Leader) E-mail, Homepage
Kaspar Sakmann E-mail, Homepage
Axel U. J. Lode E-mail, Homepage
Julian Grond E-mail
Ofir E. Alon E-mail, Homepage

MCTDHB

TC Home

MCTDHB

People

FAQ

Quick Manual

Benchmarks

Examples

OpenMCTDHB

Publications

Open
MCTDHB

(what happened to open?)

Previous work on MCTDHF

[17] M. Kitzler, J. Zanghellini, C. Jungreuthmayer, M. Smits, A. Scrinzi, and T. Brabec, Phys. Rev. A **70**, 041401 (2004).

[18] J. Caillat, J. Zanghellini, M. Kitzler, O. Koch, W. Kreuzer, and A. Scrinzi, Phys. Rev. A **71**, 012712 (2005).

[19] T. Kato and H. Kono, J. Chem. Phys. **128**, 184102 (2008).

[20] T. Kato and K. Yamanouchi, J. Chem. Phys. **131**, 164118 (2009).

[21] M. Nest, Phys. Rev. A **73**, 023613 (2006).

[22] M. Nest, R. Padmanaban, and P. Saalfrank, J. Chem. Phys. **126**, 214106 (2007).

[23] M. Nest, F. Remacle, and R. D. Levine, New J. Phys. **10**, 025019 (2008).

[24] M. Nest, Chem. Phys. Letts. **472**, 171 (2009).

Recent: Hochstuhl, Bauch, Bonitz arxiv 1010.5422 (2010)

Miranda, Fisher, Stella, Horsfield   JCP 134, 244101 & 2 (2011)

Simen Kvaal

University of Oslo
Department of Chemistry
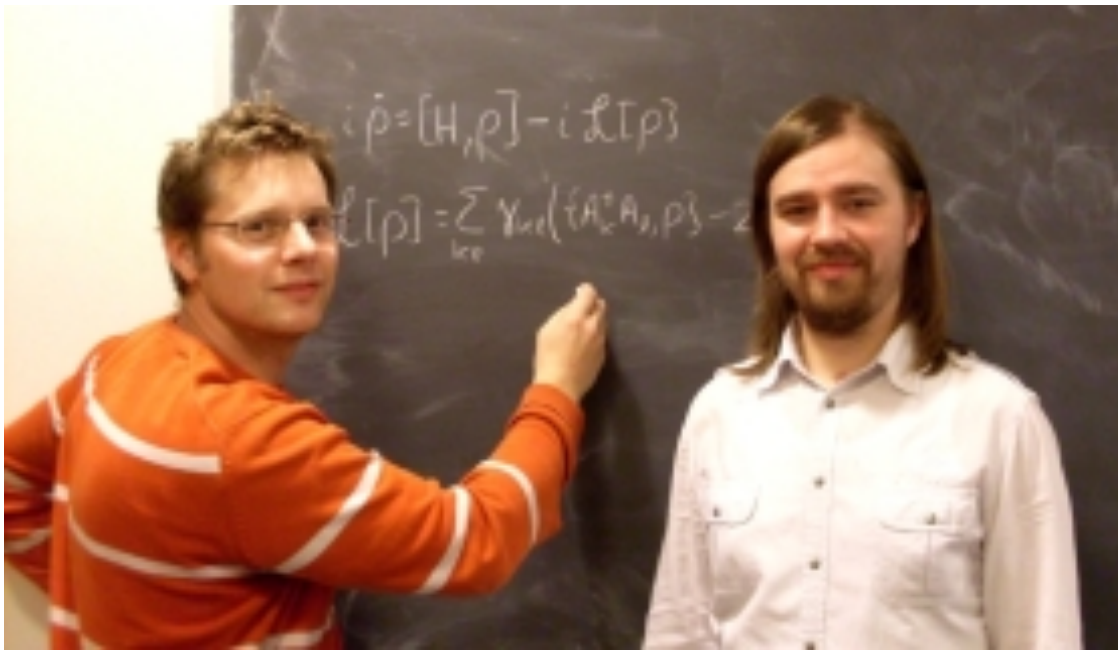
Differentiable but exact formulation of density-functional theory

Simen Kvaal, Ulf Ekström, Andrew M. Teale, and Trygve Helgaker

Multiconfigurational time-dependent Hartree method to describe particle loss due to absorbing boundary conditions

Simen Kvaal[1,2,*]

[1]*Mathematisches Institut, Universität Tübingen, Auf der Morgenstelle 10, D-72076 Tübingen, Germany*
[2]*Centre of Mathematics for Applications, University of Oslo, N-0316 Oslo, Norway*

Ab initio quantum dynamics using coupled-cluster

Simen Kvaal[a]
University of Oslo, Centre of Mathematics for Applications, N-0316 Oslo, Norway and University of Oslo, Centre for Theoretical and Computational Chemistry, N-0315 Oslo, Norway

Taylor & Francis
Taylor & Francis Group

INVITED ARTICLE

Variational formulations of the coupled-cluster method in quantum chemistry

Simen Kvaal*

*CTCC, Institutt for Kjemi, Unversitetet i OSlo, NO-0315 Oslo, Oslo, Norway*

Double ionization with absorbing potentials

Unbound systems, such as atoms being ionised, may, as the name suggests, become very large. Numerical descriptions of such systems thus require very large grids – possibly rendering simulations unfeasible. Could we avoid this pesky feature by dismissing all knowledge about the escaping particles and focus upon the ones that remain instead?

Unfortunately, the Schrödinger equation does not allow us to do so. If we introduce some term in the Schrödinger equation which removes particles beyond a certain point, such as a complex absorbing potential, the remainder of the system is also lost. We may ask whether the Schrödinger equation can be generalised in such a way that we still may describe the remaining particles as other particles are absorbed by the complex potential. As it turns out, the answer is yes. The proper generalization is provided by the Lindblad equation (see 2010 *J. Phys. B: At. Mol. Opt. Phys.* **43 065004**).

In a recent paper (published in 2011 *J. Phys. B: At. Mol. Opt. Phys.* **44 215003**), researchers from Oslo and Bergen, Norway, demonstrate how this concept may be used to describe a process in which both electrons of a helium atom are 'knocked off' by two photons. The ionisation dynamics of a simplified model atom exposed to a laser field was simulated, and the remaining system was monitored in time as electrons escaped. Calculations were performed using a complex absorbing potential on a numerical grid of smaller extension than the actual wave function. The predictions of these calculations were then compared with those of more conventional calculations on a grid large enough to contain the entire wave function. The two methods produced the same result, thus providing a proof of principle for the scheme involving a complex absorbing potential and the Lindblad equation.

Schematic of the absorbing boundary multi-particle method.
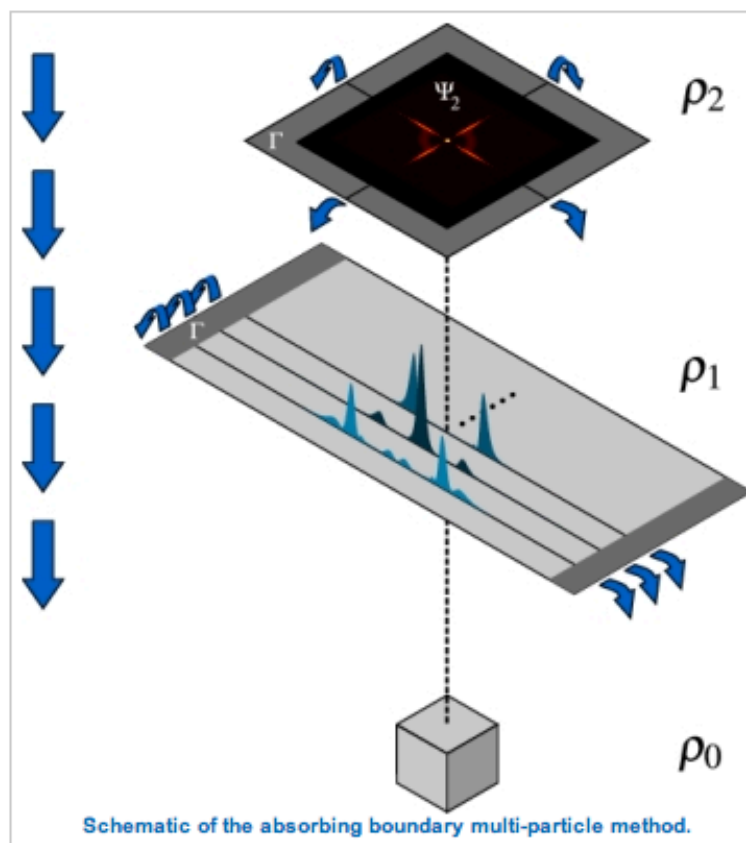
More details of the authors' work are published in *Journal of Physics B: Atomic, Molecular and Optical Physics*.

# MCTDHF wave function

INTERPOLATING POLYNOMIALS

GAUSSIAN BASIS FUNCTIONS
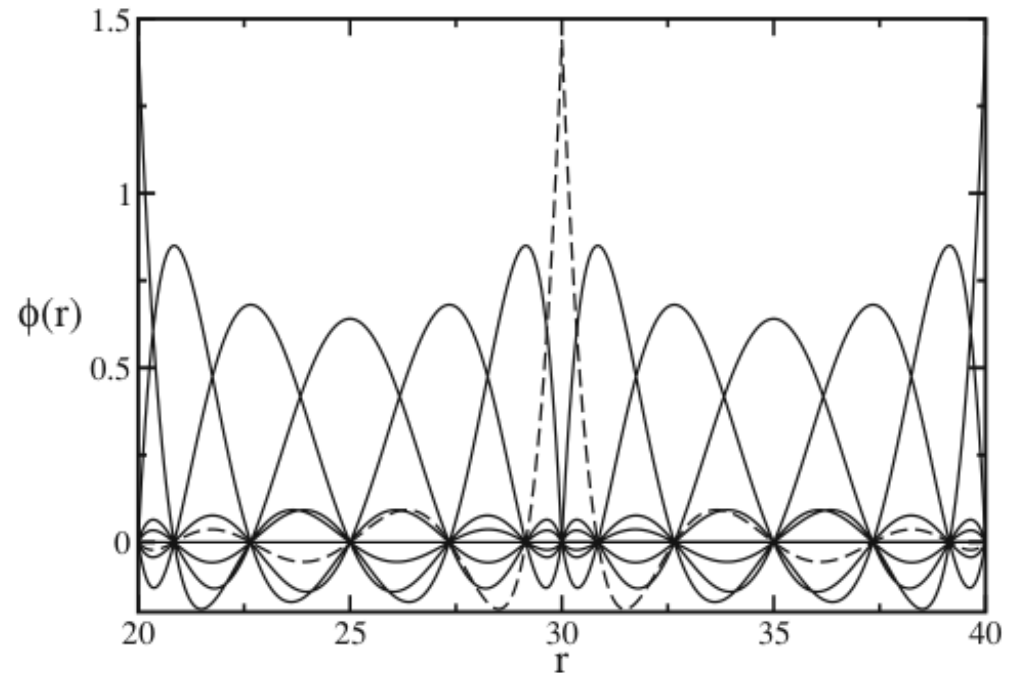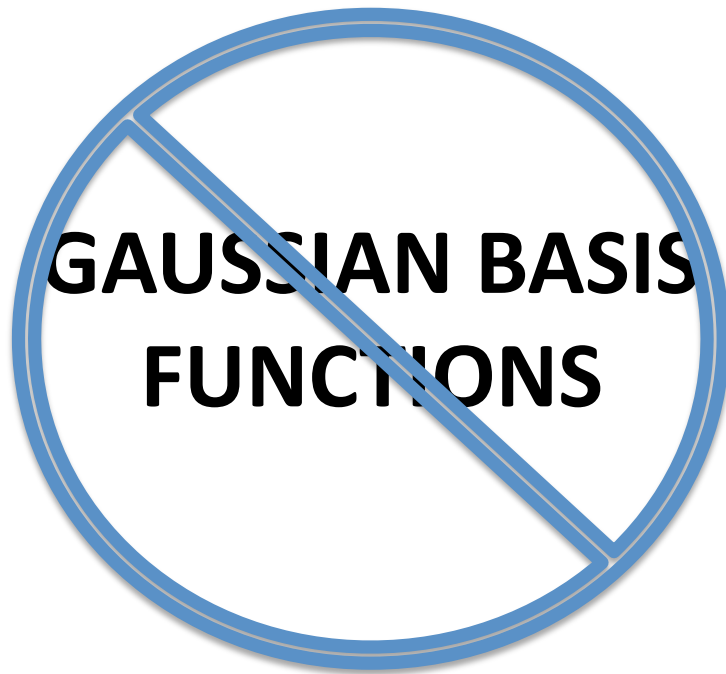
→ Grid-based representation of orbitals that makes operating with the mean field fast

Obtain complete basis limit easily with this grid method.

|	R_0	N_η	n_ξ	ξ elements	Energy
H_2	1.4	9	14	3.0, 10.0, 10.0	-1.13362957146
	same with $\theta = 15°$			1.1×10^{-9} i	-1.133629573
	same with $\theta = 30°$			1.2×10^{-9} i	-1.133629572
				HF limit	-1.1336295715 [55]
Li_2	5.051	25	20	0.75, 3× 4.0	-14.8715620178
				eliptic basis HF	-14.8715619 [56]
LiH	3.015	21	19	1.0, 3× 5.0	-7.987352237
				numerical HF	-7.987352237 [57]
CO	2.132	21	19	1.5, 7.5, 7.5	-112.79090718
	same with $\theta = 15°$			1.1×10^{-8} i	-112.79090714
	same with $\theta = 30°$			8×10^{-8} i	-112.79090714
				numerical HF	-112.790907 [57]
N_2	2.068	21	19	1.5, 7.5, 7.5	-108.99382563
				numerical HF	-108.9938257 [57]
N_2	same basis, (14/10) CAS-SCF				-109.14184793(5)
	(14/10) Columbus ccpvtz				-109.132509251
	(14/10) Columbus ccpvqz				-109.140039408

Wave function represented entirely in complex plane

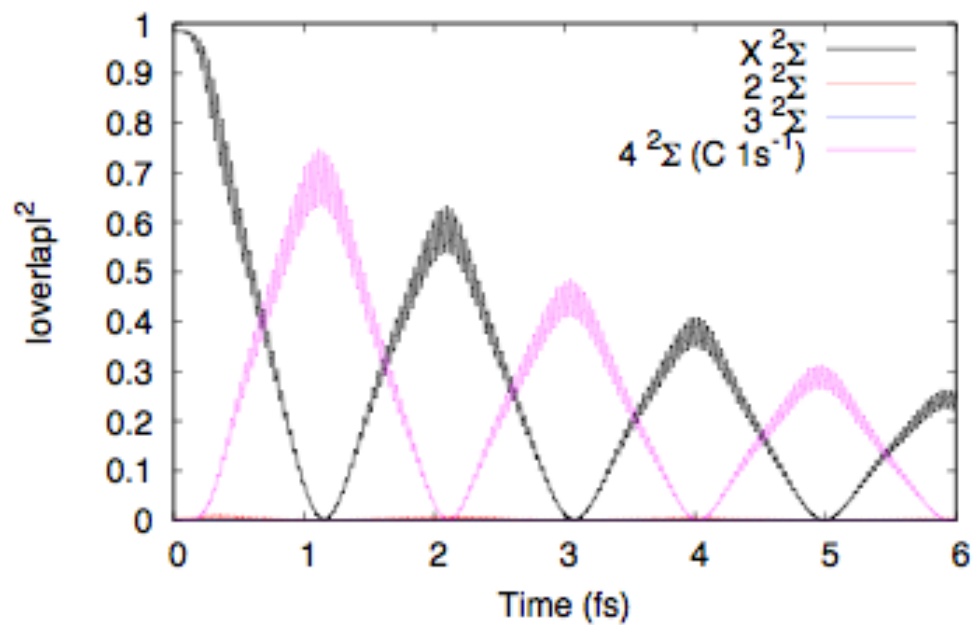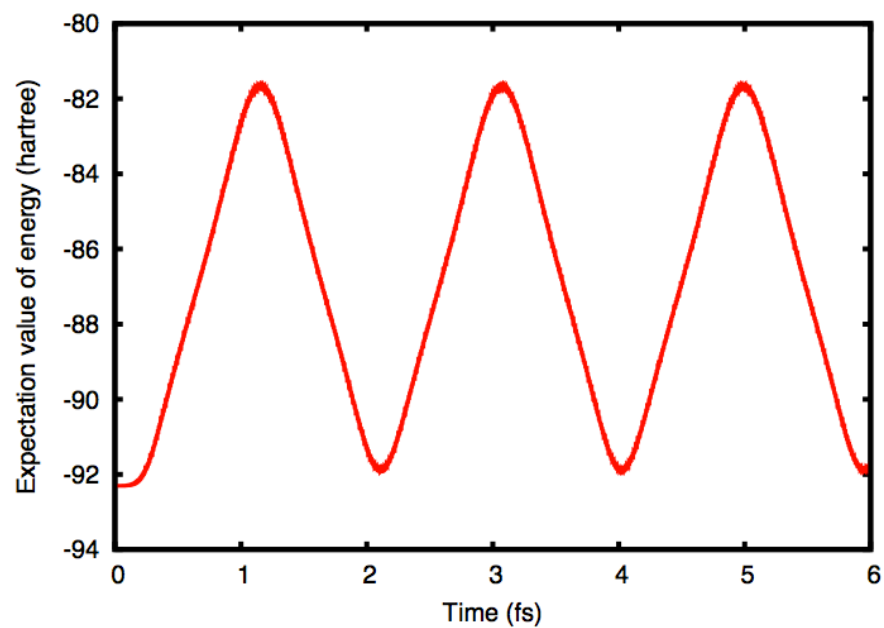# Well-behaved solution of TD Schrodinger equation for highly nonlinear pulses
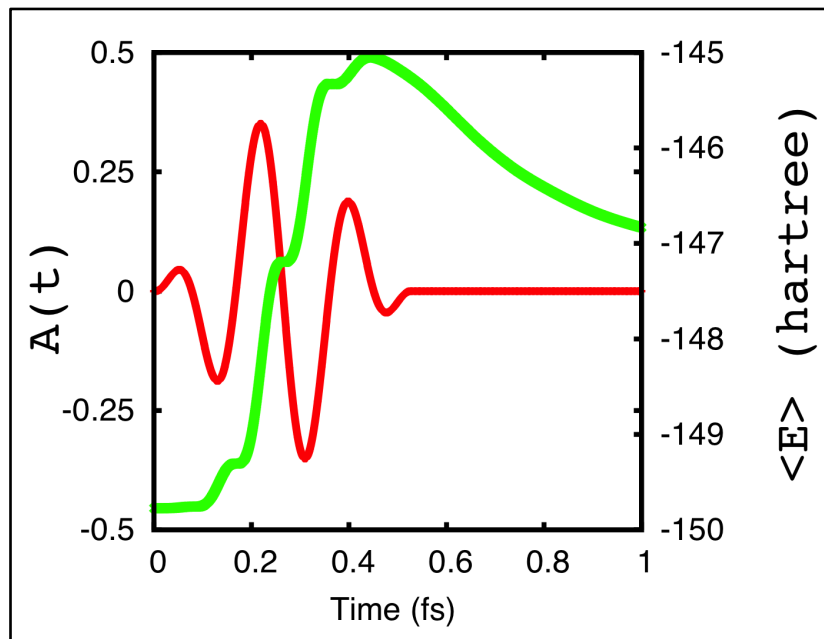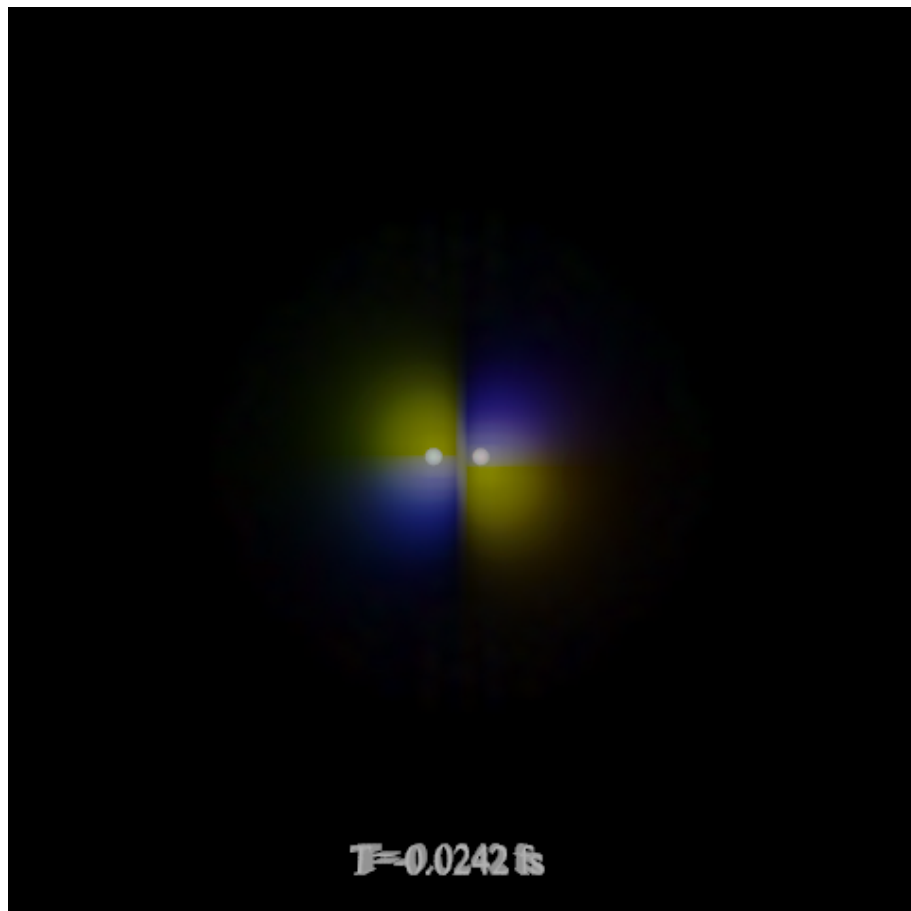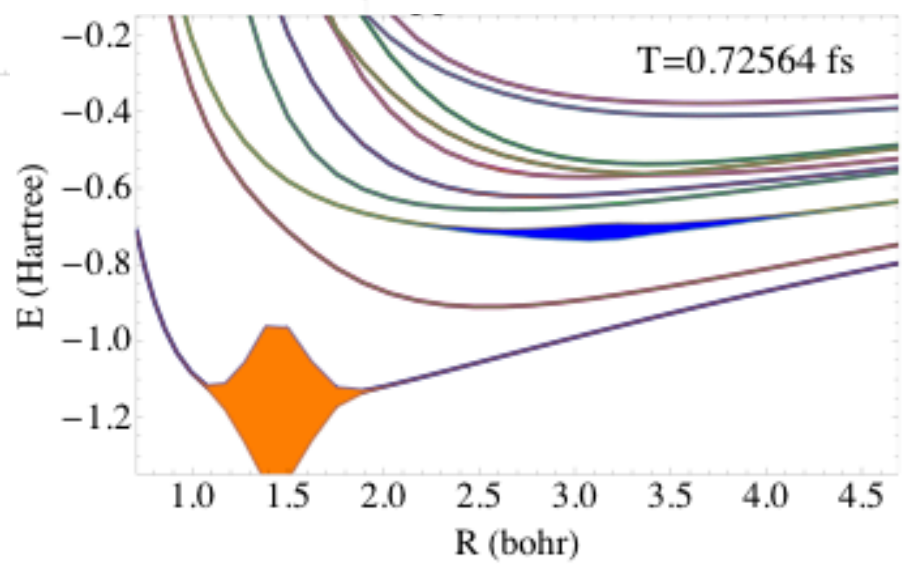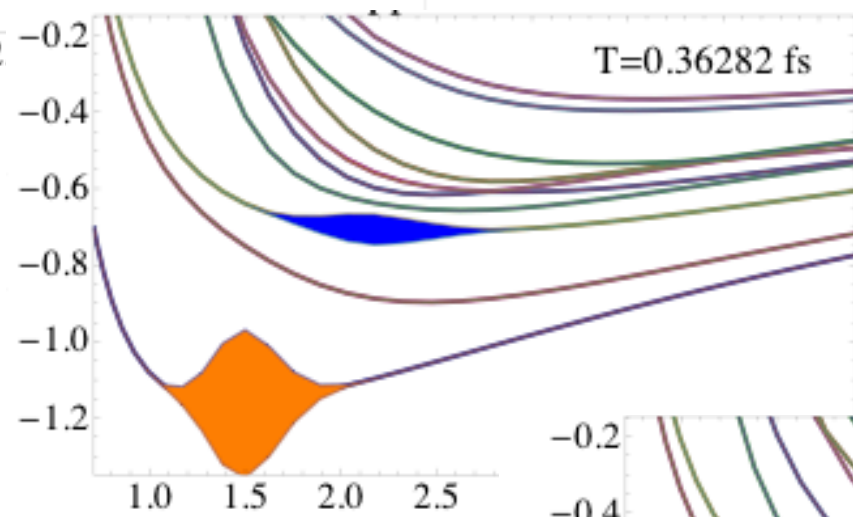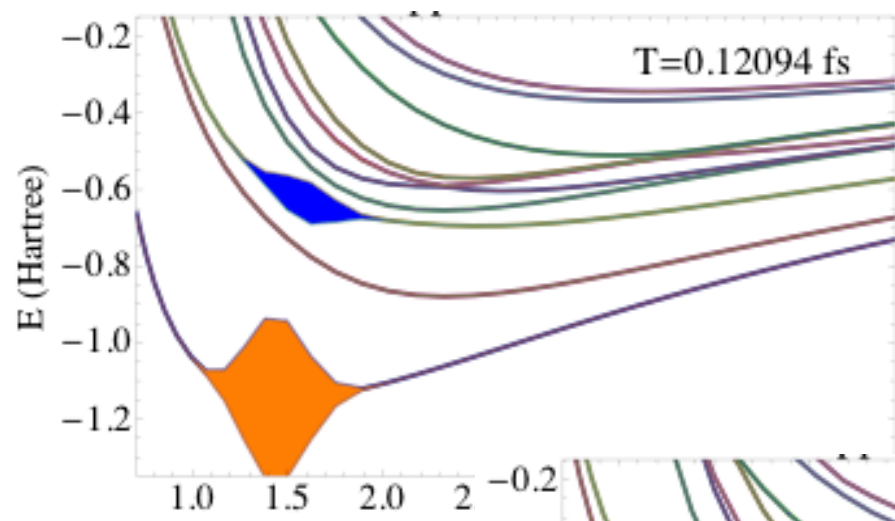

Ionizing π* orbital, O₂

16 electrons active (full CI)
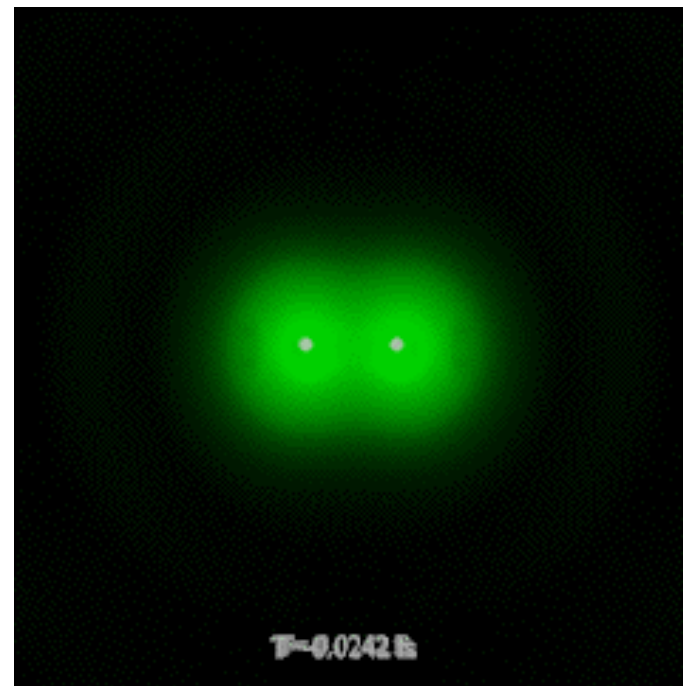
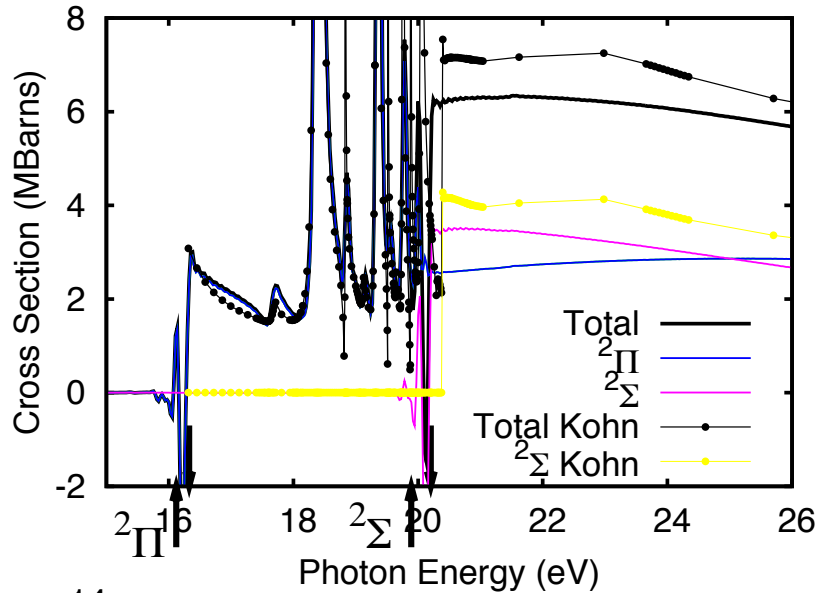# Well-behaved solution of TD Schrodinger equation for highly nonlinear pulses

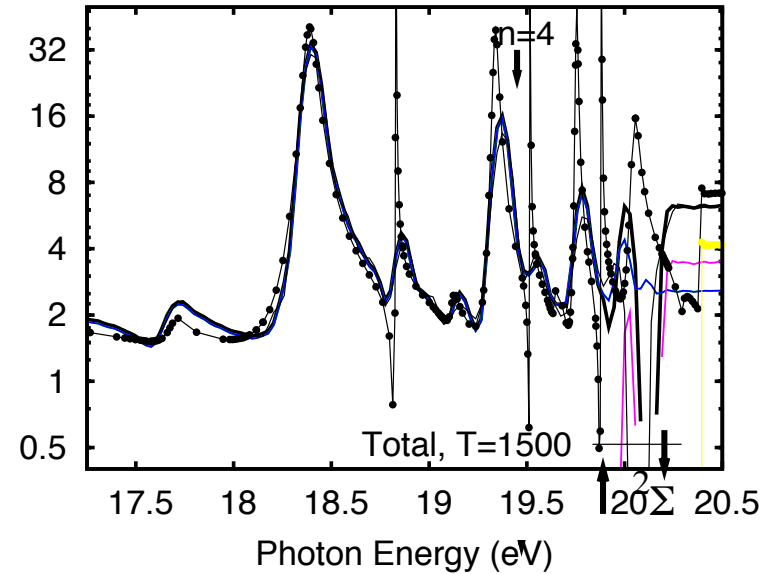## Rabi flopping in CN radical, C 1s $\longleftrightarrow$ 5σ
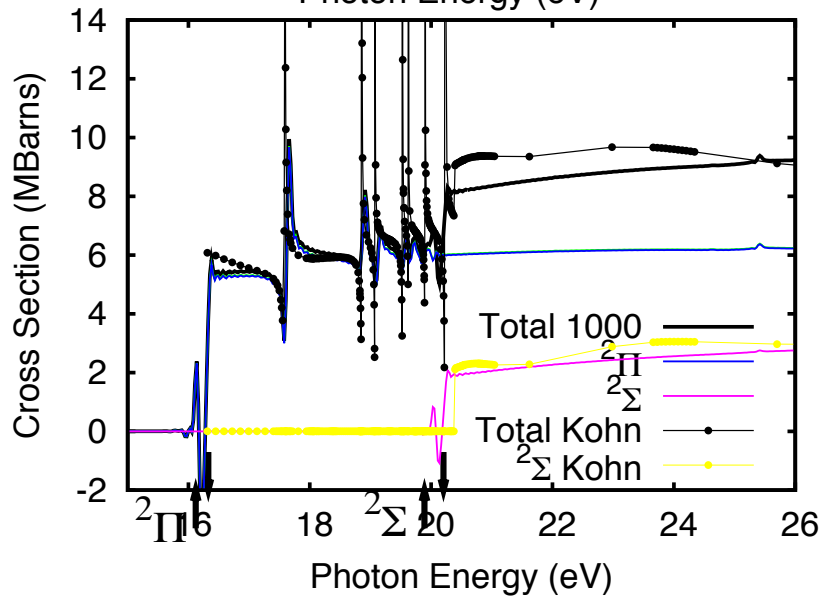
HF: Valence photoionization (9 orbitals)
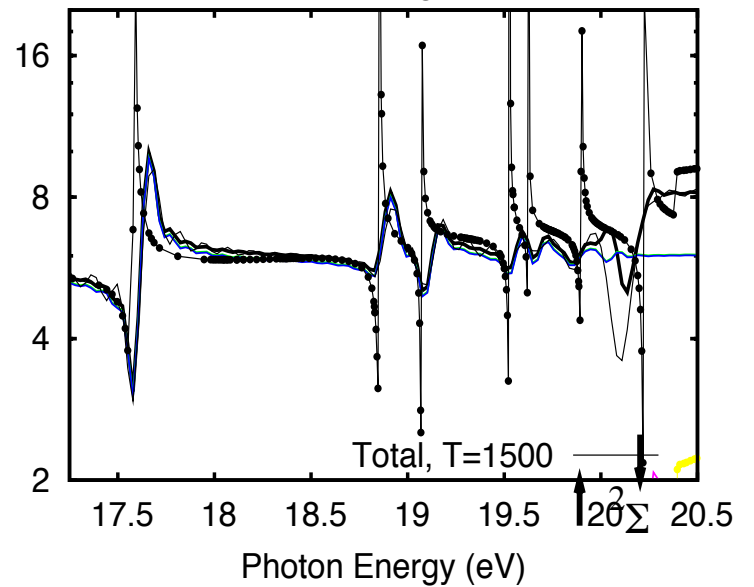
Analysis Capabilities

-Can project on eigenfunctions to obtain **populations**

-Can calculate **photoionization spectra**

-Can calculate **absorption/stimulated emission**

What it CAN'T do:

Only calculates N electron wave function!

. . . Will not follow cation after ionization.

E.g. if observed absorption is partially due to absorption by free cation, dication, etc.
    we cannot easily calculate this

. . . . TALK TO KVAAL!! PRA 84 022512 (2011)

# Population transfer between valence states via autoionizing states using two-color ultrafast π pulses in XUV and the limitations of adiabatic passage

X. Li,[1] C. W. McCurdy,[2,1] and D. J. Haxton[1]

[1]*Chemical Sciences and Ultrafast X-ray Science Laboratory, Lawrence Berkeley National Laboratory, Berkeley, California 94720, USA*
[2]*Department of Chemistry, University of California, Davis, California 95616, USA*

Population transfer between two valence states of the Li atom with a Raman process via intermediate autoionizing states well above the ionization threshold is investigated using a recently developed implementation of the muticonfiguration time-dependent Hartree Fock method. It is found that a properly chosen sequence of pump and Stokes π pulses can yield a population transfer efficiency of 53% at relatively low intensities, while the extension of the stimulated Raman adiabatic passage (STIRAP) approach to the XUV in this case is far less efficient and loses its characteristic robustness at high intensities. A rule of thumb for when STIRAP is practical is given, suggesting that at still shorter wavelengths STIRAP may be possible.
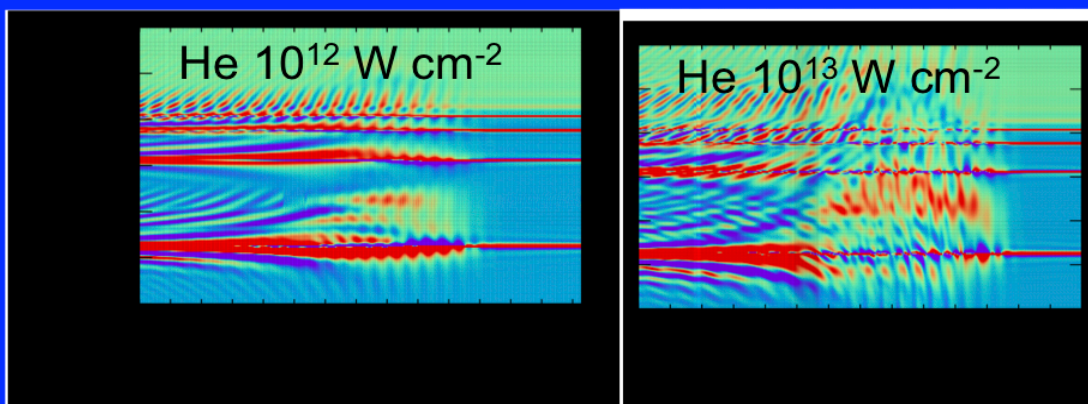
Xuan Li Project Scientist AMO Theory group
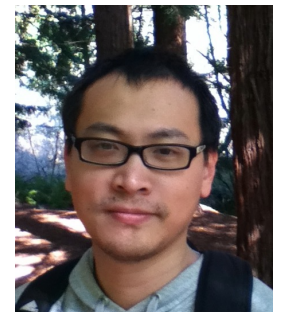
TRANSIENT ABSORPTION

$$S(\omega) = 2 \, \text{im}(\mu(\omega)E(\omega)^*)$$

Transient absorption from $\tilde{S}(\omega)$ using MCTDHF

He: both electrons active, c.f. SAE calculations of Gaarde/Schafer group PRA (2013). ECS can treat multiple ionization at higher intensities
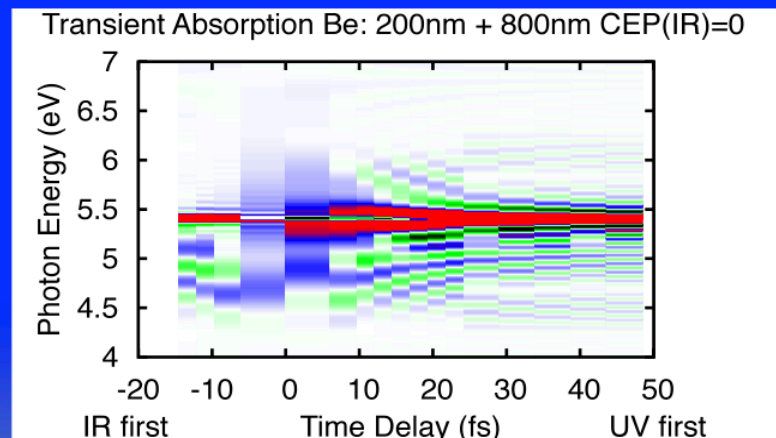
Requires MCTDHF calculation of

$$\mu(t) = \langle \Psi(t) | \hat{\mu} | \Psi(t) \rangle$$

for t up to 10s of femtoseconds

Be: 4 electrons active. Intense IR pulse (10.5 fs @ 9.6 x10^{12} W cm^{-2} IR creates polarization that is probed by weaker UV (6.2 eV 088 fs pulse) – with carrier phase sensitivity

Transient Absorption Be: 200nm + 800nm CEP(IR)=0

Quantum interference in attosecond transient absorption of laser-dressed helium atoms

Shaohao Chen, Mengxi Wu, Mette B. Gaarde, and Kenneth J. Schafer

Department of Physics and Astronomy, Louisiana State University, Baton Rouge, Louisiana 70803, USA

(Received 29 December 2012; published 8 March 2013)

Light-induced states in attosecond transient absorption spectra of laser-dressed helium

Shaohao Chen,[1,*] M. Justine Bell,[2,3,*] Annelise R. Beck,[2,3] Hiroki Mashiko,[2] Mengxi Wu,[1] Adrian N. Pfeiffer,[2,3] Mette B. Gaarde,[1] Daniel M. Neumark,[2,3] Stephen R. Leone,[2,3,4] and Kenneth J. Schafer[1]

Chemical Physics Letters

FRONTIERS ARTICLE

Probing ultrafast dynamics with attosecond transient absorption

Annelise R. Beck[a,b,*], Daniel M. Neumark[a,b], Stephen R. Leone[a,b,c]

[a] *Department of Chemistry, University of California Berkeley, Berkeley, CA 94720, USA*
[b] *Ultrafast X-ray Science Laboratory, Chemical Sciences Division, Lawrence Berkeley National Laboratory, Berkeley, CA 94720, USA*
[c] *Department of Physics, University of California Berkeley, Berkeley, CA 94720, USA*

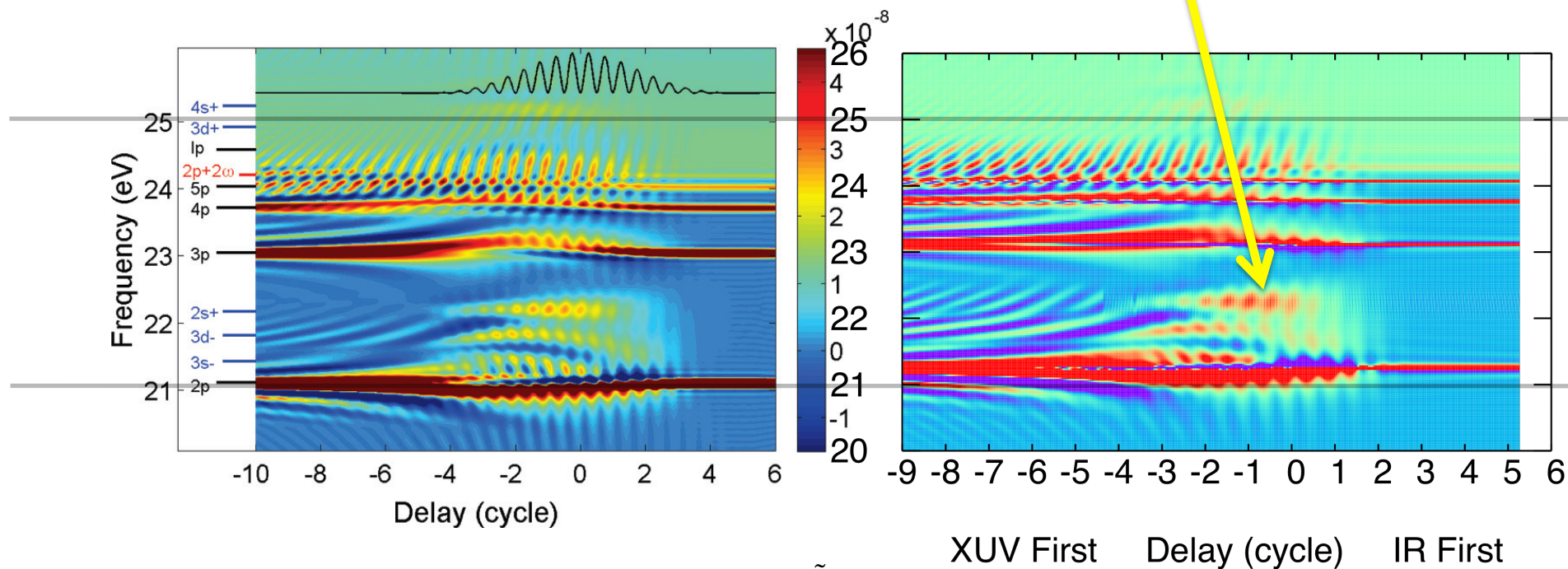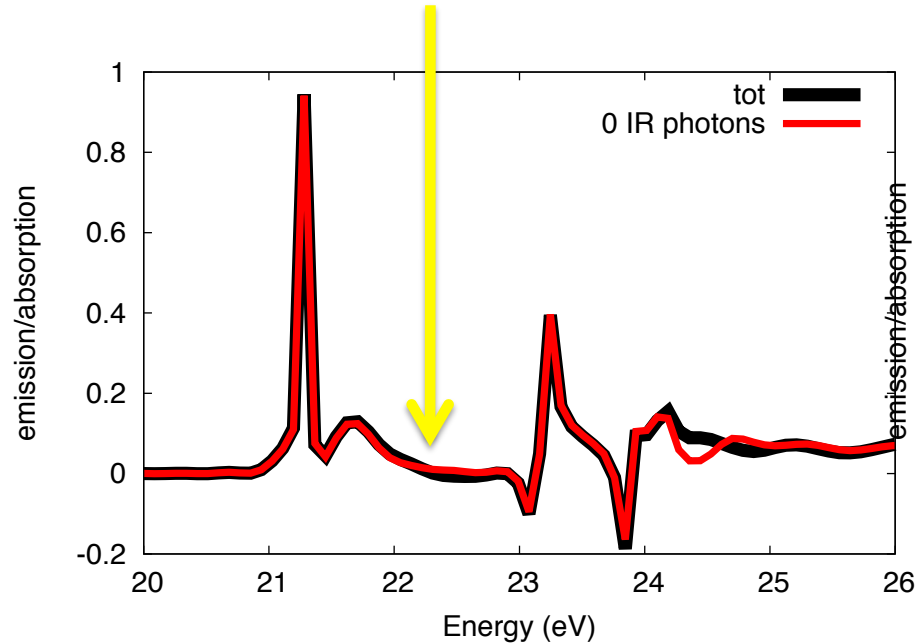This feature is He 1s2s + 1 IR photon

FIG. 1. (Color online) Single atom response function $\tilde{S}(\omega, t_d)$ in helium where t_d is the time delay in IR cycles between the IR laser pulse (800 nm, 3×10^{12} W/cm^2, 4 cycles, cos^2 envelope, sine-like carrier envelope) and the attosecond pulse (330 as, centered at 25 eV). The IR intensity oscillations are shown in black in the top panel.

Opposite circular polarization

No feature if opposite circular polarizations

Same circular polarization

This feature is He 1s2s + 1 IR photon
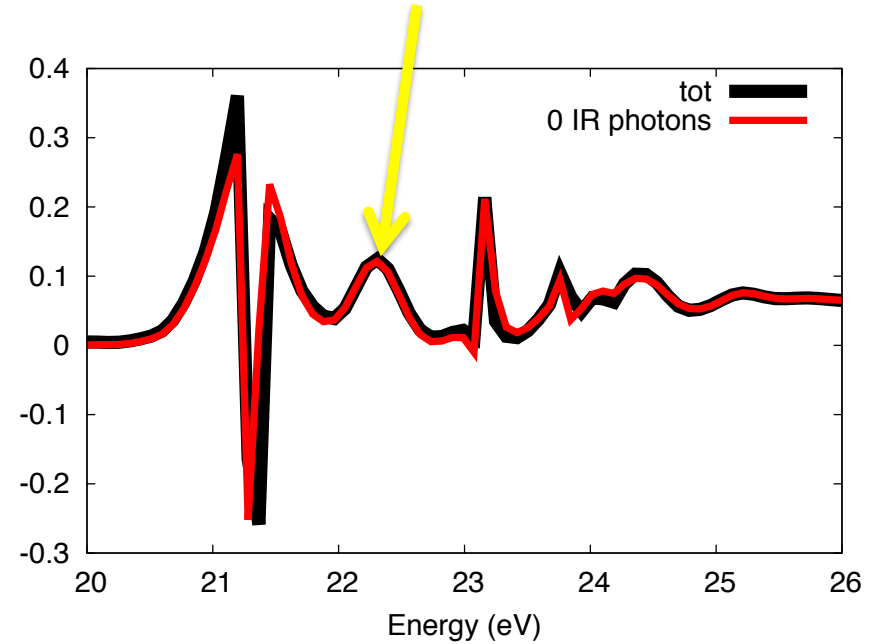
Circular polarization gives you more information.
At ~22.2eV it absorbs XUV and emits IR
  22.2-1.6 = 20.6 He 1s2s
Since it is an S state, polarizations must be the same

Multi-fragment vector correlation imaging. A search for hidden dynamical symmetries in many-particle molecular fragmentation processes
Mol Phys 110, 1863 (2012)
F Trinter, L.Ph.H Schmidt, T Jahnke, M.S. Schöffler, O Jagutzki, A Czasch, J Lower,
T.A Isaev, R. Berger, A.L. Landers, Th. Weber, R. Dörner, H. Schmidt-Böcking

DECOMPOSE transient signal w.r.t # IR Photons!

Absorption, Helium; 330as 25eV,
11fs FWHM 780nm, 2.7e11 W cm^{-2}

IR First   Delay (cycle)   XUV First
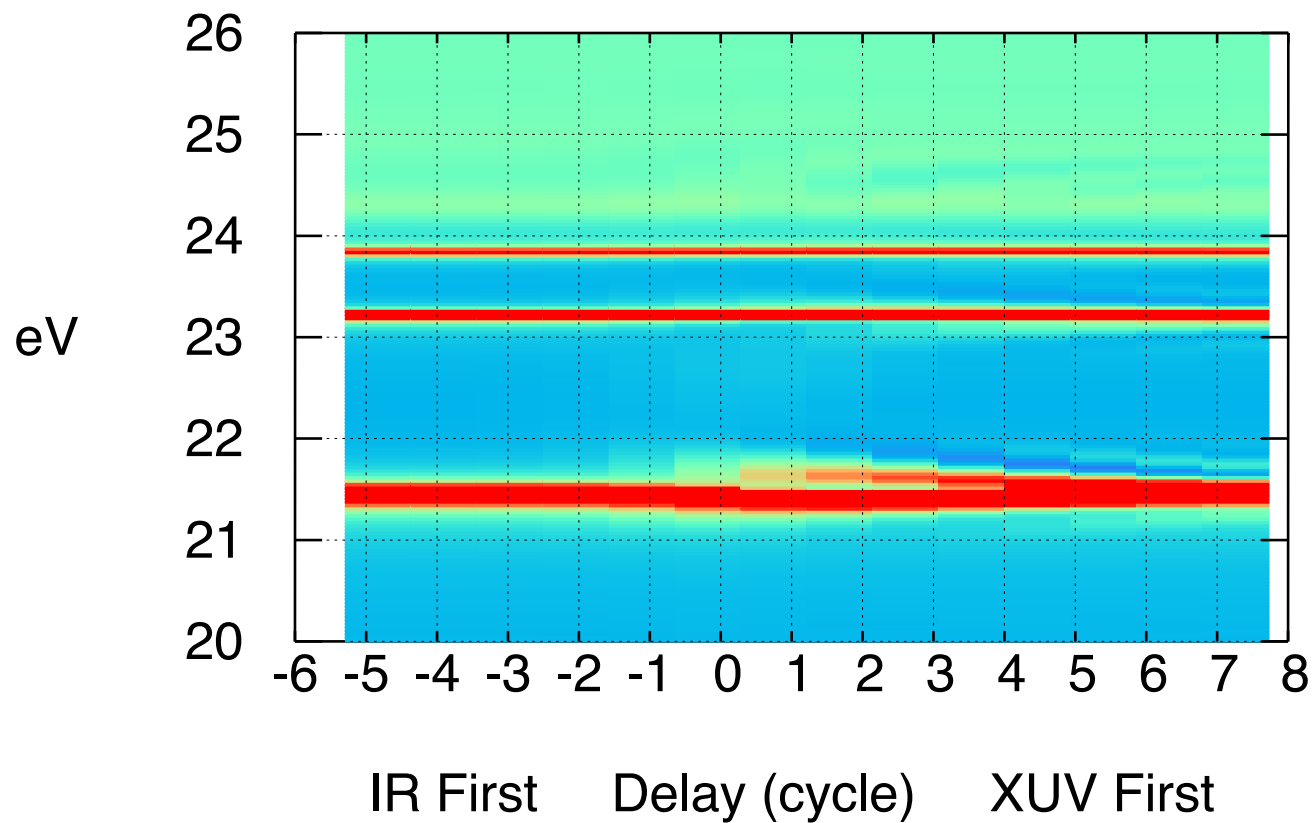
DECOMPOSE transient signal w.r.t # IR Photons!

0,0 photon
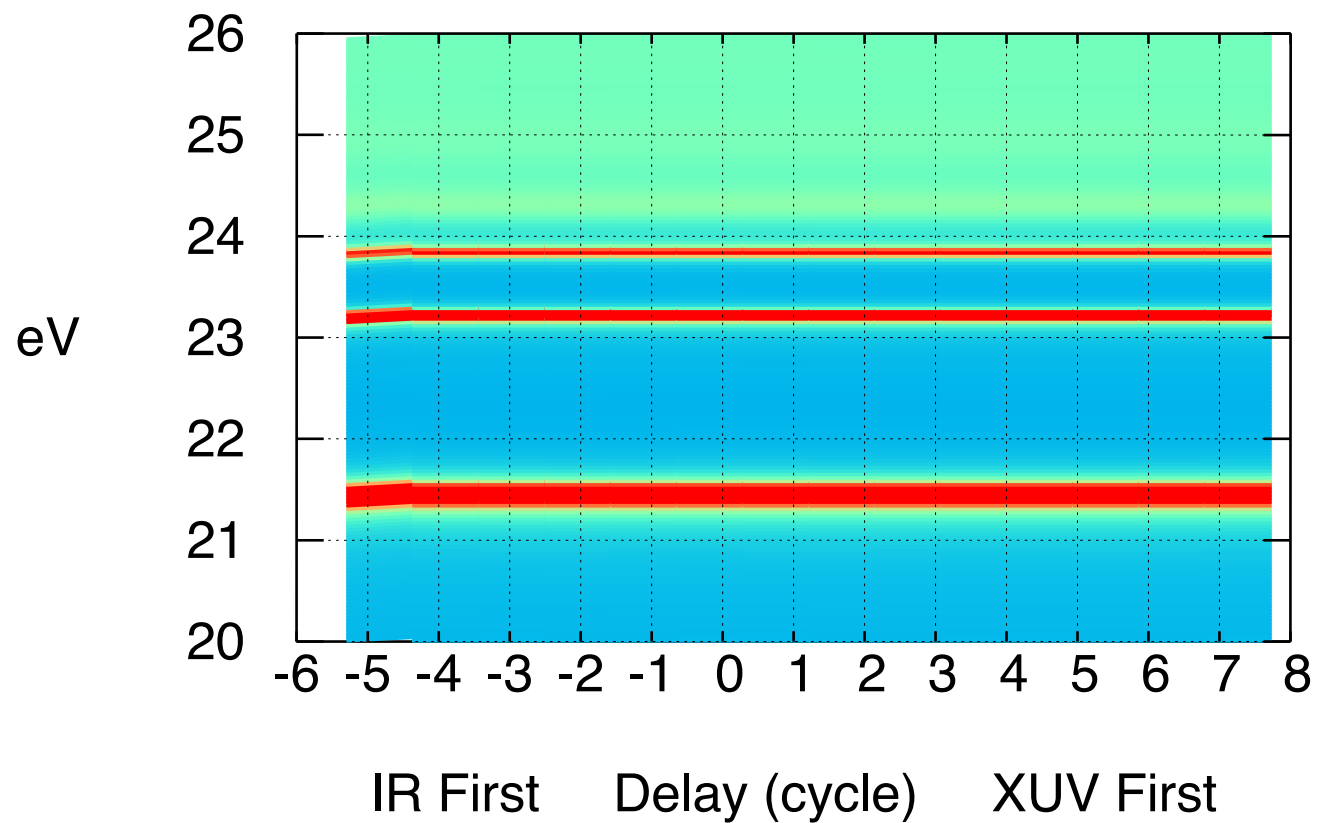
FIG. 4: (Color Online) Four views of the two dimensional spectrum induced by a monochromatic probe pulse. a) ω_{out} vs n_{IR} b) ω_{out} vs ϕ_s/π, c) $t - t_0$ vs n_{IR}, d) $t - t_0$ vs ϕ_s/π.

Non-perturbative Calculations of Multidimensional Spectra in the XUV

Proposed work: Explore various kinds of multidimensional spectra for electronic excitation of dimers like Ne_2 with MCTDHF to see coupled excitations, etc. in a correlated ab initio treatment.

But how? The phase matching condition is macrosopic
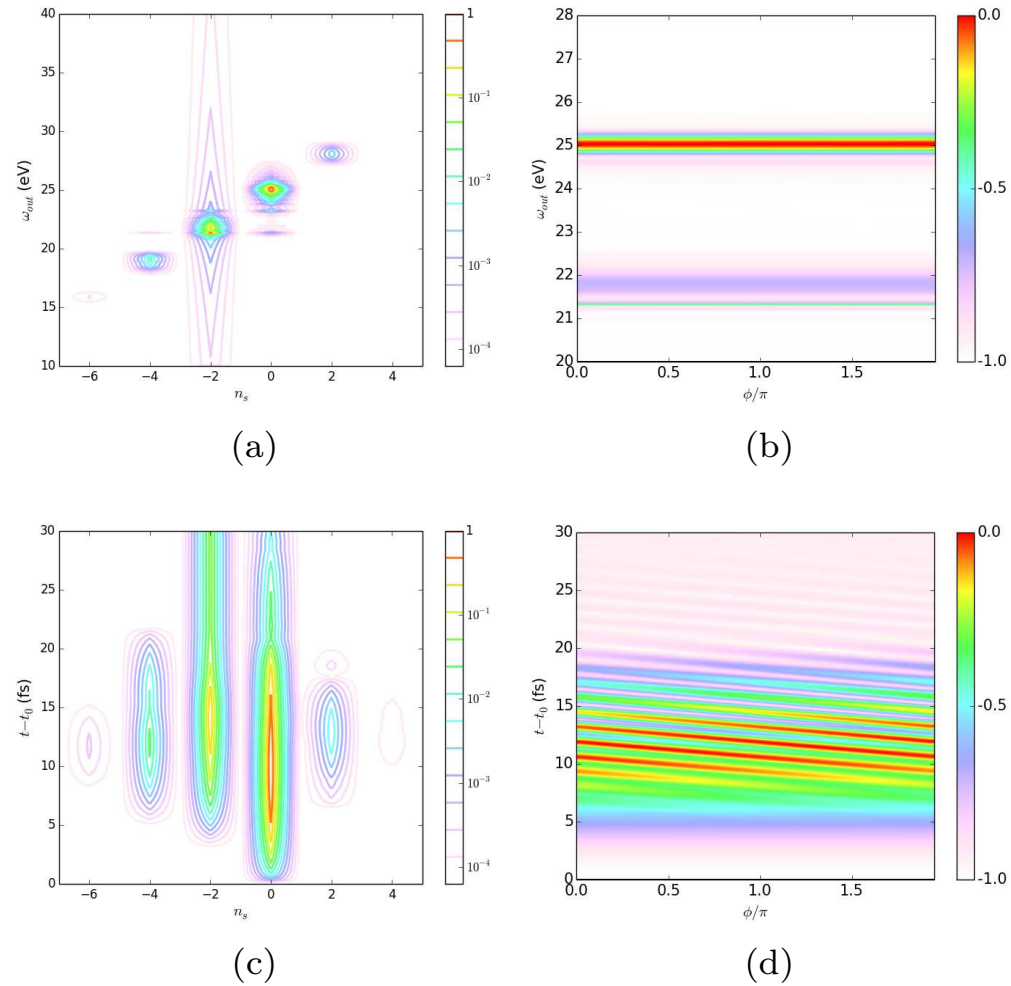
$$\tau \qquad T \qquad k_s = -k_1 + k_2 + k_3$$

time
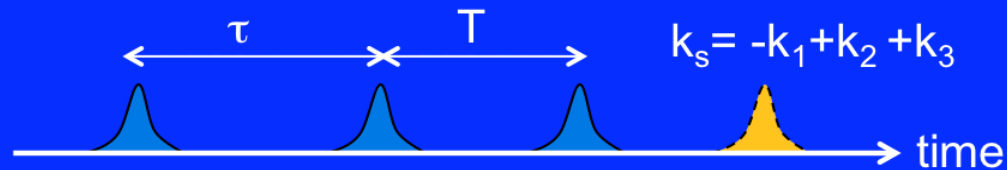
MCTDHF calculates total polarization for isolated atom or molecule

$$P(t) = \langle \Psi(t) | \hat{\mu} | \Psi(t) \rangle$$

The four wave mixing signal is due to a component of this quantity selected by phase matching direction
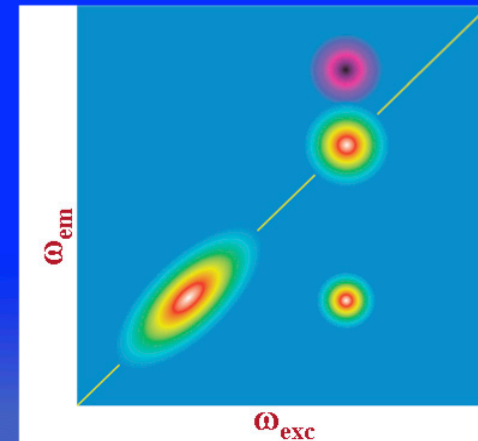
Non-perturbative Calculations of Multidimensional Spectra in the XUV

Signal in the phase matched direction comes one component of this expansion of the polarization for specific l, m, n

$$P(t) = \sum_{\ell,n,m} P_{\ell,n,m}(t) e^{i(\ell\vec{k}_1 + m\vec{k}_1 + n\vec{k}_1)\cdot\vec{r}}$$

Multidimensional spectra from Fourier transform of this.

Calculate polarization for a number of independent sets of carrier phases of the pulses .

$$\mathcal{P}(t, \varphi_1, \varphi_2, \varphi_3) = \sum_{\ell,m,n} P_{\ell,m,n}(t) \ e^{i(\ell\varphi_1 + m\varphi_2 + n\varphi_3)}$$

And solve linear equations for the $P_{\ell,m,n}(t)$ at each time [S. Meyer & V. Engle, (2000) L. Seidner, G. Stock & W. Domcke (1995)]

Phase matching has been implemented, and preliminary MCTDHF calculations are underway on atoms.

Transient Absorption Above the Ionization Potential for Atoms and Molecules

Two overlaping (or not) pulses

τ

UV/XUV above IP

IR/VIS

time

CCD Camera

Grating

Sn Filter

Gas Sample

Toroidal Au mirror

Time delay=0.887fs
Time delay=8.87fs
Time delay=17.74fs
XUV only

Absorption signal (a.u.)

Photoenergy (eV)

1e-03

0e+00
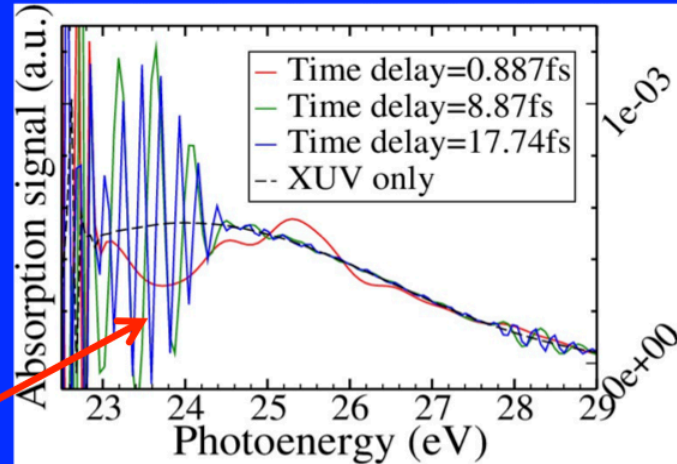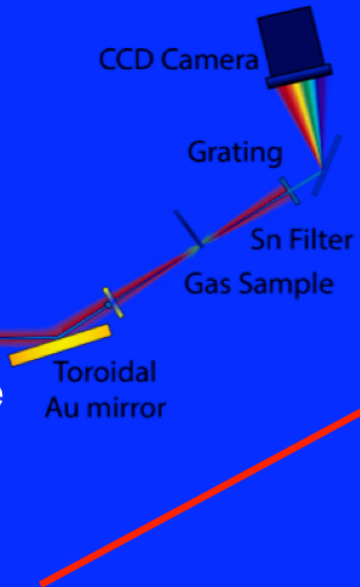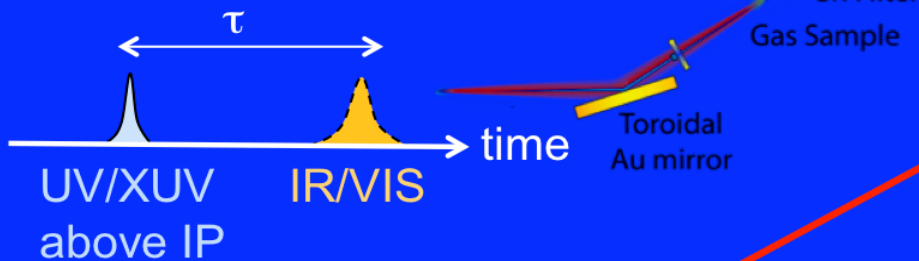
MCTDHF calculations on Neon
10 electrons

Transient absorption in the continuum has considerable structure in time delay and frequency

What is being measured such experiments?

MCTDHF Calculations Suggest a Way to Measure the Time-Dependent Dipole Without Detecting Ions

Probing Time-Dependent Molecular Dipoles on the Attosecond Time Scale

Ch. Neidel, J. Klei, C.-H. Yang, A. Rouzée, and M.J.J. Vrakking*

Max-Born Institut, Max-Born Strasse 2A, 12489 Berlin, Germany

K. Klünder, M. Miranda, C. L. Arnold, T. Fordell, A. L'Huillier, M. Gisselbrecht, and P. Johnsson

Department of Physics, Lund University, P.O. Box 118, SE-221 00 Lund, Sweden

M. P. Dinh and E. Suraud

Laboratoire de Physique Théorique—IRSAMC, University Paul Sabatier Toulouse 3, 118 Route de Narbonne, 31062 Toulouse Cedex, France

P.-G. Reinhard

Institut für Theoretische Physik, Universität Erlangen, Staudtstrasse 7, D-91058 Erlangen, Germany

V. Despré, M. A. L. Marques, and F. Lépine[†]

Institut Lumière Matière, Université Lyon 1, CNRS, UMR 5306, 10 Rue Ada Byron, 69622 Villeurbanne Cedex, France
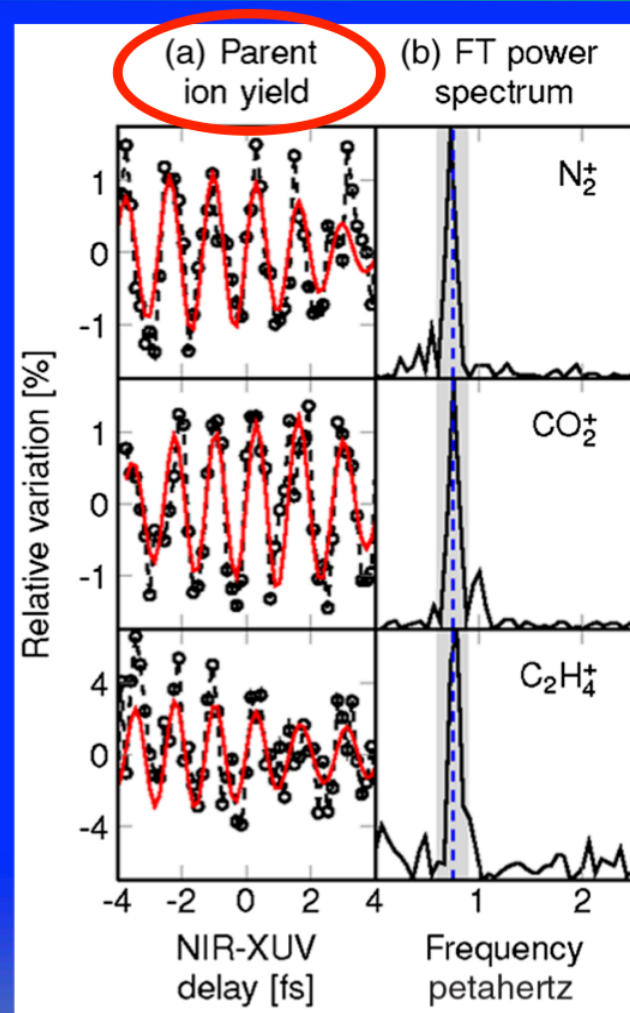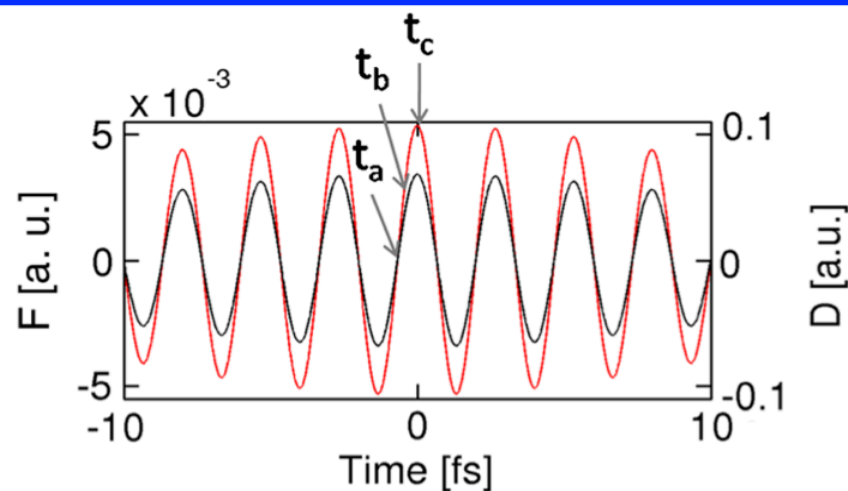
NO S. RAMAN

Ultrafast population transfer to excited valence levels of a molecule driven by x-ray pulses

D. J. Haxton[1] and C. W. McCurdy[2,3]

[1]*Chemical Sciences, Lawrence Berkeley National Laboratory, Berkeley, California 94720, USA*
[2]*Chemical Sciences and Ultrafast X-ray Science Laboratory, Lawrence Berkeley National Laboratory, Berkeley, California 94720, USA*
[3]*Department of Chemistry, University of California, Davis, California 95616, USA*

Two color core hole stimulated Raman in NO

$(1s)^2 \pi_g^1 \rightarrow 1s^1 \pi_g^2$

$^2\Delta$, $^2\Sigma^-$, $^2\Sigma^+$ overall
$^1\Delta$, $^3\Sigma^-$, $^1\Sigma^+$ valence shell
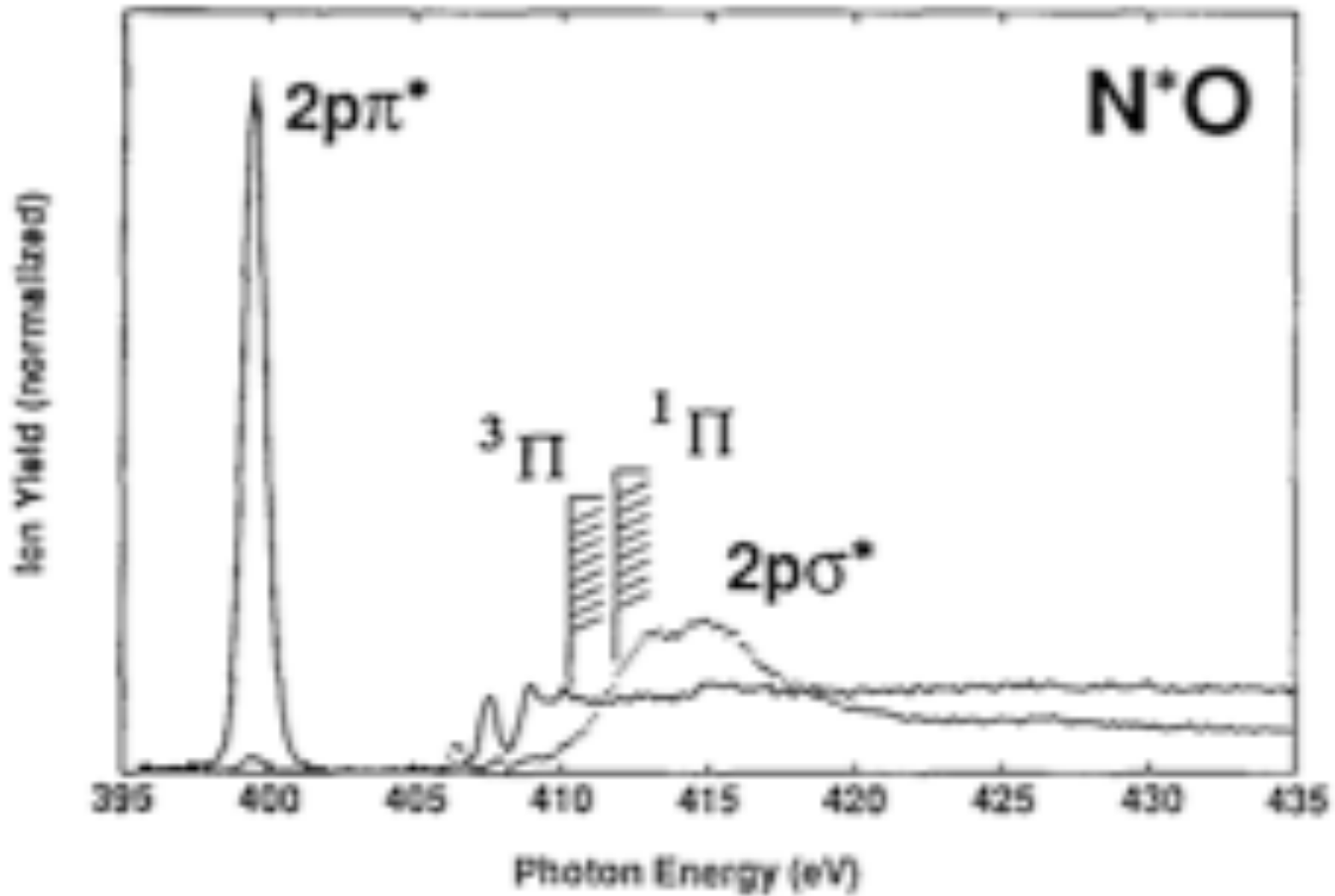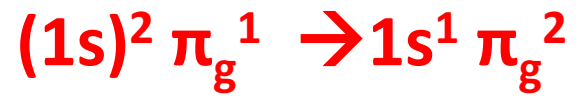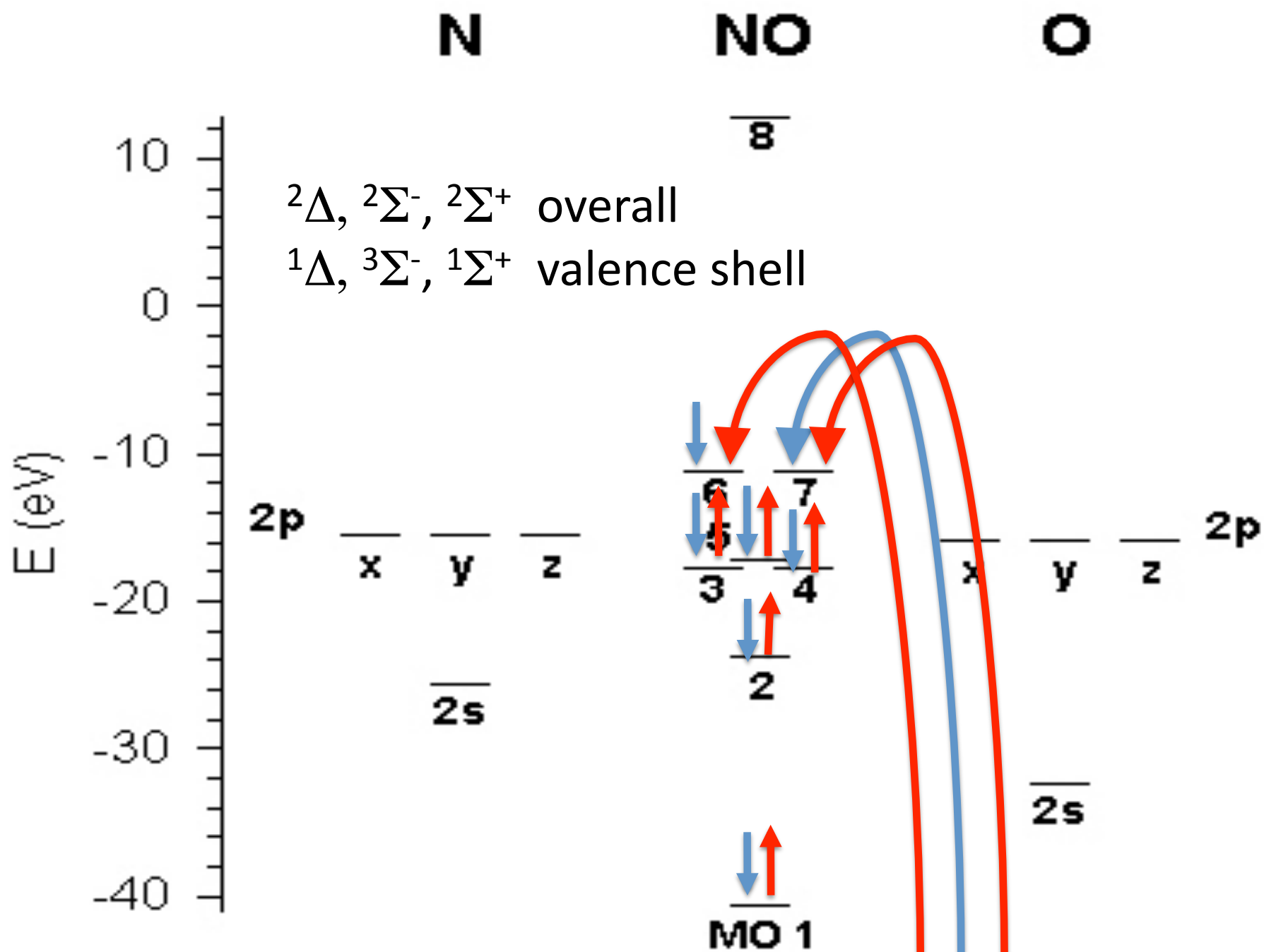
The first electron can be in any of the three spots.

Depending on which spot it's in, the transition illustrated here from sigma to N 1s takes you the B' $^2\Delta$, G $^2\Sigma^-$, and I $^2\Sigma^+$ states.
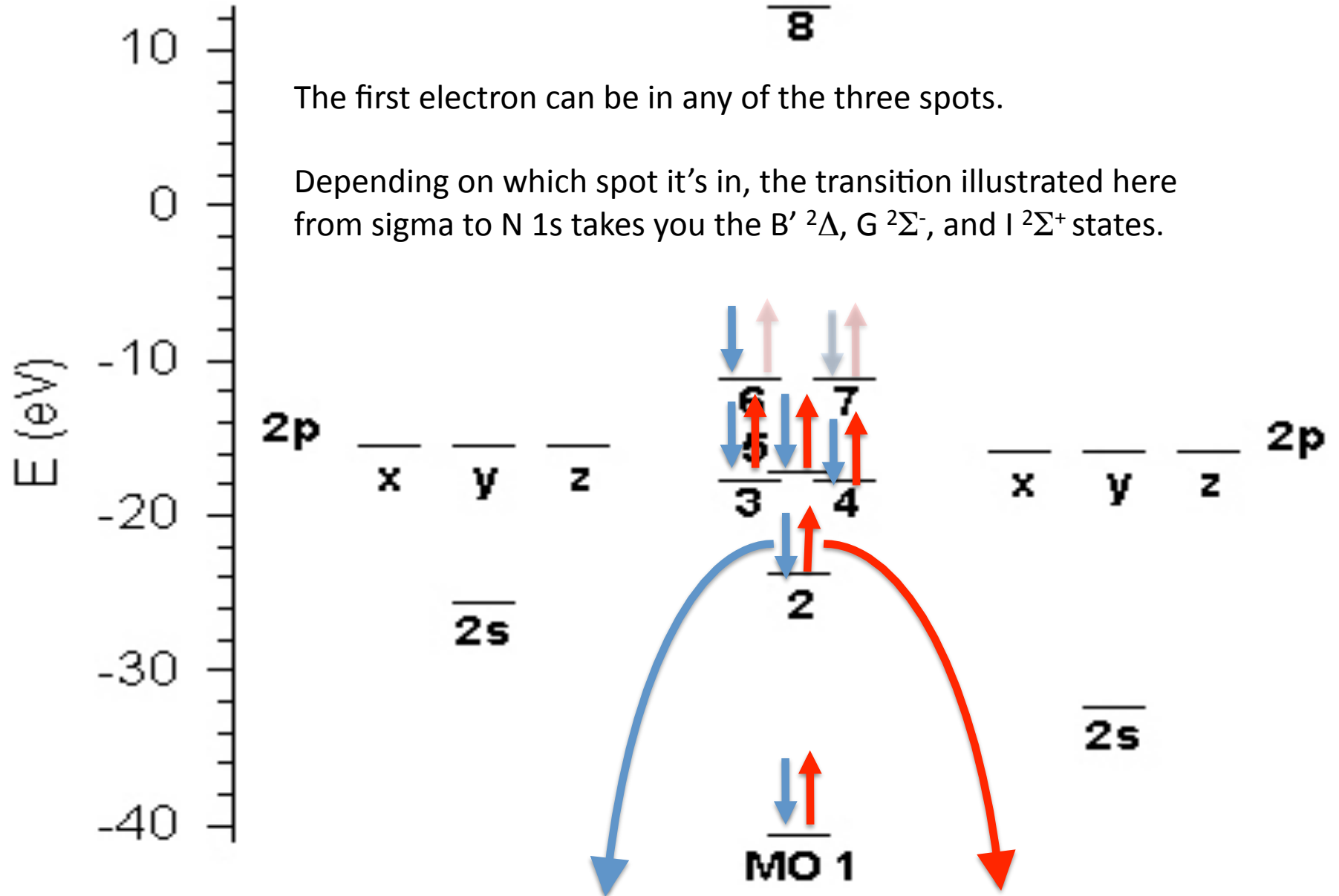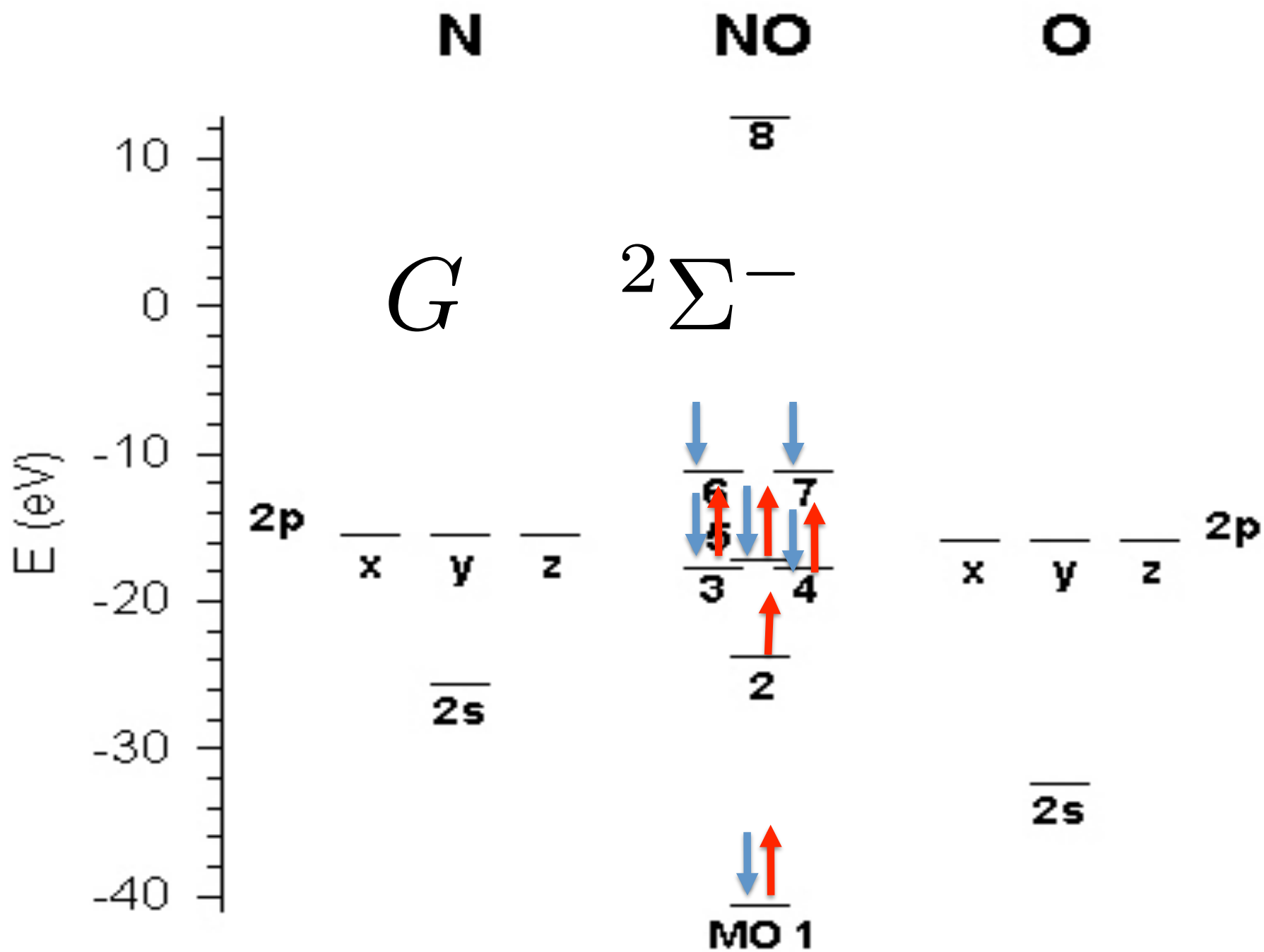
Parameters of pulse used

Sin^2 envelope FWHM 0.66fs, duration 1.32fs

H-bar Omega = 402.6, 393.3eV

Intensity=5 x 10^{16}, 3 x 10^{17} W cm^{-2}
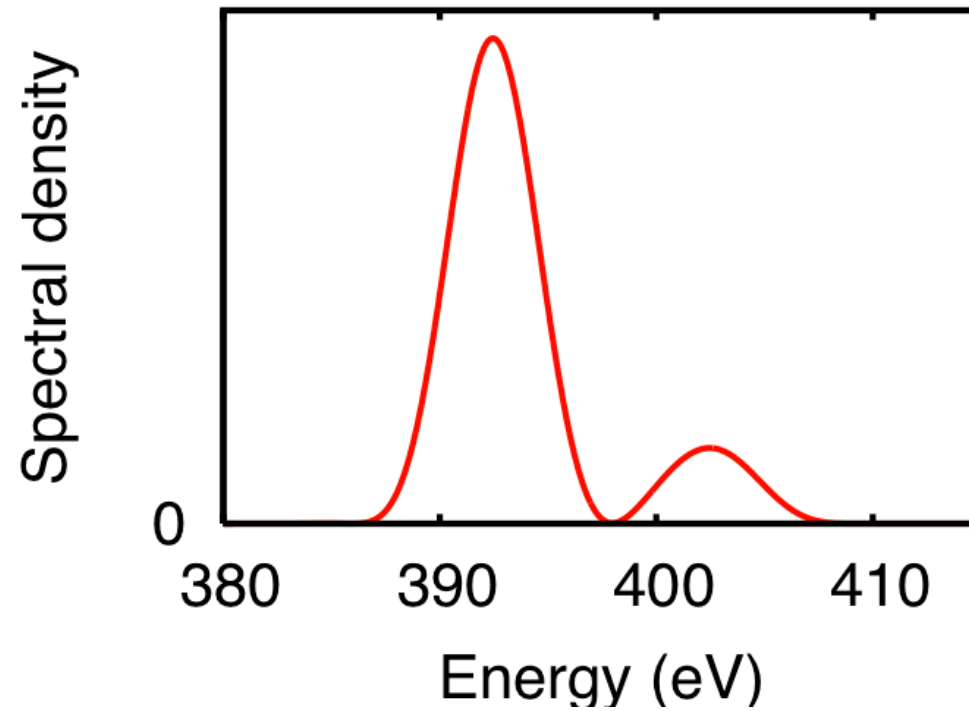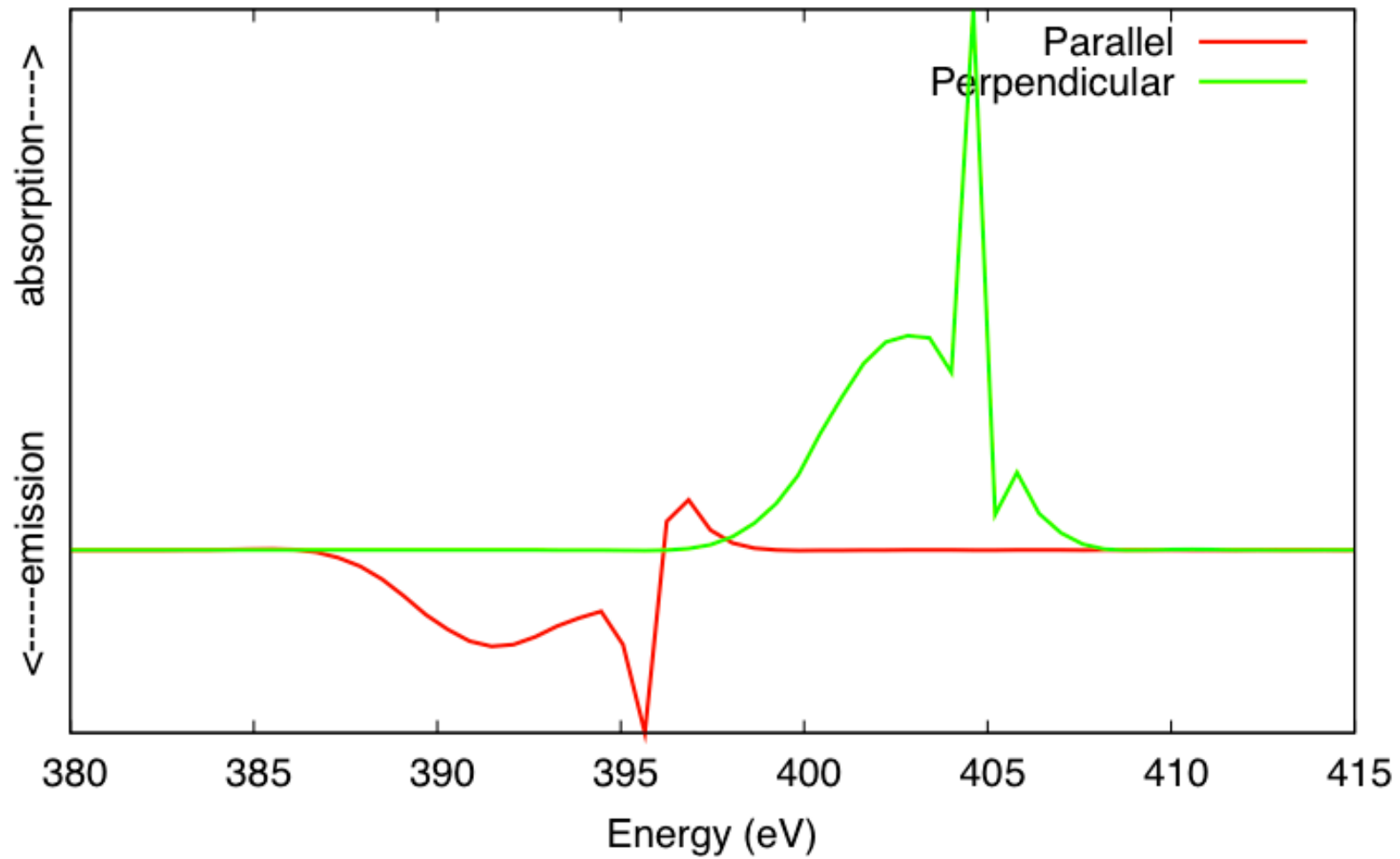
The Raman signal

Frequency dependent response function

$$\tilde{\mathbf{S}}(\omega) = \mathbf{2}\mathrm{Im}[\tilde{\mu}(\omega)\tilde{\mathcal{E}}(\omega)^*]$$

Emission/absorption of energy $\propto \omega\tilde{\mathbf{S}}(\omega)$

FT of $\langle\mathbf{\Psi(t)}|\hat{\mu}|\mathbf{\Psi(t)}\rangle$ FT of field
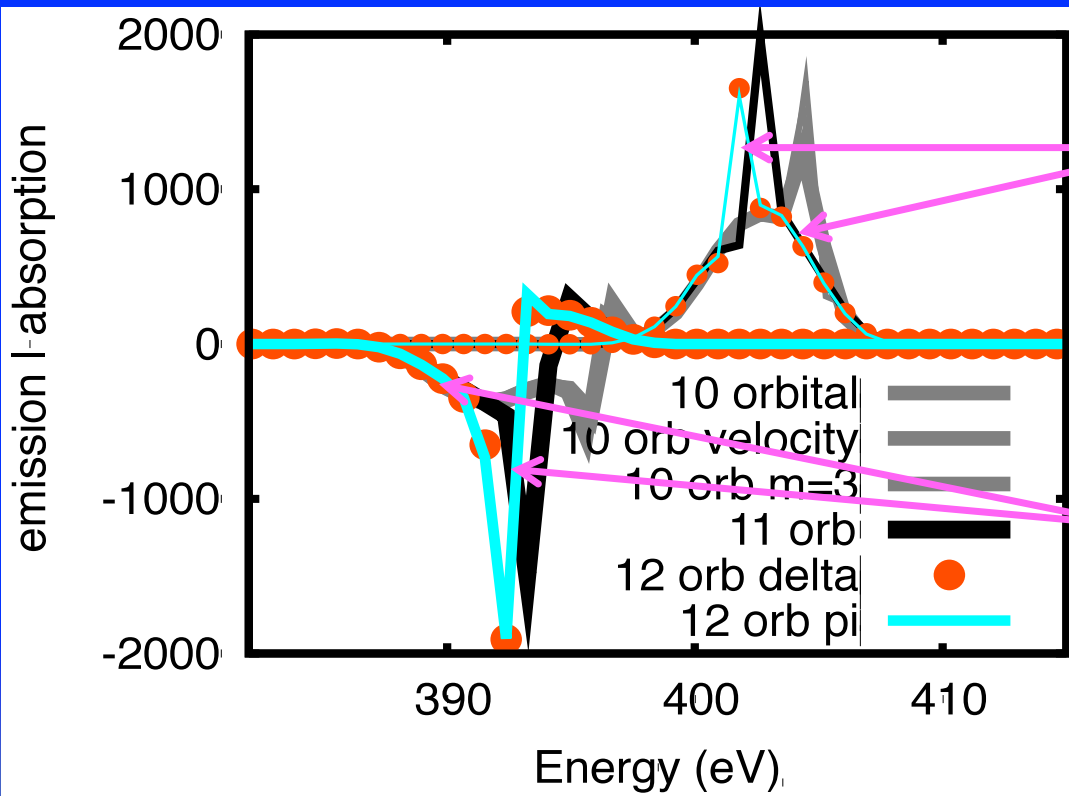
Absorption: peak near 400 eV and background with energy profile of pulse

Raman emission: peak near 393 eV and background with energy profile of pulse -- Raman via the continuum

Convergence with respect to orbitals – core states

Nitric.SLANT.BOTH-together-lowtol.allstates.double$_z$pulse.long-12shifted
T=   70.40000 atomic units

CORE EXCITED STATES
N $1s^{-1}\pi^{*2}$ configuration
Doublets
Labeled by π^{*2} coupling

$^3\Sigma\ 1s^{-1}$
$^1\Sigma\ 1s^{-1}$
$^1\Delta\ 1s^{-1}\ (m_L=+2)$
$^1\Delta\ 1s^{-1}\ (-2)$

Convergence with respect to orbitals – core states

Nitric.SLANT.BOTH-together-lowtol-12orb.shifted.double$_z$pulse.long
T=   52.72000 atomic units

CORE EXCITED STATES
N $1s^{-1}\pi^{*2}$ configuration
Doublets
Labeled by π^{*2} coupling

$^3\Sigma\ 1s^{-1}$
$^1\Sigma\ 1s^{-1}$
$^1\Delta\ 1s^{-1}\ (m_L=+2)$
$^1\Delta\ 1s^{-1}\ (-2)$

Population (log scale)

Time (fs)

Convergence with respect to orbitals – valence states

Nitric.SLANT.BOTH-together-lowtol.allstates.double$_z$pulse.long-12shifted
T=   70.40000 atomic units

$^2\Pi$ (m_L=+/-1)
G $^2\Sigma$
I $^2\Sigma$
B' $^2\Delta$

Initial $^2\Pi$ π^{*1} state
m_L=+1 component

Final $(5\sigma)^{-1}\pi^{*2}$
states

VALENCE
STATES

Population (log scale)

Time (fs)

Convergence with respect to orbitals – valence states

Nitric.SLANT.BOTH-together-lowtol-12orb.shifted.double$_z$pulse.long
T=   52.72000 atomic units

Legend:
- $^2\Pi$ (m_L=+/-1) — black
- G $^2\Sigma$ — magenta
- I $^2\Sigma$ — green
- B' $^2\Delta$ — gray

Initial $^2\Pi\,\pi^{*1}$ state
m_L=+1 component

Final $(5\sigma)^{-1}\pi^{*2}$
states

VALENCE
STATES

Population (log scale)
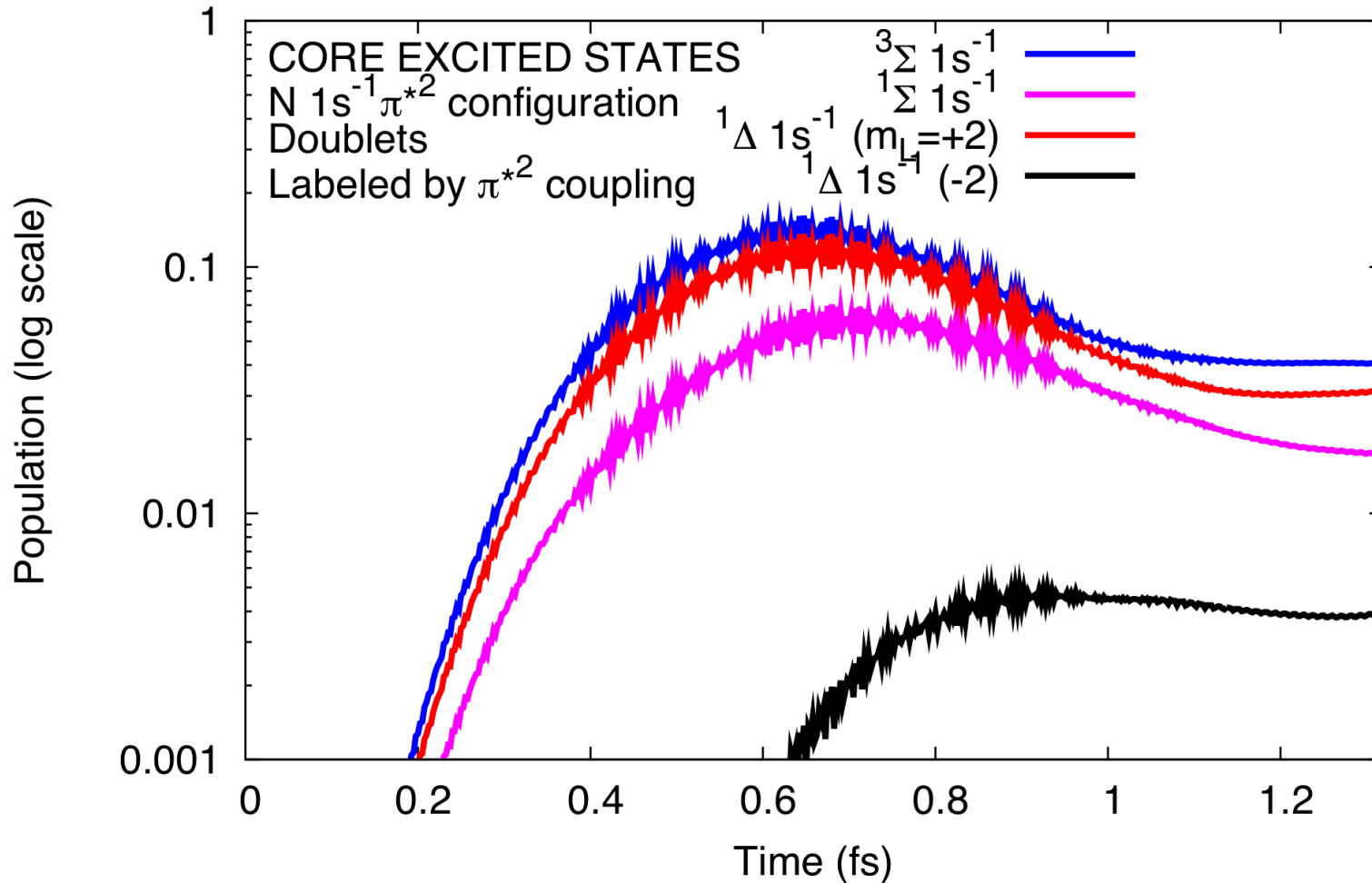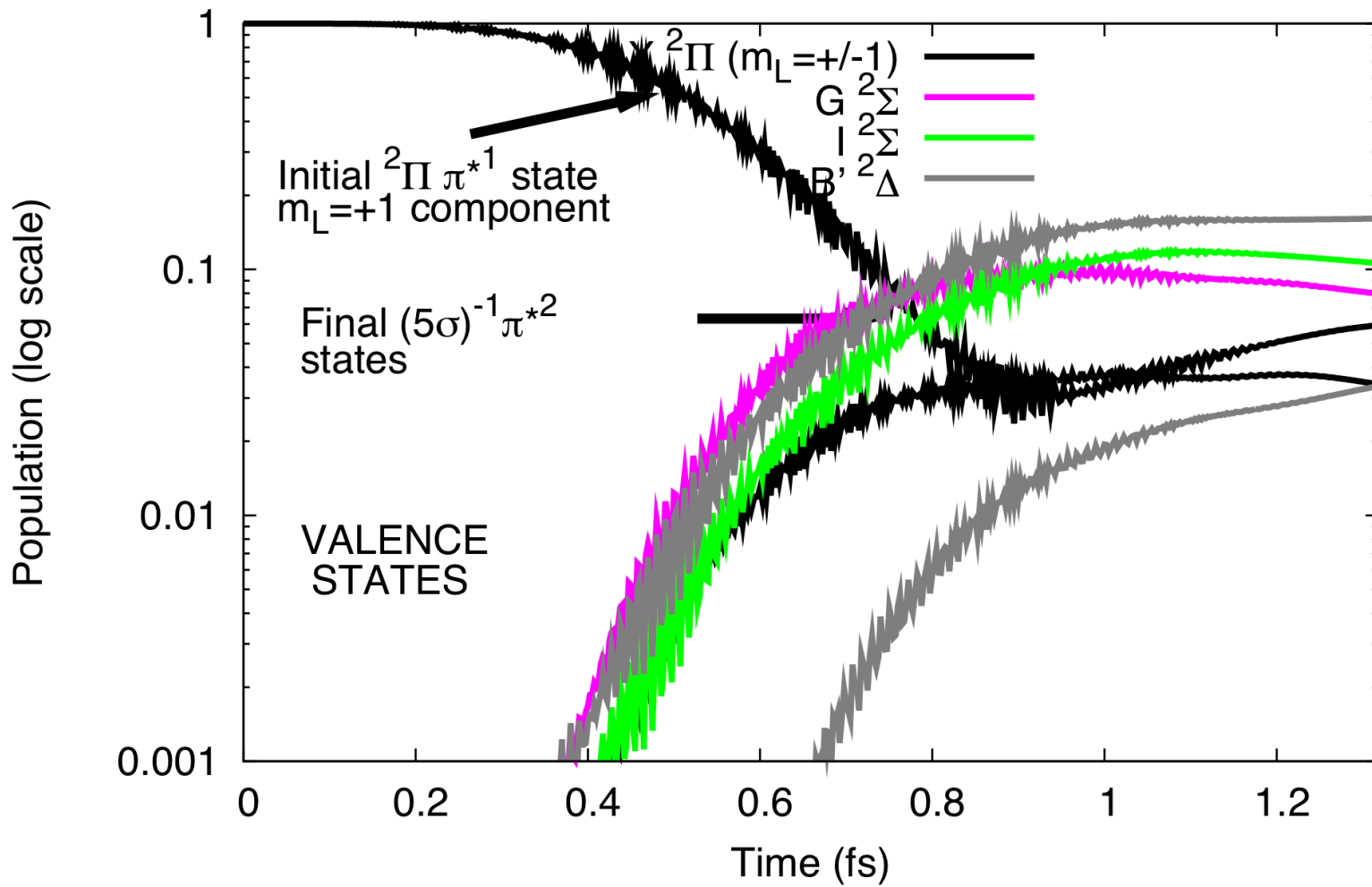
Time (fs)
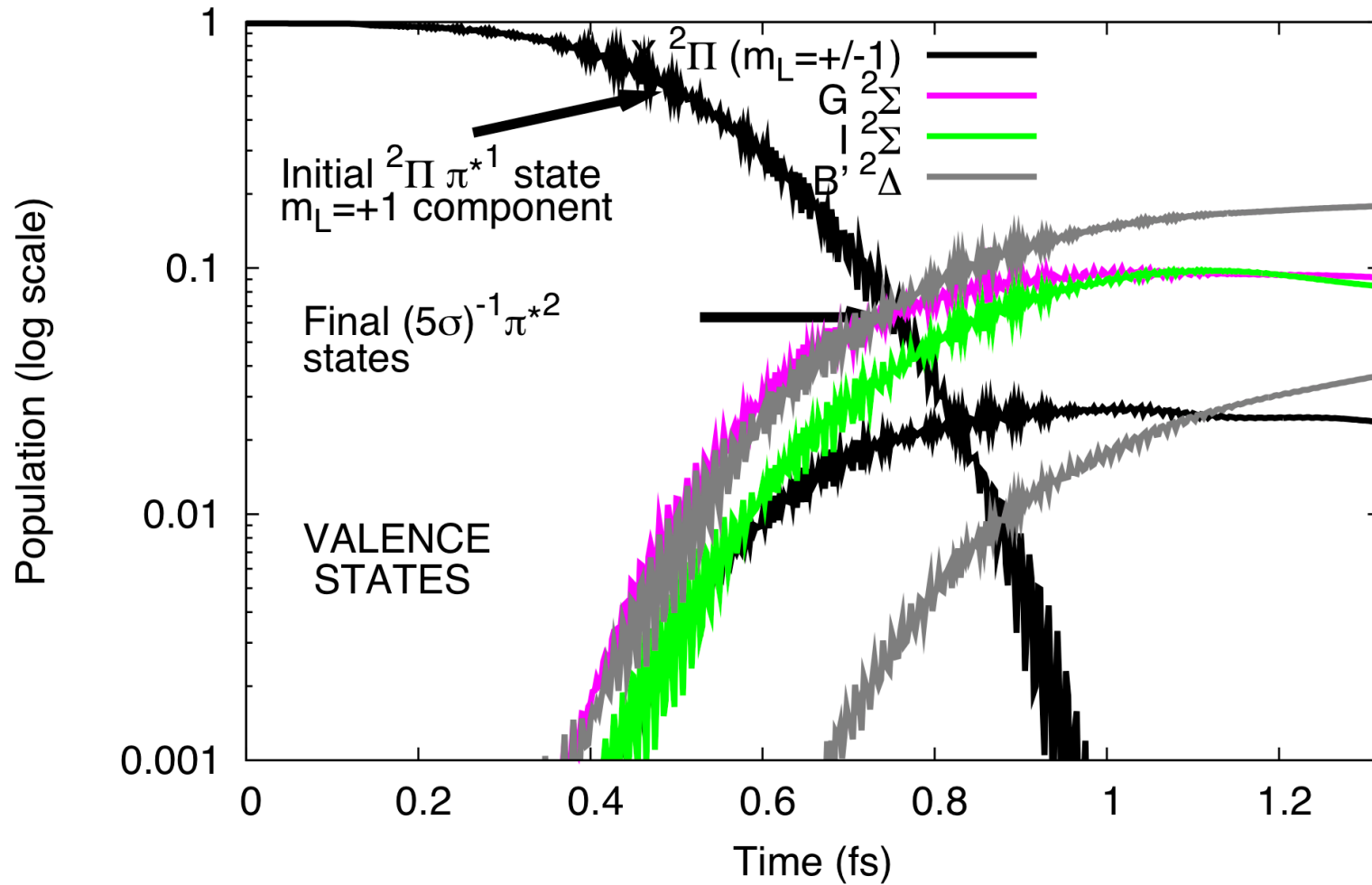
WITH NUCLEAR MOTION

With ECS we can calculate ionization and, hypothetically, dissociation
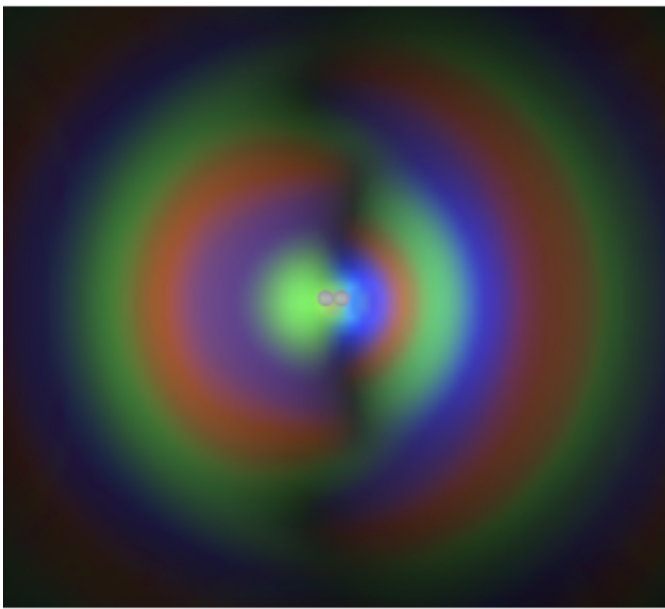
O2 10th full CI orbital ionized.   H$_2$ excited and dissociating.
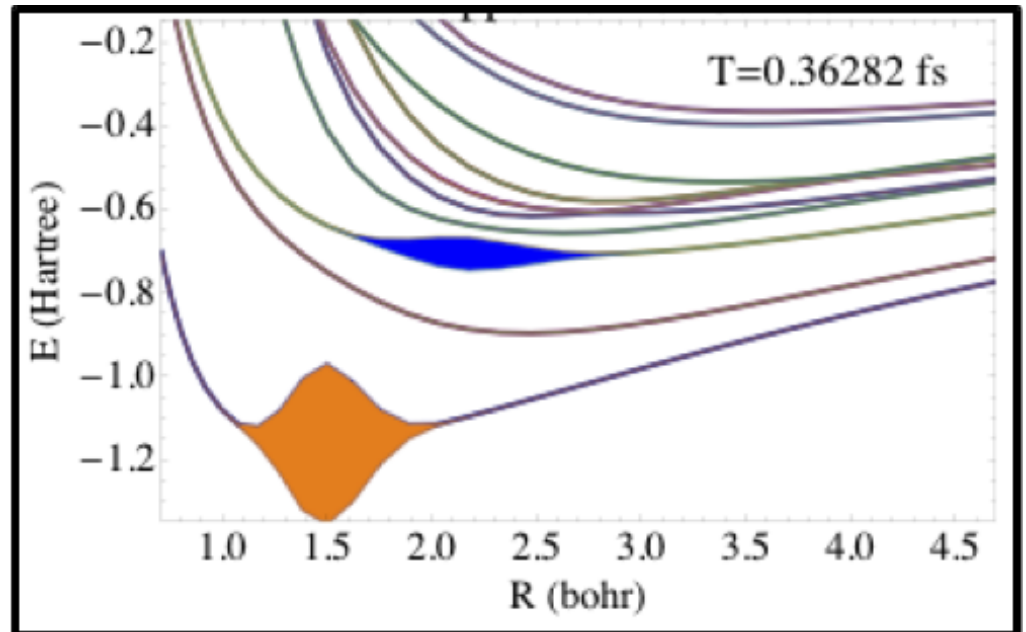
(For dissociation a CAP – complex absorbing potential – works too.)

How does one most appropriately include nuclear motion within MCTDHF?

Orbitals in electronic and R, cf. Nest 2009? Only electronic?

Ideally, **full primitive basis** in nuclear DOF(s) for correlated motion.
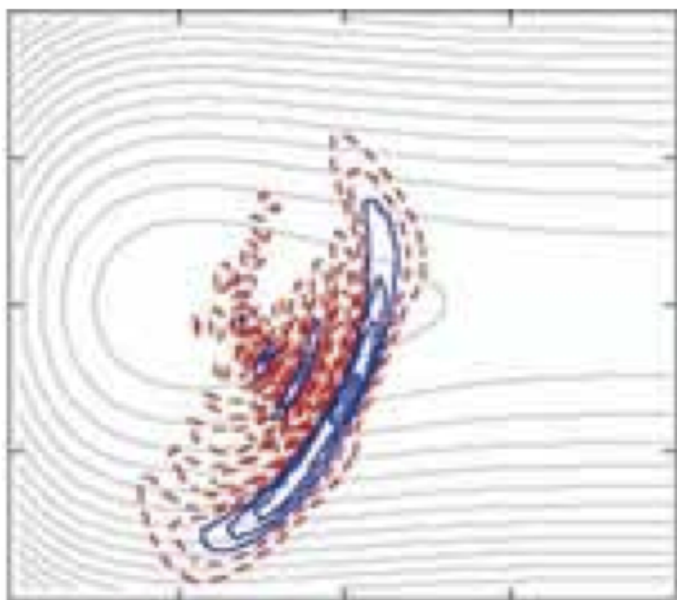
J. Cina, U. Oregon
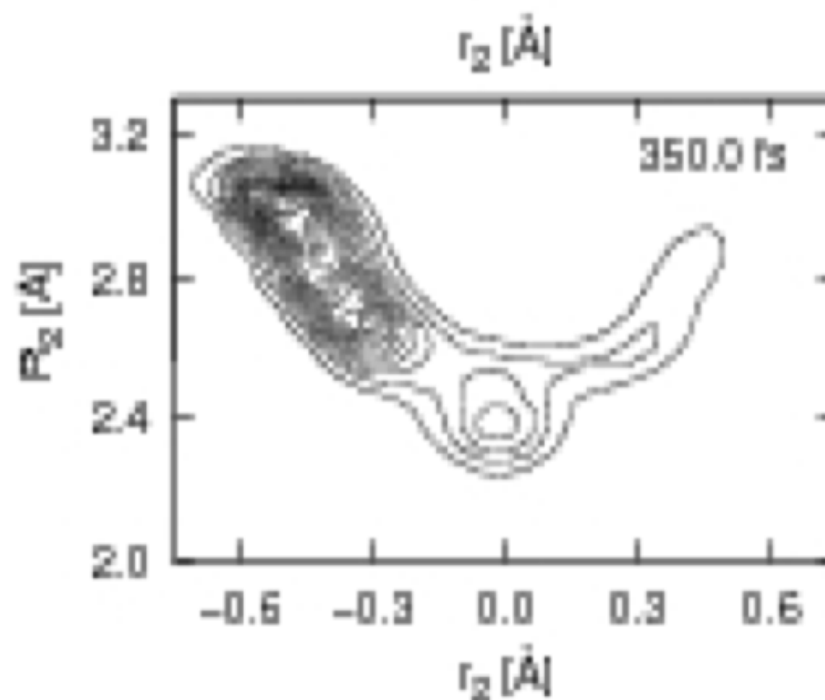
Vendrell and Meyer, JCP 122, 104505 (2005)

Vibrational transitions converge with respect to number of orbitals.

Natural orbital occupations are close to those of Born Oppenheimer wave function – Prolate coordinates are good

Can do other things too like
construct Schmidt decomposition
of wave function in prolate
coordinates

$$\Psi(\vec{r_1}, \vec{r_2}, ..., R) =$$
$$\sum_{\alpha} \lambda_{\alpha} \phi_{\alpha}(\vec{r_1}, \vec{r_2}, ...) \chi_{\alpha}(R)$$

to analyze correlation of
nuclear and electronic motion
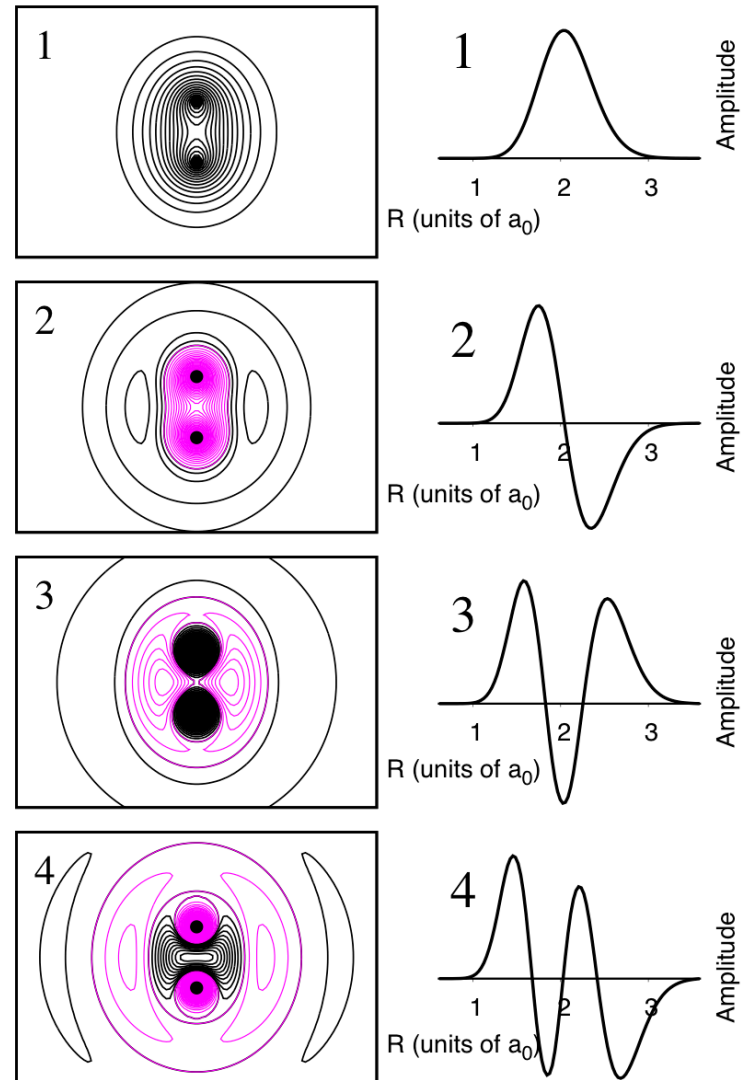
Toy calculation on BH

a) $\langle H_0 \rangle$
b) Occupancy of *natural orbitals*
c) Projection of *natural configuration*
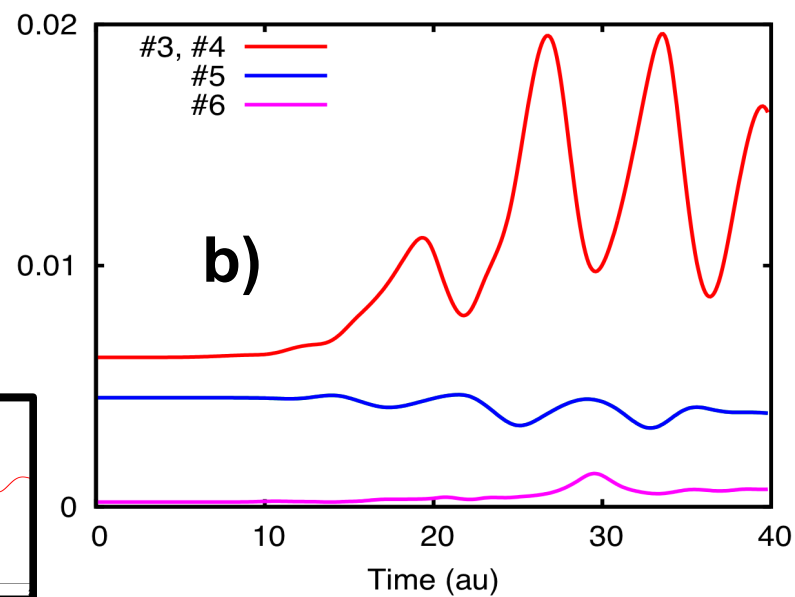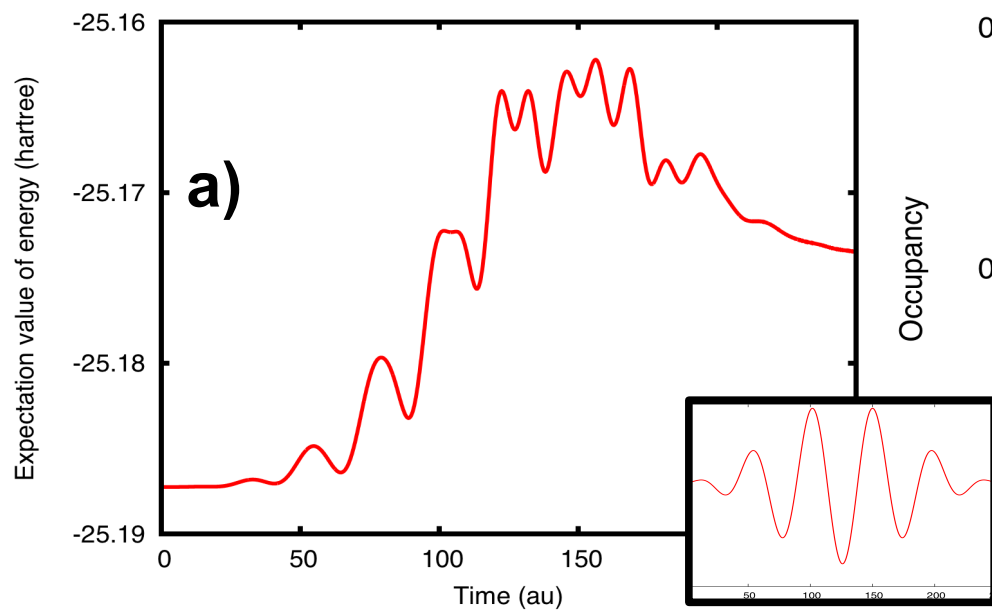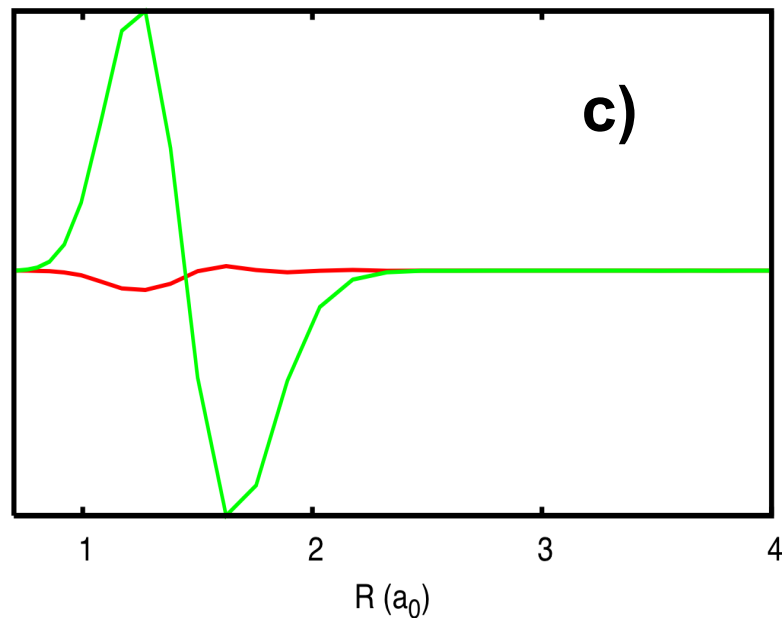
Dissociative ionization of H_2^+
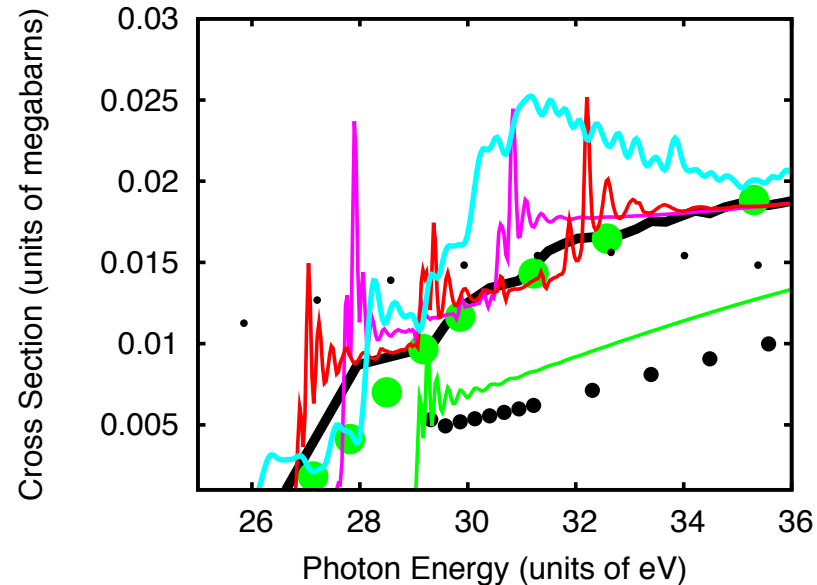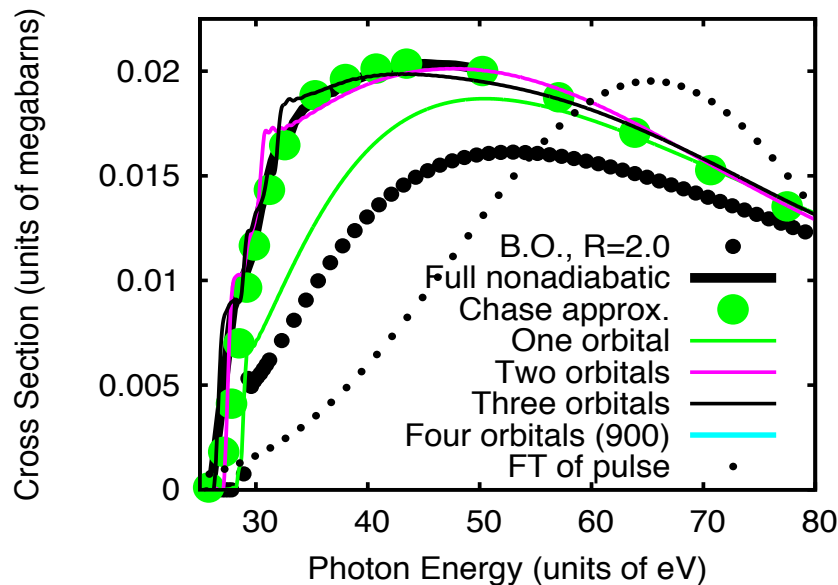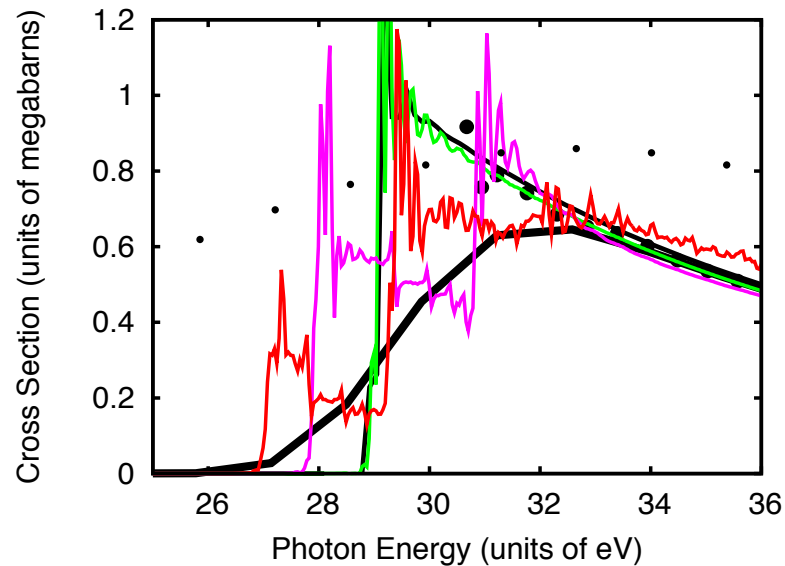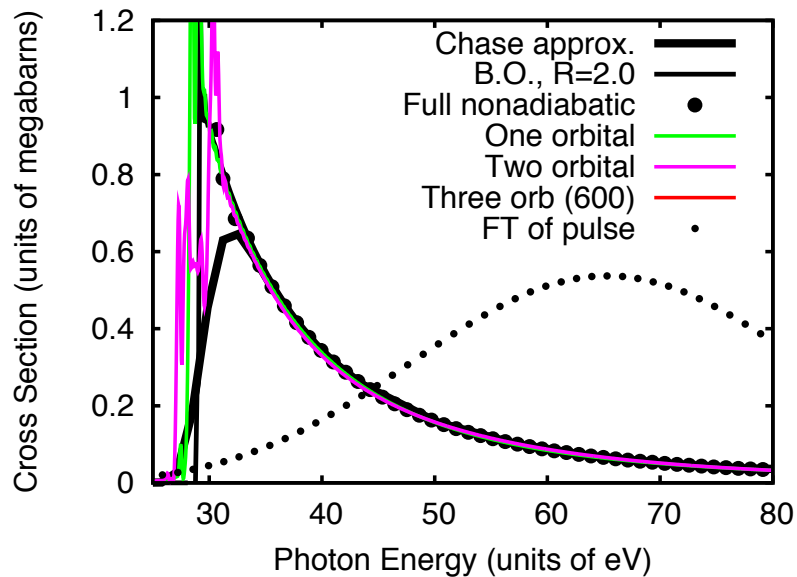
Goal for first quantitative calculation:

Calculate dissociative excitation of Q1 and Q2 autoionizing series in H_2, as per studies by Bozek, Gay et al and as calculated by Martin et al. Requires projecting on Born-Op states and applying CAP (Complex Absorbing Potential) flux formalism of Meyer et al.

Enforcing the phase convention and accounting for adaptive basis is tricky; work in progress.

H2 Dissociative flux
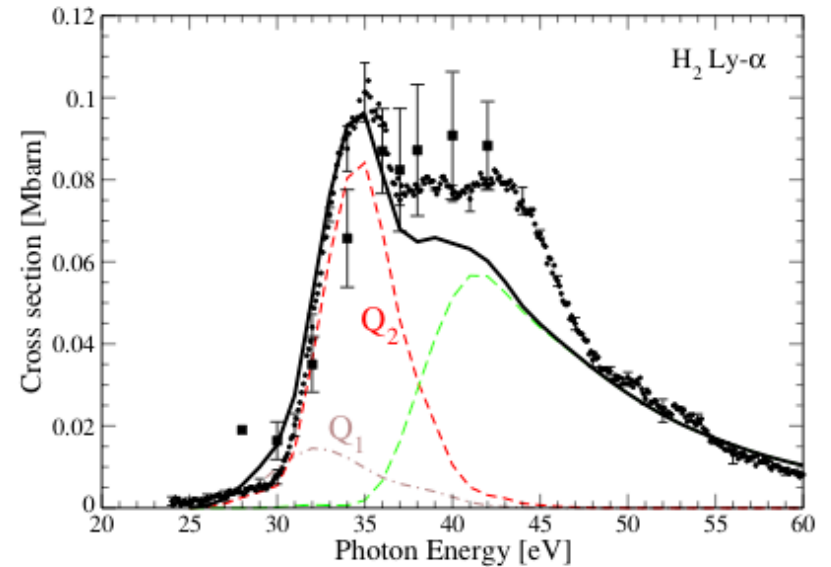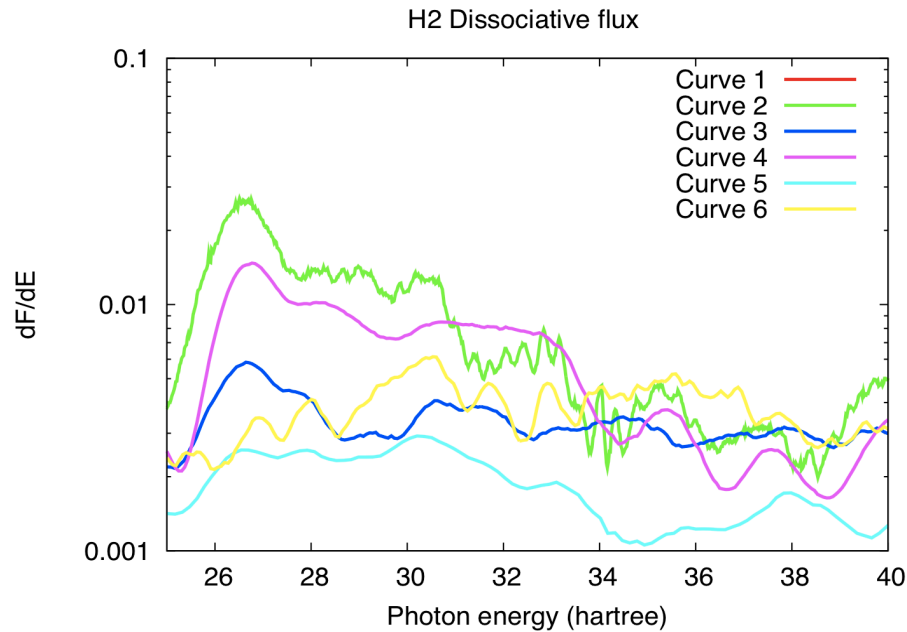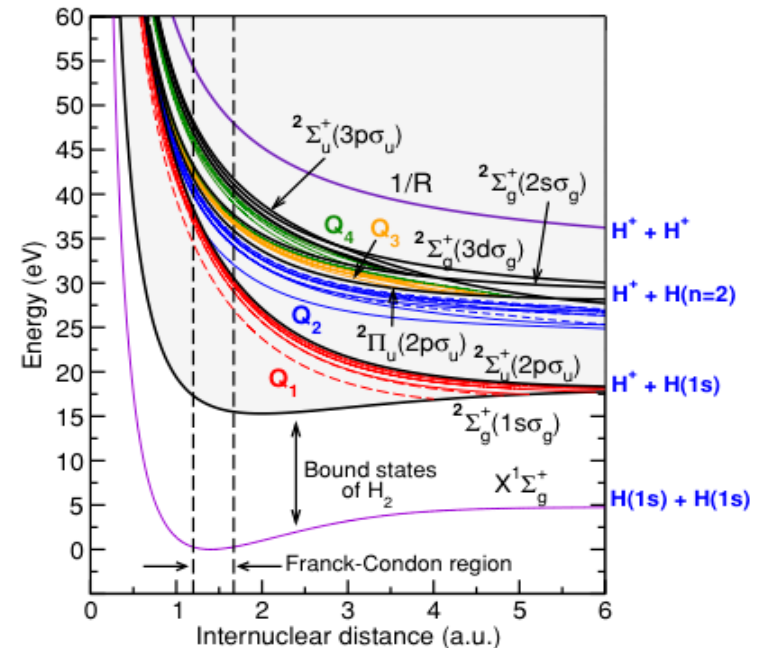
Bozek et al, J Phys B 39, 4871

Comparison flux/autocorr for dissociation: no-ionization 4-spf H2+
0.5 Hartree, 0.4fs, 0.9 x 10^{16} W cm^{-2}

Autocorrelation
CAP Flux BO state 1
CAP Flux BO state 2
CAP Flux BO state 3
CAP Flux BO state 4

Internormalized

Photon energy (ha

H2 Dissociative flux

Curve 1
Curve 2
Curve 3
Curve 4
Curve 5
Curve 6

dF/dE

Photon energy (hartree)
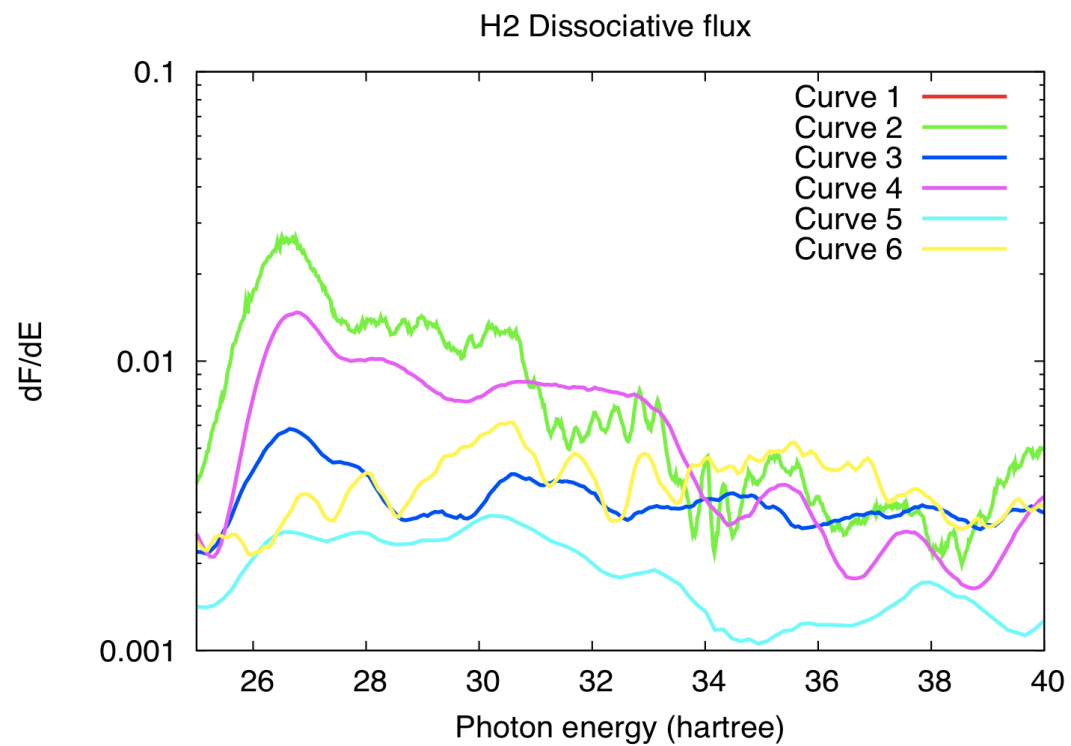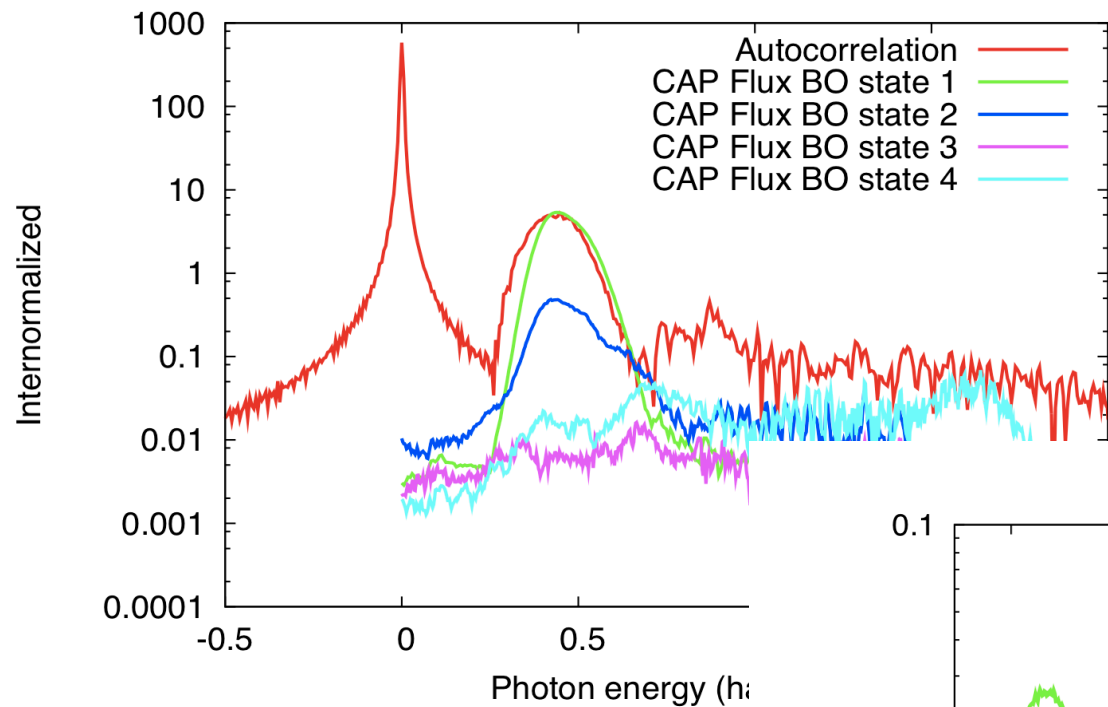
Where the project is going

TWO CHALLENGES to make the MCTDHF (MCTDH, MCTDHB, quantum dynamics in general) method scalable to large systems

1) Restricted configuration spaces – two methods
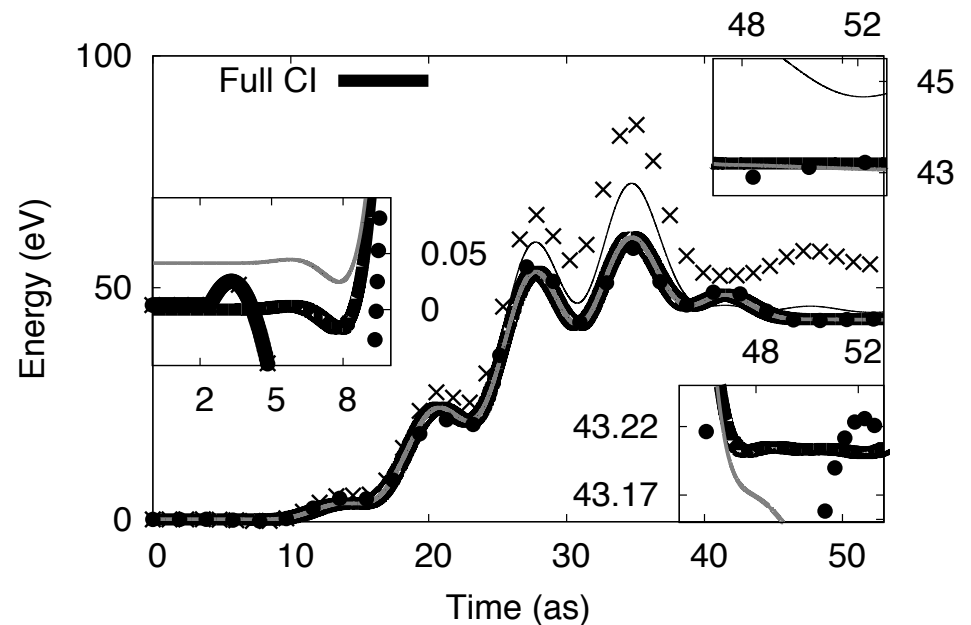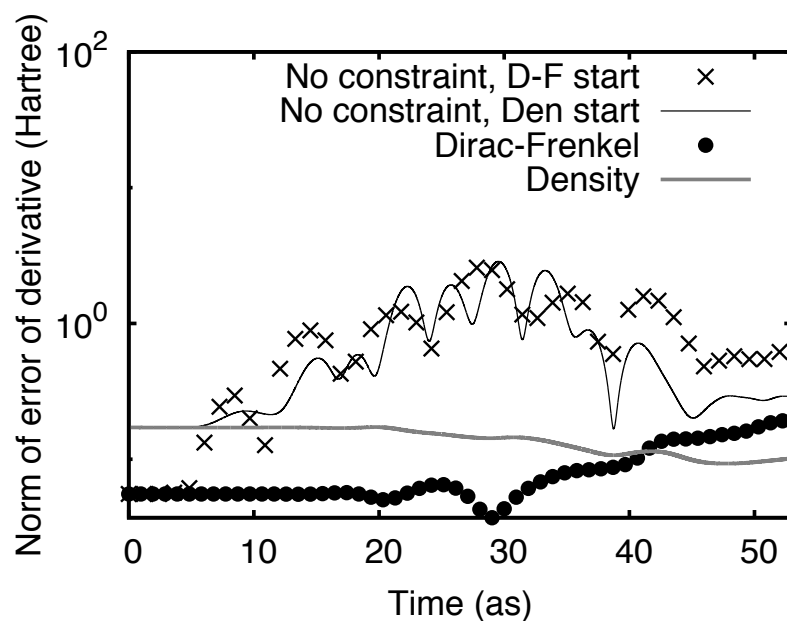
2) Mean field approximation to decouple orbitals from one another for short times (A WHALE)

RESTRICTED

Two methods for restricted configuration spaces within the multiconfiguration time-dependent Hartree-Fock method

Daniel J. Haxton[1] and C. William McCurdy[1,2]

[1]*Lawrence Berkeley National Laboratory, Chemical Sciences, Berkeley, California 94720, USA*
[2]*Department of Chemistry, University of California, Davis, California 95616, USA*

POLYATOMIC

Final goal: *Nonadiabatic Polyatomic with Ionization*

For Diatomics:
Improved nonadiabatic diatomic treatment.
New coordinate system.
Also add rotation

.

versus

R=2
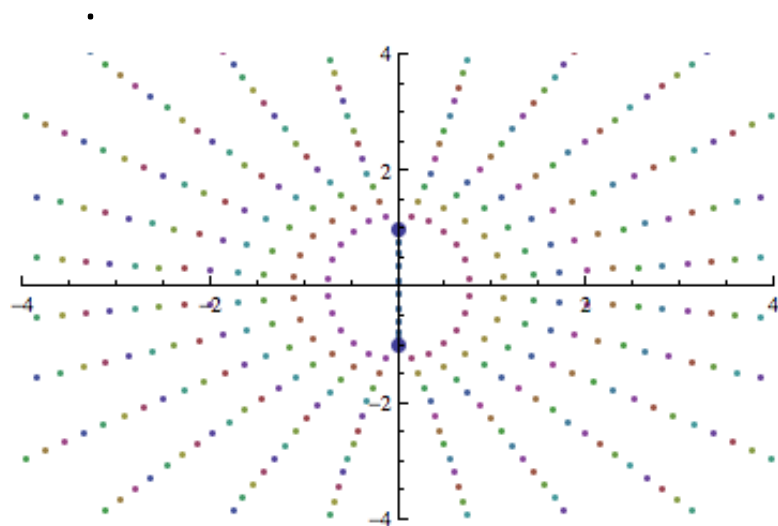
(schematic)
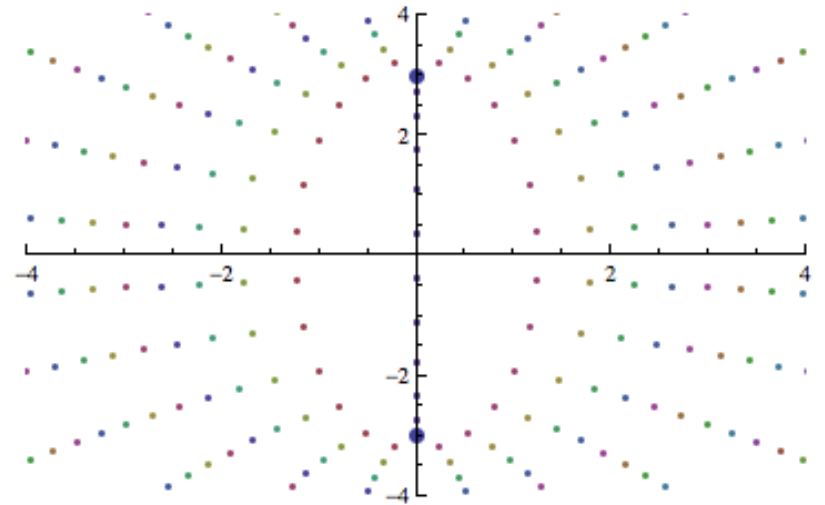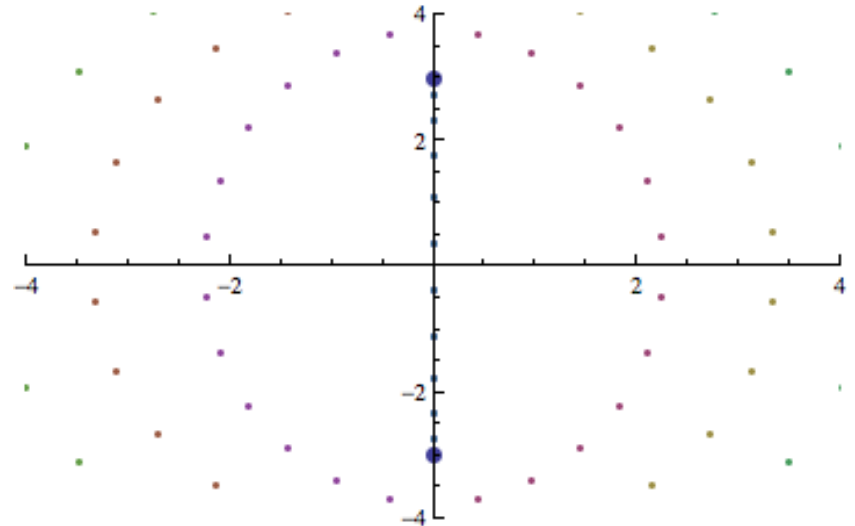
R=6

Polyatomic treatment with nonadiabatic nuclear motion.

Numerical technology: 3D Cartesian coordinate representation

V MATRIX – POTENTIAL ENERGY MATRIX, INCLUDING TWO ELECTRON OPERATOR -- IS DIAGONAL!!!
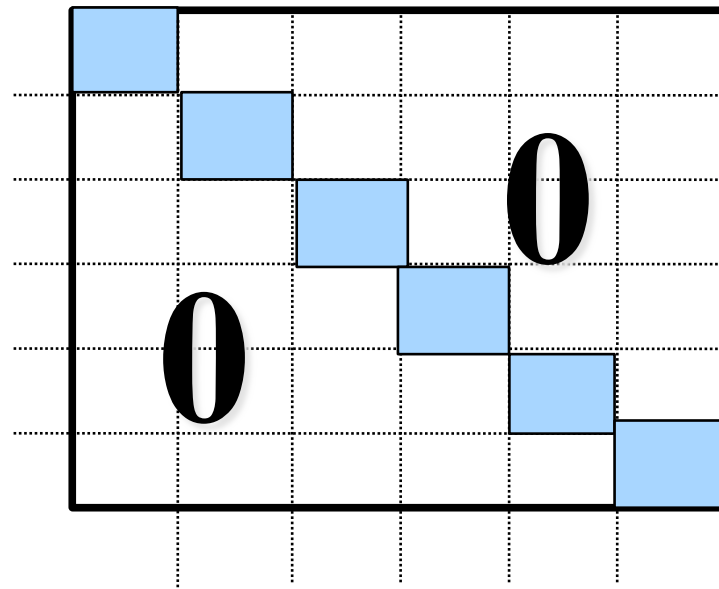
$$i \, d/dt \, \psi = (T + V) \, \psi$$

KINETIC ENERGY T IS ALSO EFFICIENT IN 3D

METHANE!

Looks like we need a grid with about 0.4 bohr spacing and a box about
24 bohr wide to get the lowest valence excitation energy about right

63 points on a side
~0.4 spacing
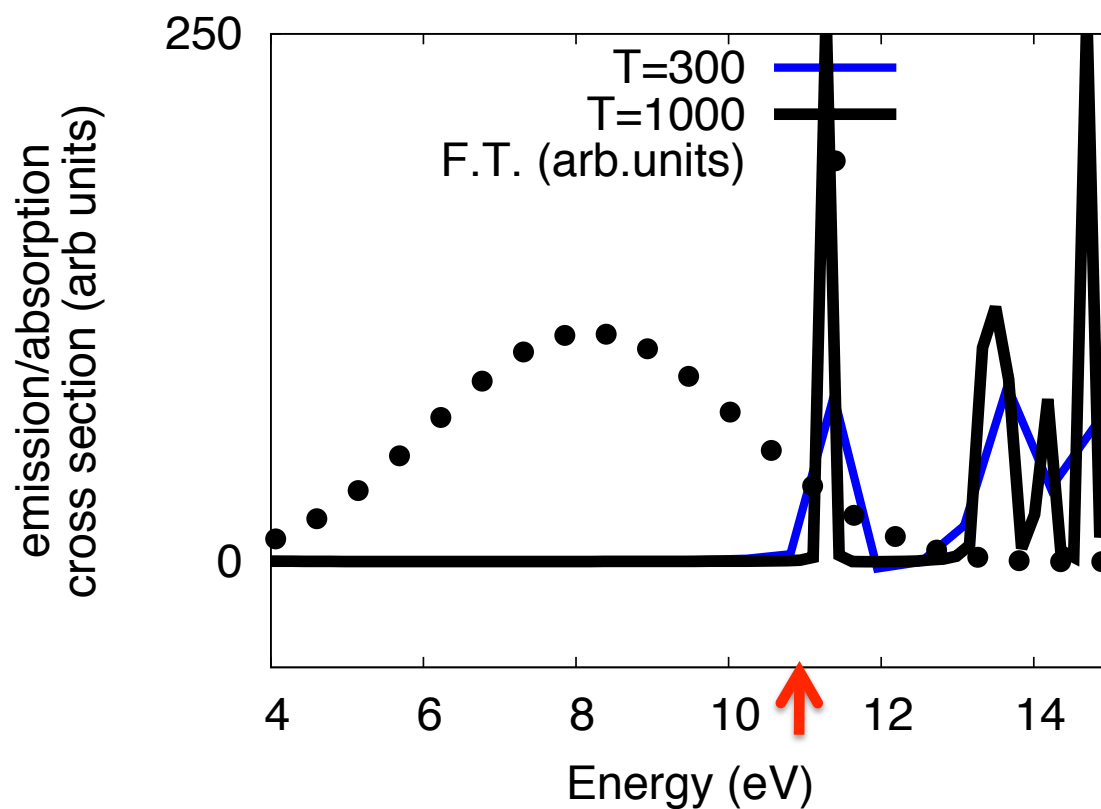
METHANE!

Looks like we need a grid with about 0.4 bohr spacing and a box about 24 bohr wide to get the lowest valence excitation energy about right

31 points on a side
~0.4 spacing
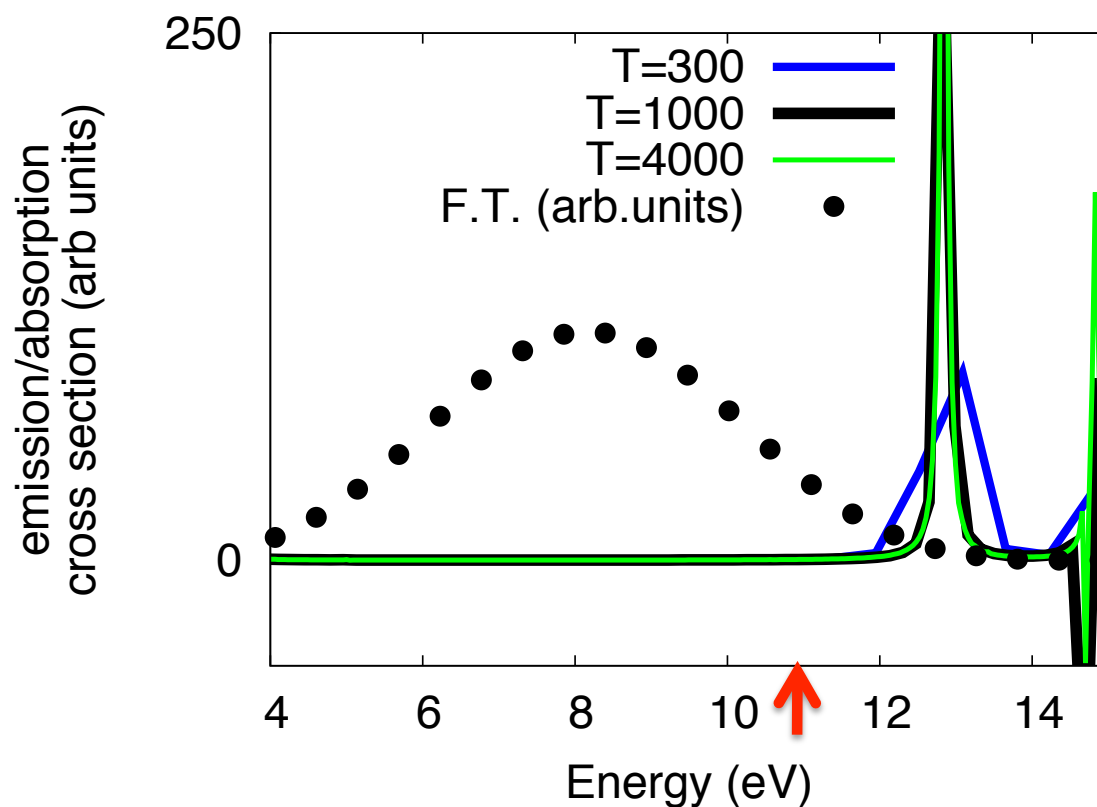
METHANE!

Looks like we need a grid with about 0.4 bohr spacing and a box about
24 bohr wide to get the lowest valence excitation energy about right

63 points on a side
~0.2 spacing
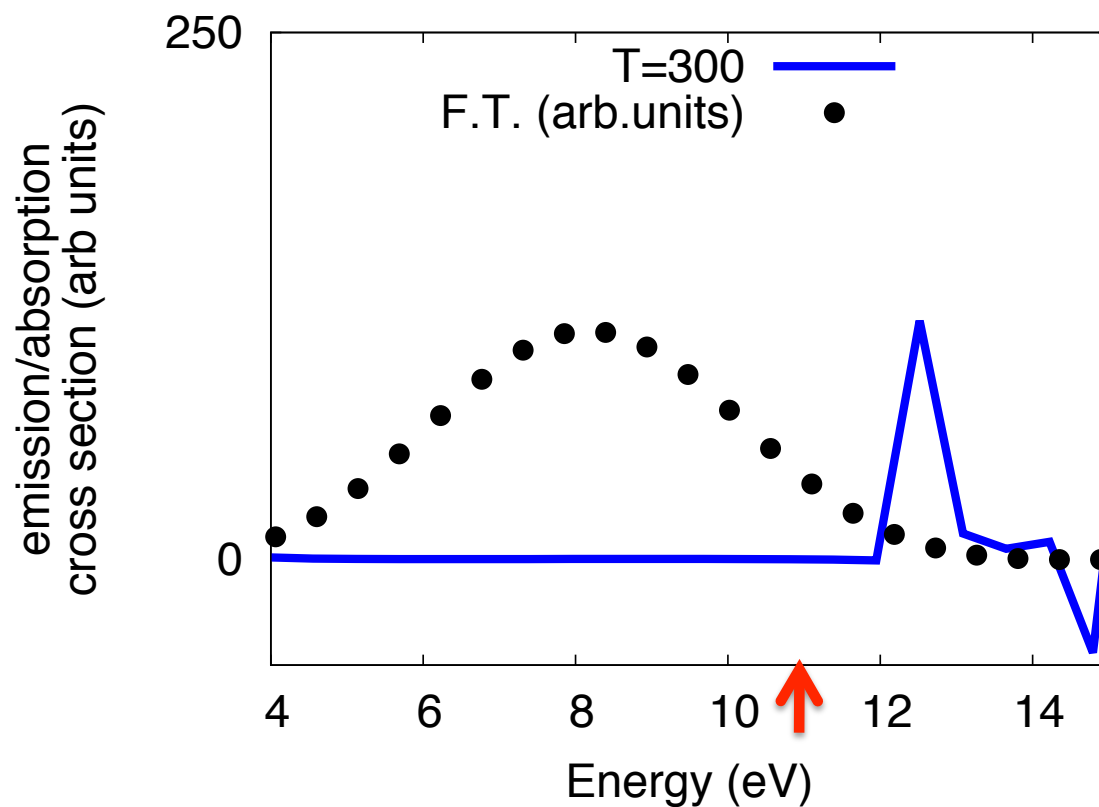
MPI scaling of methane calc
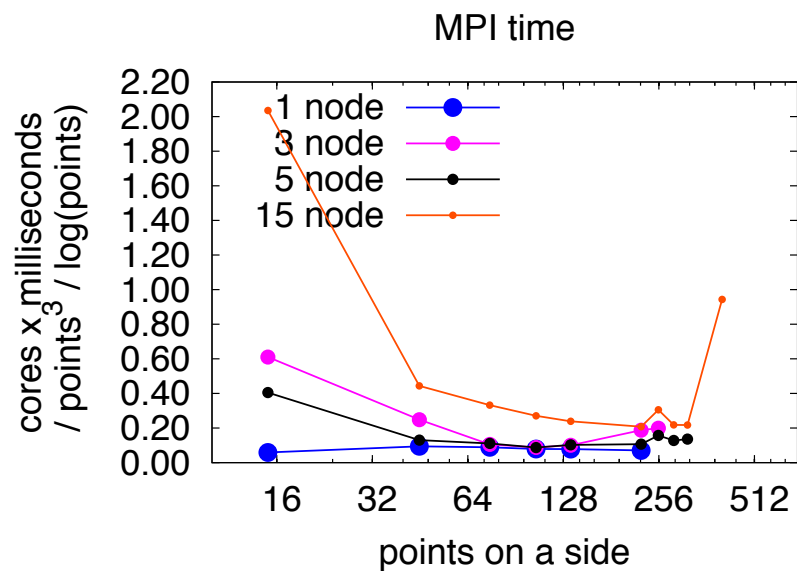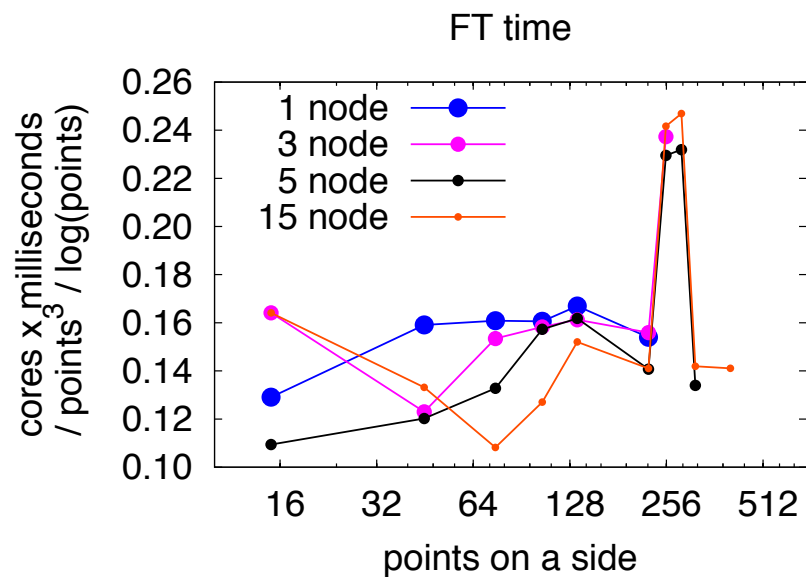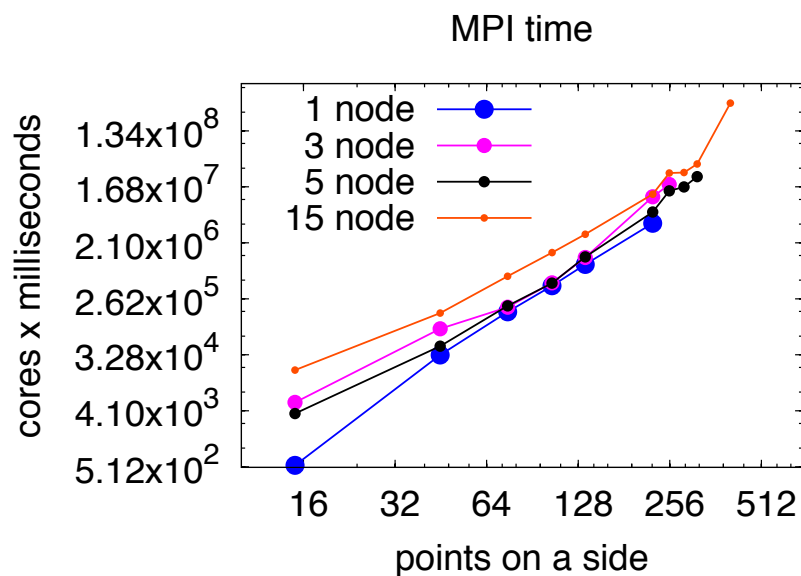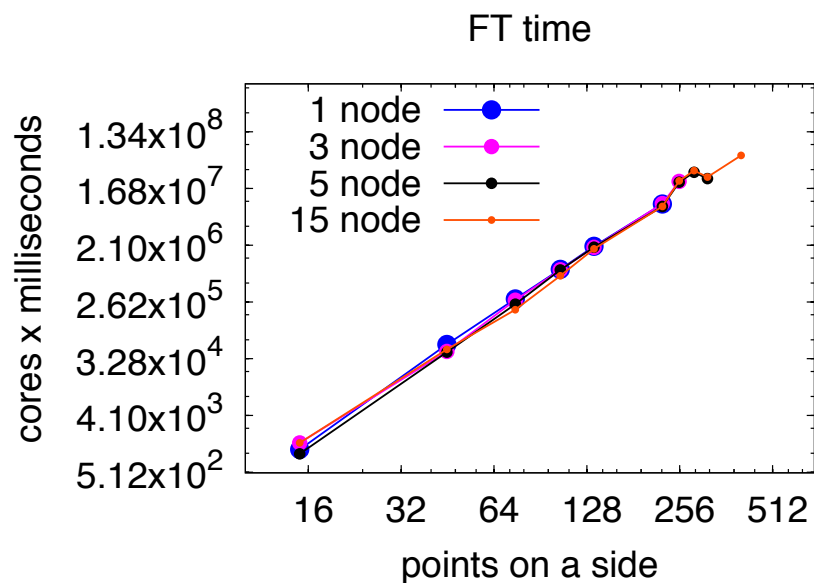
CUBANE

A Density Functional Theory and Electron Momentum Spectroscopy Study into the Complete Valence Electronic Structure of Cubane

W. Adcock,[†] **M. J. Brunger,**[*,‡] **I. E. McCarthy,**[†] **M. T. Michalewicz,**[§] **W. von Niessen,**[||] **F. Wang,**[⊥] **E. Weigold,**[#] **and D. A. Winkler**[§]

Low-energy electron scattering by cubane: Resonant states and Ramsauer−Townsend features from quantum calculations in the gas phase

F. A. Gianturco[a)]
Department of Chemistry and INFM, The University of Rome, La Sapienza, Piazzale A. Moro 5, 00185 Rome, Italy

R. R. Lucchese
Department of Chemistry, Texas A&M University, College Station, Texas 77843-3255

A. Grandi and N. Sanna
Supercomputing Center for University and Research, CASPUR, via de Tizii 6b, 00185 Rome, Italy

Table 2

Transition energy (eV), orbital character, one-photon oscillator strength, two-photon absorptivity and polarization ratios for the low-lying excited states of cubane

State	Dominant character	E	f	$W^{(2)}_{f\leftarrow 0}$ ᵃ	$\Omega^{(2)}_1$	$\Omega^{(2)}_2$
$^1T_{2g}$	$3t_{2g}\to 3s$	6.79		1.88×10^{-52}	3/2	4/3
$^1A_{2u}$	$3t_{2g}\to 3p$	6.95				
^1E_u		6.97				
$^1T_{1u}$		6.99	0.09120			
$^1T_{2u}$		7.54				
$^1T_{1g}$	$3t_{2g}\to 3d$	7.86				
$^1A_{1g}$		7.87		2.55×10^{-51}	7×10^{-5}	3×10^4
$^1T_{2g}$		7.99		3.22×10^{-53}	3/2	4/3
$^1T_{1g}$		8.04				
^1E_g		8.06		2.45×10^{-52}	3/2	4/3
$^1T_{2g}$		8.16		6.13×10^{-53}	3/2	4/3
$^1T_{2g}$	$3t_{2g}\to 4s$	7.91		2.57×10^{-52}	3/2	4/3
^1E_u	$3t_{2g}\to 4p$	7.96				
$^1T_{2u}$		8.00				
$^1T_{1u}$		8.10	0.00157			
$^1A_{2u}$		8.13				
$^1T_{1g}$	$3t_{2g}\to 4d$	8.50				
$^1A_{1g}$		8.51		6.28×10^{-52}	3×10^{-4}	6×10^3
$^1T_{2g}$		8.52		7.83×10^{-53}	3/2	4/3
^1E_g		8.54		1.19×10^{-52}	3/2	4/3
$^1T_{1g}$		8.57				
$^1T_{2g}$		8.60		8.98×10^{-55}	3/2	4/3
$^1T_{2g}$	$3t_{2g}\to 5s$	8.49		2.23×10^{-55}	3/2	4/3
$^1A_{1u}$	$3t_{2g}\to 4f$	8.58				
$^1A_{2u}$		8.58				
$^1T_{1u}$		8.58	0.00018			
$^1T_{1u}$		8.58	0.00303			
$^1T_{2u}$		8.58				
^1E_u		8.59				
^1E_u		8.59				
$^1T_{1u}$		8.59	0.00099			
$^1T_{2u}$		8.59				
$^1T_{2u}$	$1t_{2u}\to 3s$	6.92				
$^1T_{1g}$	$1t_{2u}\to 3p$	7.39				
$^1A_{2g}$		7.43				
^1E_g		7.49		5.70×10^{-53}	3/2	4/3
$^1T_{2g}$		7.56		3.06×10^{-52}	3/2	4/3
$^1T_{1u}$	$1t_{2u}\to 3d$	8.43	0.09123			
^1E_u		8.46				
$^1T_{1u}$		8.47	0.00018			
$^1T_{2u}$		8.49				
$^1A_{1u}$		8.52				
$^1T_{2u}$		8.54				
$^1T_{2u}$	$1t_{2u}\to 4s$	8.42				
$^1A_{2g}$	$1t_{2u}\to 4p$	8.42				
$^1T_{1g}$		8.47				
^1E_g		8.67				
$^1T_{2g}$		8.72		1.88×10^{-53}	3/2	4/3
$^1T_{1u}$	$1t_{2u}\to 4d$	9.05	0.02572			
^1E_u		9.07				
$^1T_{1u}$		9.08	0.00270			
$^1T_{2u}$		9.08				
$^1A_{1u}$		9.11				

A *CONTINUUM* of electronic and nuclear motion awaits starting just above 6eV!

What is its structure?

In terms of reduced density operators for electrons and nuclei, natural configurations for instance

Galasso,
Chem. Phys.
184, 107 (1994)
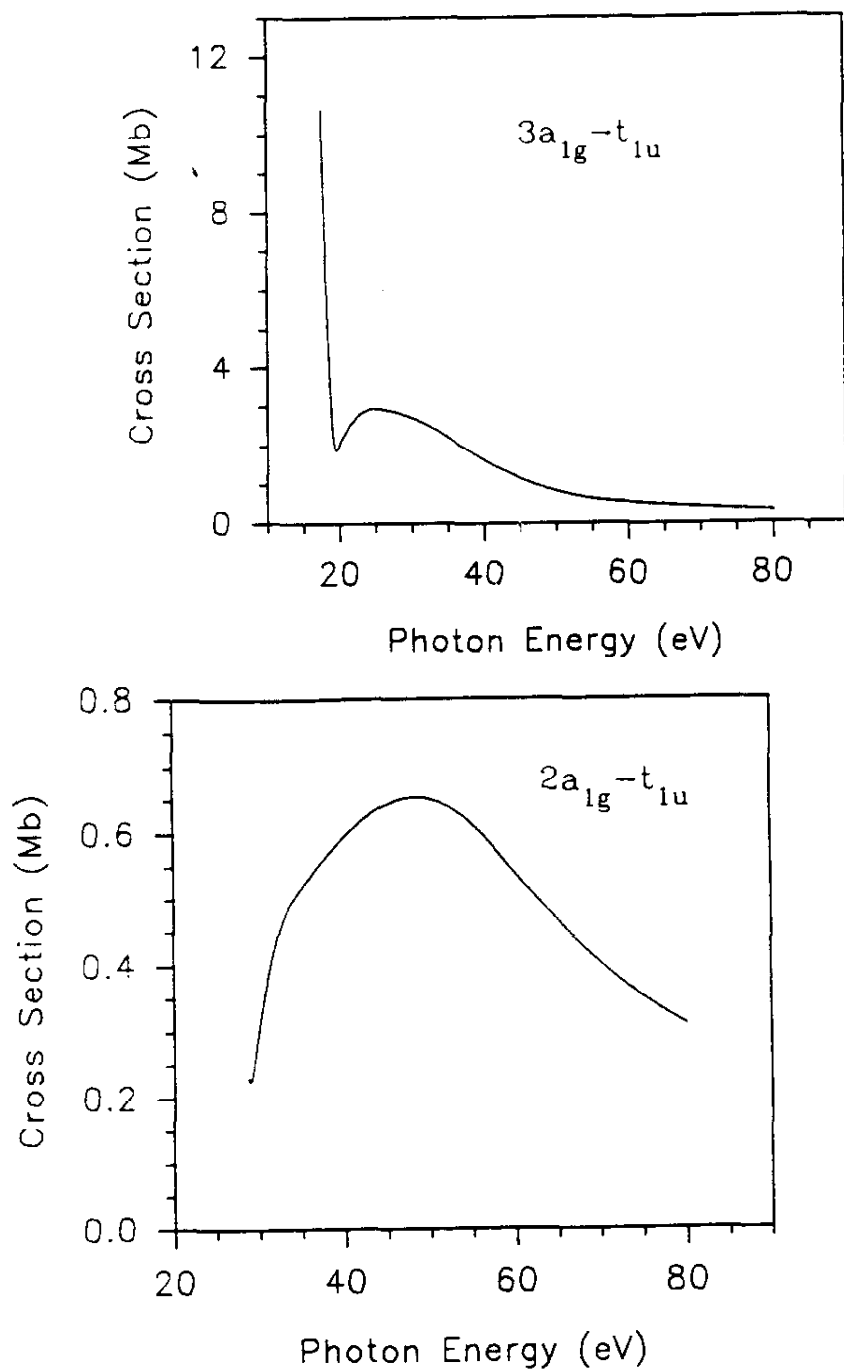
Fig. 1. Calculated cross section profiles relative to the $2a_{1g}$, $3a_{1g}$ and $2a_{2u}$ ionizations of cubane.

Calculations of giant resonances and cross section profiles of valence ionizations of cubane by the LCAO Density Functional Stieltjes Imaging approach.

M. Stener, P. Decleva, A. Lisini.
J Mol Struct (Theochem) 357, 125 (1995)

C_8H_8, Si_8H_8, and Ge_8H_8 Molecules
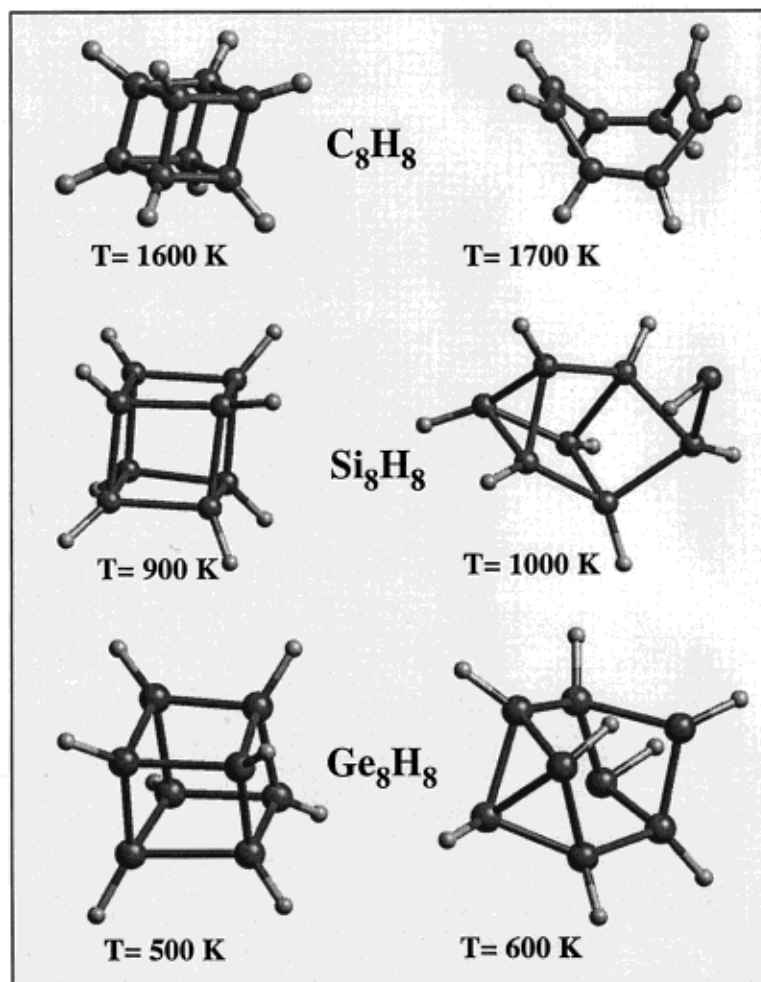
A First-Principles Study of the Structure and Dynamics of C8H8, Si8H8, and Ge8H8 Molecules

C. Kilic, T. Yildirim, H. Mehrez, S. Ciraci

Figure 4. High-temperature structures of the X_8H_8 molecules calculated by quantum molecular dynamics with a plane-wave basis set. The first column shows the structures before transformation, while the second column illustrates how the structure is transformed after a 1 ps relaxation of the original molecule at the given temperature.

Theoretical Studies of the Cubane Molecule

Jerome M. Schulman,*[1a] C. Rutherford Fischer,[1b] Paul Solomon,[1a] and Thomas J. Venanzi[1c]

Abstract: Molecular orbital calculations were performed on cubane using ab initio STO-3G, SCF-Xα, MINDO/3, and INDO methods. The photoelectron ionization energies were calculated from the above by Koopmans' theorem and, in addition, by Slater's transition-state approximation in the SCF-Xα method. An analysis of the molecular orbital energy splitting pattern has been made utilizing the concept of interactions between symmetry-adapted combinations of localized CC and CH orbitals.
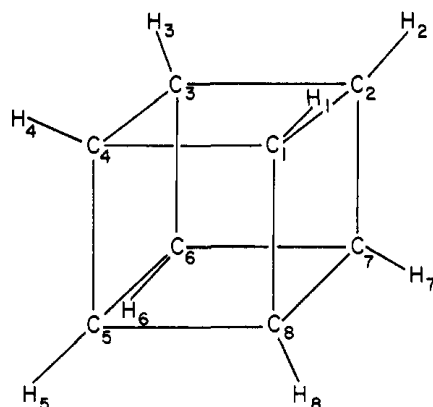
Figure 1. The cubane molecule including the atomic numbering system used here.

Table I. Valence Orbital Energies of Cubane Calculated by Several Methods[a]

| Orbital | Negative orbital energy, au | | | |
	STO-3G	SCF-Xα	MINDO/3	INDO
$1a_{1g}$	1.219	0.835	1.709	2.489
$1t_{1u}$	0.947	0.646	1.055	1.467
$1t_{2g}$	0.739	0.522	0.735	0.990
$2a_{1g}$	0.693	0.505	0.641	1.076
$1a_{2u}$	0.617	0.443	0.584	0.769
$2t_{1u}$	0.555	0.378	0.487	0.728
$1e_g$	0.548	0.361	0.528	0.952
$1t_{2u}$	0.350	0.211	0.349	0.494
$2t_{2g}$	0.344	0.188	0.338	0.393

[a] Bond lengths of R_{CC} = 1.55 Å, R_{CH} = 1.06 Å were employed except in the MINDO/3 calculation where the geometry was optimized to R_{CC} = 1.568 Å, R_{CH} = 1.106 Å.

Table II. Ionization Energies of Cubane (eV)[a]

Symmetry of ionized state	STO-3G eq 1	SCF-Xα transition-state method
$^2T_{2g}$	10.2	10.2
$^2T_{2u}$	10.4	10.8
^2E_g	14.5	14.9
$^2T_{1u}$	14.6	15.4
$^2A_{2u}$	15.9	16.5
$^2A_{1g}$	17.5	18.5
$^2T_{2g}$	18.4	19.9
$^2T_{1u}$	22.8	22.7
$^2A_{1g}$	28.4	28.0

[a] Reference 9 gives observed ionization energies (eV) at 8.74, 13.62, 15.34, 16.87, and 17.26.

interatomic, and outer-sphere regions, and (4) the angular momentum *l* values to be used in the inner- and outer-sphere regions.

For the atomic spheres we employed the criterion of Norman[11] that each hydrogen and carbon sphere contain one and six electrons, respectively, when the atomic charge densities were superposed, giving r_C/r_H = 1.426. The extent of sphere overlap was determined by Norman's condition[11] that the virial theorem be satisfied, which furnished r_C = 1.74 Å (and r_H = 1.22 Å). Overlap of the carbon spheres was 19− of the CC bond length and the carbon-hydrogen sphere overlap was somewhat greater. The outer sphere was made tangent to the hydrogen spheres. Values of α_C = 0.759 28 and α_H = 0.777 25 were taken from the work of Schwarz[12] and Rosch et al.,[13] while for the intersphere and outer-sphere regions a weighted average, α = 0.761 85, was employed. Finally, as to the choice

Figure 5. Schematic diagrammatic representation of the cubane orbital energies. On the left, 12 degenerate CC LMOs interact to form five CC energy levels of a_{1g}, t_{1u}, e_g, t_{2g}, and t_{2u} symmetries; on the right, eight degenerate CH LMOs interact to form four CH energy levels of a_{1g}, t_{1u}, t_{2g}, and a_{2u} symmetry. In the center the cubane molecular orbital levels are shown. Six are formed from interactions between CC and CH orbitals of like symmetry (a_{1g}, t_{1u}, and t_{2g}); the e_g(CC), t_{2u}(CC) and a_{2u}(CH) are symmetry determined. The location of the 12 CC LMO's relative to the 8 CH LMO's is not known with certainty.

Calculations of giant resonances and cross section profiles of valence ionizations of cubane by the LCAO Density Functional Stieltjes Imaging approach

M. Stener*, P. Decleva, A. Lisini

Dipartimento di Scienze Chimiche, Università di Trieste, Via Giorgieri 1, I-34127, Italy

Received 3 February 1995; accepted 11 April 1995

Abstract

Valence partial channel photoionization cross sections for each final symmetry of cubane have been evaluated at the local density level. The muffin-tin potential approximation is avoided by the use of large basis set LCAO calculations and the Stieltjes Imaging approach. The "giant resonances" which are expected from symmetry considerations have only actually been determined for outer valence ionizations, while they are not present in the inner valence. Minimal basis set calculations have been successfully used throughout the discussion in order to assess the position and the intensity of the transitions to virtual valence orbitals. Eventually, we analyze the total cross sections for each final state and their ratios, which might be compared with further experimental data that are not yet available. The previous partial final symmetry analysis allows the assignment of the features which could be experimentally observable,

Figure 1 shows the photoelectron spectrum of cubane, as obtained with either He(Ia) or He(IIa) radiation. The positions of the band maxima (I_j^m) are collected in *Table 1* and for comparison the ionization energies measured by *Dewar & Worley* [2] who have used a cylindrical grid spectrometer. Due to the unavoidable short-comings of these early instruments only the onset of each multiple band could be obtained. If this limitation is taken into account, the agreement of these early data with the ones presented in this work is remarkably good, as can be seen by referring to the band shapes displayed in *Figure 1*.

The He(Ia) photoelectron spectrum of cubane has been recorded both in Basel and in Darmstadt using samples from two independent sources [1] [3]. The ranges quoted in *Table 1* for the I_j^m values give an idea of the closeness of the two determinations. Recently, the photoelectron spectrum of cubane has also been recorded by *Schmidt* [4] whose results are in complete agreement with those presented here.
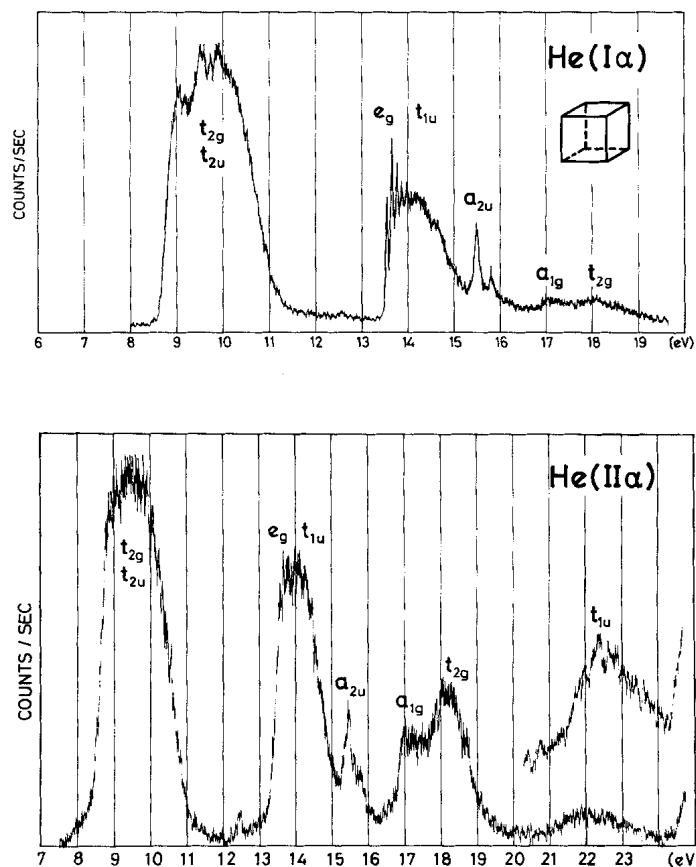
Fig. 1. *Photoelectron spectrum of cubane*

44. The Electronic Structure of Cubane as Revealed by Photoelectron Spectroscopy

P Bischof, P E Eaton, R Gleiter, E Heilbronner, T B Jones, H Musso, A Schmelzer, R Stobei

a

Cubane, $\phi = 0°$

(——) Envelope of all fitted components

b

Cubane, $\phi = 10°$

(——) Envelope of all fitted components
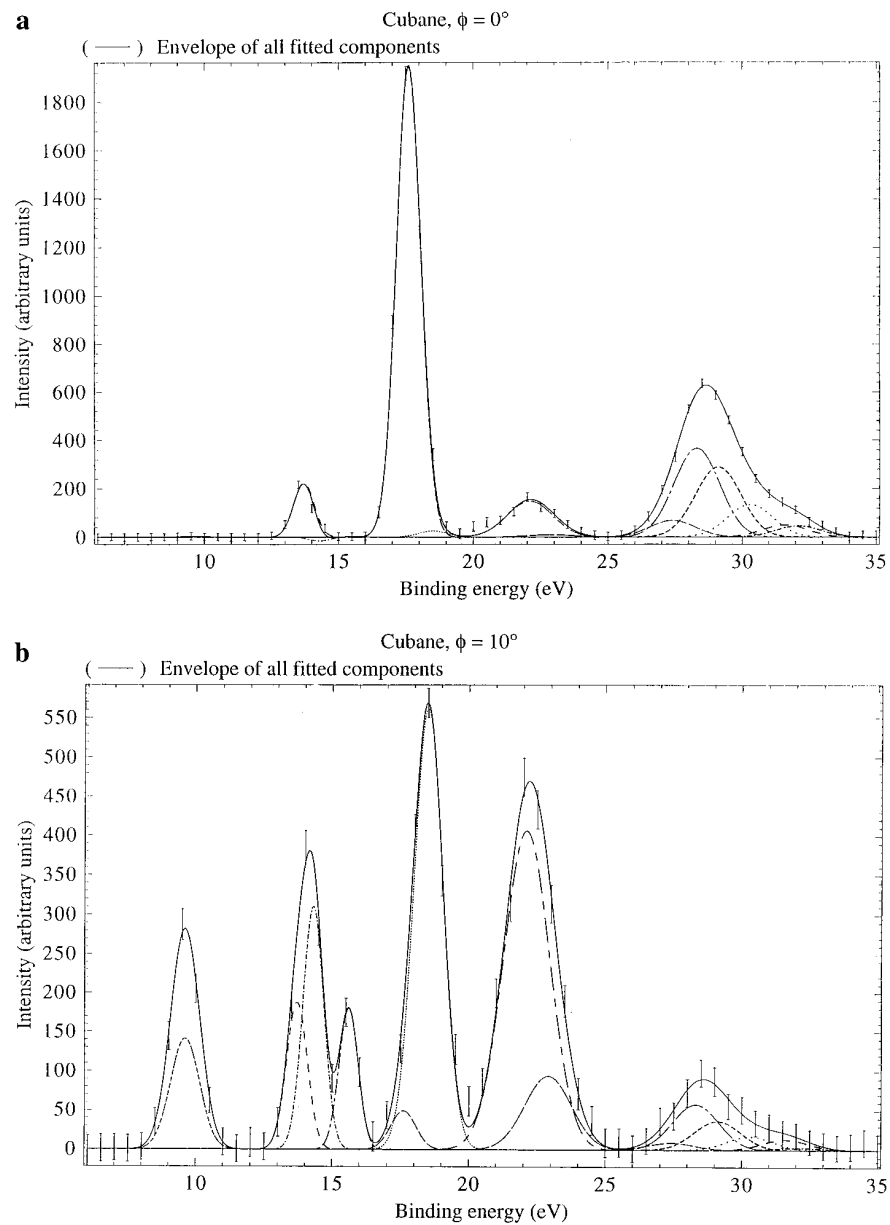
Figure 1. Typical binding-energy spectra from our 1000 eV noncoplanar symmetric EMS investigation into cubane. The curves show the fits to the spectra at (a) $\phi = 0°$ ($p \sim 0.09$ au) and (b) $\phi = 10°$ ($p \sim 0.75$ au) using the known energy resolution.

Atomic, Molecular, and Optical theory group LBNL

Bill (C. William) McCurdy

Xuan Li

Tom Resicgno

Chen Zhang
MCTDHF

Cynthia Trevisan
(Cal Maritime)
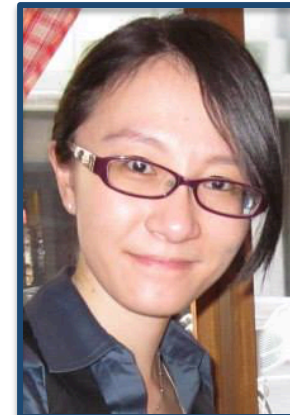
Frank Yip (")

Zach Walters

Ann Orel (UC Davis)

Brant Abeln

BERKELEY LAB
LAWRENCE BERKELEY NATIONAL LABORATORY

uxsl
ultrafast x-ray science laboratory

Triple Toeplitz Matvec

...it's a drink; what's in it?

it requires a processing step, just mixing perhaps, which will be called the "Fourier Transform" or maybe "Fourier Transfoam" or something
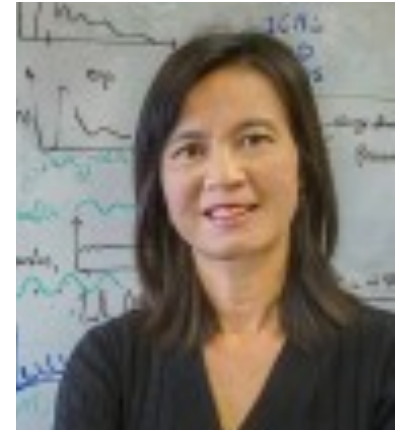
Sam Willams, Sherry (Xiaoye) Li,
Khaled Ibrahim,
Computer Science Division LBL
(DOE SCIDAC COLLABORATION)

Thorsten Kurth,
Nuclear Science Division LBL

Brant
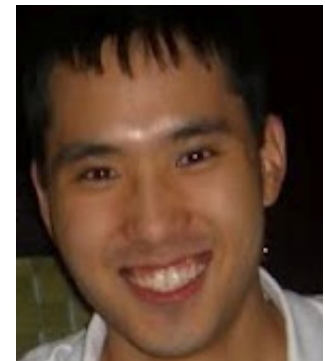
"Polynomial multiplication is local in Fourier space"

FIN. EXTRA:

SURFACES

The idea:

Calculate accurate ultrafast quantum dynamics of metal-adsorbate systems,
    focusing on the pump-probe framework.

IR, UV/Vis, X-ray pump; X-ray probe.
                                Electronic excitation followed by e/n dynamics.

The motivation:

1) A new direction for theory at the UXSL, parallel with its mission;
    a compass for future experimental work here

2) Much existing experimental work on surfaces, but ultrafast studies just
    beginning; great opportunity to improve understanding of interesting
    fundamental processes for both theory and experiment

3) Method development. Wide-ranging applicability. Distribute code to community.

.... The exact topic of a recent seminar at the UXSL!

Anders Nilsson, SLAC   5/5/11

"Probing the reactive state in catalysis"

"...I will show recent experiments using LCLS to probe the ***laser induced desorption*** of CO on Ru(0001) with 200 femtosecond resolution....

... we observe considerable dynamics in the relevant occupied and unoccupied pi-states and in the occupied sigma-states of CO."

What happens at the molecule-metal interface?

Fermi sea electrons undergo bonding with molecule

The electronic and vibrational structure of the molecule is affected
→ K-edge; transition energies; Auger branching ratios

Bonding interaction leads to orientation on the surface

In many cases the bonding is understood as charge transfer: the anion is then bound by its image charge

What happens at the molecule-metal interface?

Fermi sea electrons undergo bonding with molecule

The electronic and vibrational structure of the molecule is affected
→ K-edge; transition energies; Auger branching ratios

Bonding interaction leads to orientation on the surface

In many cases the bonding is understood as charge transfer: the anion is then bound by its image charge
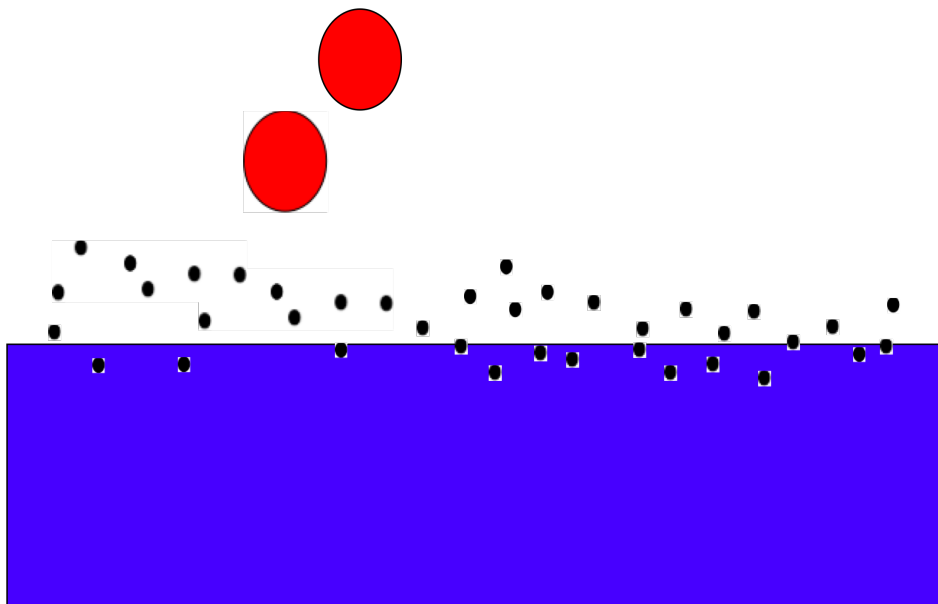
What happens at the molecule-metal interface?

Fermi sea electrons undergo bonding with molecule

The electronic and vibrational structure of the molecule is affected
→ K-edge; transition energies; Auger branching ratios

Bonding interaction leads to orientation on the surface

In many cases the bonding is understood as charge transfer: the anion is then bound by its image charge

The phenomena of DIET and DIMET

Desorption Induced by (Multiple) Electronic Transitions
Review: P. Saalfrank, Chem Rev 106, 4116 (2006)

UV/Vis femtosecond lasers promote DIMET, observed via nonlinear intensity dependence.

These figures* depict atom-surface Born-Op. potentials.

z
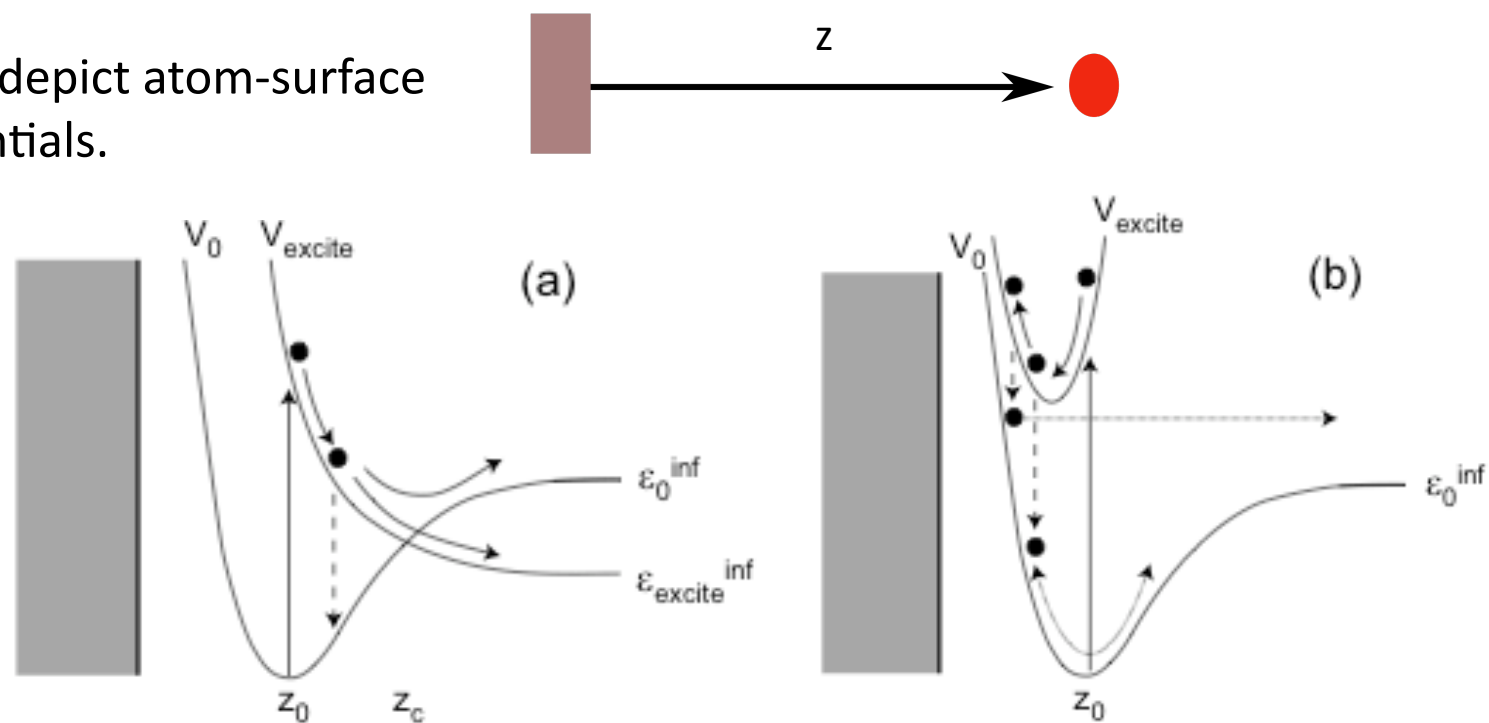
*JW Gadzuk, Laser Spectroscopy and Photochemistry on Metal Surfaces

Work in Kapteyn/Murnane group (JILA, CU-Boulder):

Ultrafast studies similar to what we would model. High harmonic setup.

→ Dissociation of O_2 on Pt: monitor photoelectron spectrum. 500fs timescale.

"Direct observation of surface chemistry using ultrafast soft-X-ray pulses"
M. Bauer, H.C. Kapteyn et al., **PRL** 87, 025501 (2001)

→ Other work on O_2 and CO: monitor electronic (O_2) and vibrational (CO) degrees of freedom.

E.g. M. Bauer, C. Lei, R. Tobey, M.M. Murnane,
H. Kapteyn, Surface Science 532-535 (2003) 1159
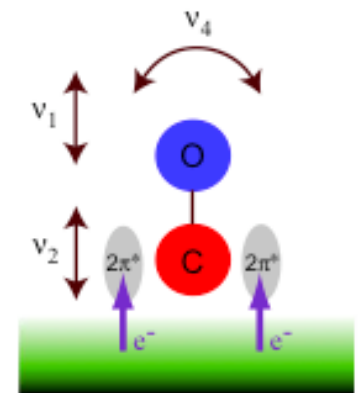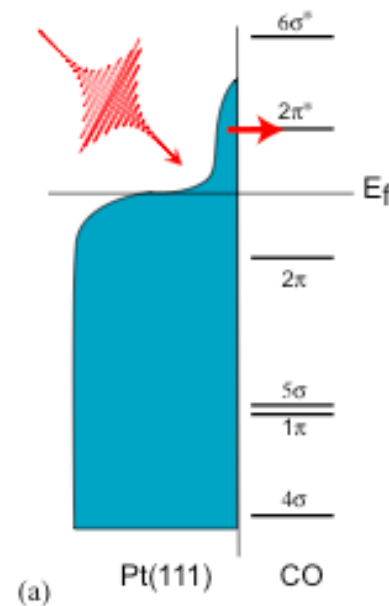
Figure credit C-F Lei
(thesis CU-Boulder)

Work in Kapteyn/Murnane group (JILA, CU-Boulder):

Direct Measurement of Core-Level Relaxation Dynamics on a Surface-Adsorbate System

L. Miaja-Avila,[1,*] G. Saathoff,[1,4] S. Mathias,[2] J. Yin,[1] C. La-o-vorakiat,[1] M. Bauer,[3] M. Aeschlimann,[2] M. M. Murnane,[1] and H. C. Kapteyn[1]

[1]*JILA, University of Colorado and National Institute of Standards and Technology, and Department of Physics, University of Colorado, Boulder, Colorado 80309-0440, USA*
[2]*Department of Physics, University of Kaiserslautern, 67663 Kaiserslautern, Germany*
[3]*Institut für Experimentelle und Angewandte Physik, Christian-Albrechts-Universität zu Kiel, 24908 Kiel, Germany*
[4]*Max-Planck-Institute of Quantum Optics, Hans-Kopfermann-Straße 1, 85748 Garching, Germany*
(Received 28 March 2008; published 21 July 2008)

The coupling between electronic states in a surface-adsorbate system is fundamental to the understanding of many surface interactions. In this Letter, we present the first direct time-resolved observations of the lifetime of core-excited states of an atom adsorbed onto a surface. By comparing laser-assisted photoemission from a substrate with a delayed Auger decay process from an adsorbate, we measure the lifetime of the $4d^{-1}$ core level of xenon on Pt(111) to be 7.1 ± 1.1 fs. This result opens up time-domain measurements of surface dynamics where energy-resolved measurements may provide incomplete information.

A good experimental result to work with – verify that we can reproduce this lifetime.

"Core Hole Clock" method pioneered by W. Wurth, D. Menzel et al.

(Universitat Hamburg & Technische Universitat Munchen, Germany)

A popular technique to measure *charge transfer times* for adsorbed core hole states.

Not "time resolved" in the usual sense: Charge transfer times determined in proportion to the already-determined Auger lifetime.

A long list of experimental results on charge transfer times:

Sulfer on Ru(0001) CPL 434, 214 (2007), Nature 436, 373 (2005)
Argon on Copper   CPL 427, 91 (2006)
Argon on Ru(0001) J Elec Spec 93, 135 (1998)
CO on Ru(0001)   PRL 80, 1774 (1998)

etc. represent more experimental results helpful for initial studies.

Experiments by D.J. Auerbach, A.M. Wodtke & collaborators
(IBM & UCSB respectively)

"Conversion of large-amplitude vibration to electron excitation at a metal surface"

J.D. White, A.M. Wodtke et al., **Nature** 433, 503 (2005)

Vibrationally hot NO quenched on Cs/Au surface through nonadiabatic mechanisms.

"… [We] unambiguously demonstrate the direct conversion of vibrational to electronic excitation*, thus questioning one of the basic assumptions currently used in theoretical approaches to describing bond dissociation at metal surfaces*"

"Vibrational promotion of electron transfer"

Y. Huang, C.T. Rettner, D.J. Auerbach, A.M. Wodtke, **Science** 290, 111 (2000)

Demonstrated effect of charge transfer on NO/Au scattering.

"The signature of the electron transfer process is *a highly efficient multiquantum vibrational relaxation event*."

Vibrational relaxation / electronic friction :

a highly nonadiabatic process, *so fundamental*, but difficult to calculate!

Here is a story:

"Chemically accurate simulation of a prototypical surface reaction:
   H_2 dissociation on Cu(111)" G.-J. Kroes, D. Auerbach et al. **Science** 326, 832 (2009)

   used a (substantially tweaked) Born-Oppenheimer surface to obtain good results.
   The same potential was used in

"Apparent failure of the Born-Oppenheimer static surface model for vibrational
excitation of molecular hydrogen on copper"
   G.-J. Kroes, D. Auerbach et al. **PNAS** 107, 20881 (2010)

   and the results for vibrational excitation were off by a factor of 3.

Why our MCTDHF algorithm has a chance at a good general treatment

$$|\Psi(t)\rangle = \sum_{\kappa a} A_{\kappa a}(t)\, |\vec{n}_a(t)\rangle \chi_\kappa(R)$$

Wavefunction is sum of Slater determinants for electrons times DVR functions χ for nuclear

$$|\vec{n}_a(t)\rangle = \mathscr{A}\left(|\phi_{n_{a1}}(t)\rangle \times ...|\phi_{n_{aN}}(t)\rangle\right)$$

Slater dets are made of orbitals,

$$\langle \vec{x}|\phi_i(t)\rangle = \phi_i(x, y, z, t; R)$$

The orbitals being functions of all three spatial dimensions and time.

Why our MCTDHF algorithm has a chance at a good general treatment

$$|\Psi(t)\rangle = \sum_{\kappa a} A_{\kappa a}(t) \, |\vec{n}_a(t)\rangle \chi_\kappa(R)$$

Wavefunction is sum of Slater determinants for electrons times DVR functions χ for nuclear

$$|\vec{n}_a(t)\rangle = \mathscr{A}\left(|\phi_{n_{a1}}(t)\rangle \times ...|\phi_{n_{aN}}(t)\rangle\right)$$

Slater dets are made of orbitals,

$$\langle\vec{x}|\phi_i(t)\rangle = \phi_i(x, y, z, t; R)$$

The orbitals being functions of all three spatial dimensions and time.

The implementation is already parallelized over nuclear degree of freedom.
We may include surface/torsion DOFs easily.

Why our MCTDHF algorithm has a chance at a good general treatment

$$|\Psi(t)\rangle = \sum_{\kappa a} A_{\kappa a}(t) \, |\vec{n}_a(t)\rangle \chi_\kappa(R)$$

Wavefunction is sum of Slater determinants for electrons times DVR functions χ for nuclear

$$|\vec{n}_a(t)\rangle = \mathscr{A}\left(|\phi_{n_{a1}}(t)\rangle \times ... |\phi_{n_{aN}}(t)\rangle\right)$$

Slater dets are made of orbitals,

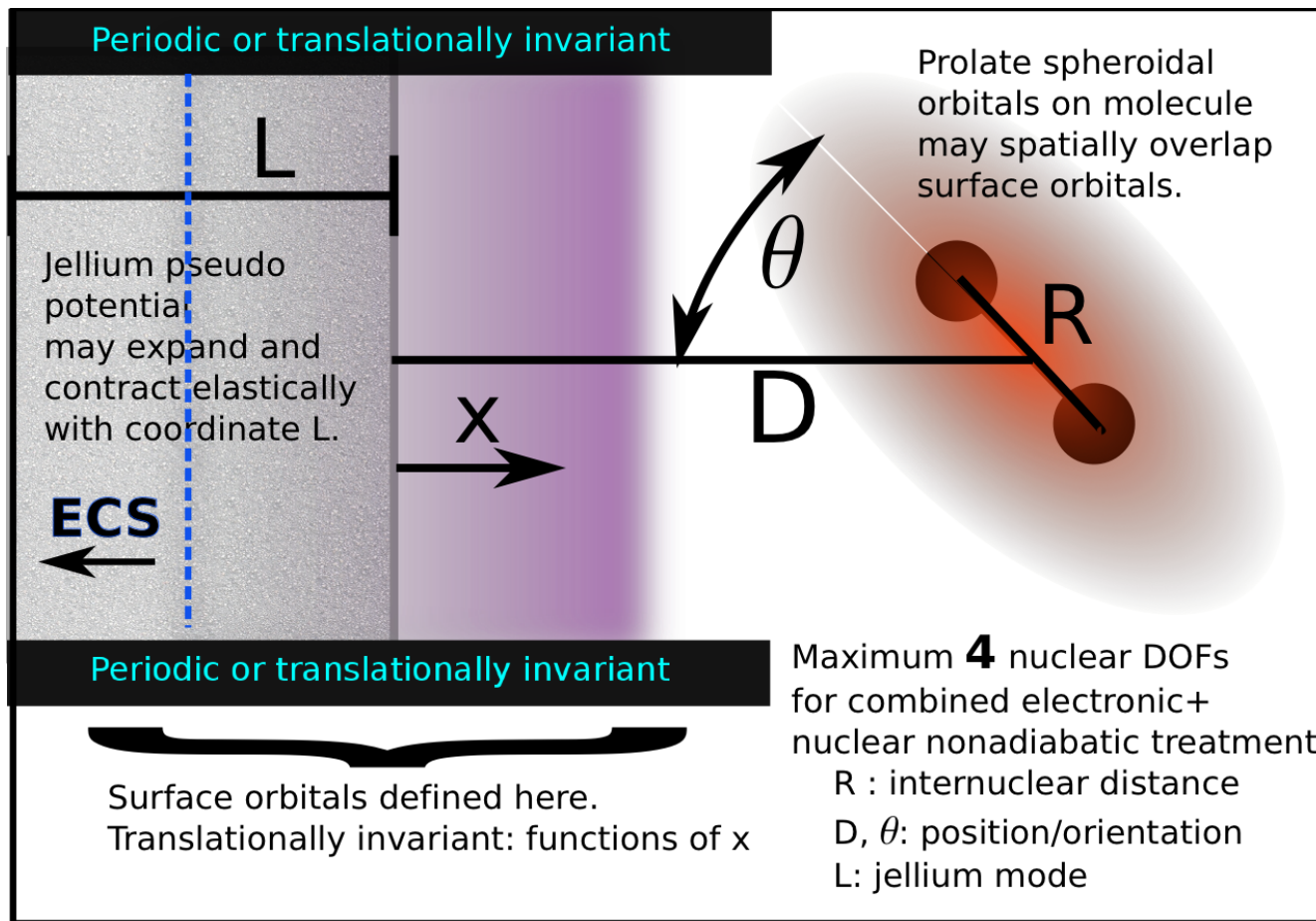$$\langle\vec{x}|\phi_i(t)\rangle = \phi_i(x, y, z, t; R)$$

The orbitals being functions of all three spatial dimensions and time.

Propagating the orbitals is the hard part. Nonlinear differential equation in 3D!
Our numerical implementation has proven its mettle; continuing to improve.
The surface orbitals should not particularly complicate this aspect.

Periodic or translationally invariant

Prolate spheroidal orbitals on molecule may spatially overlap surface orbitals.

L

Jellium pseudo potential may expand and contract elastically with coordinate L.

ECS

θ

R

D

X

Periodic or translationally invariant

Maximum **4** nuclear DOFs for combined electronic+ nuclear nonadiabatic treatment

R : internuclear distance

D, θ: position/orientation

L: jellium mode

Surface orbitals defined here.
Translationally invariant: functions of x

$$H(L, D, \theta, R, \vec{x}) \approx T + \frac{k}{2}(L - L_0)^2 + \frac{Z_1 Z_2}{R}$$

$$+ \sum_{i,a=1,2} \frac{-Z_a}{r_{ia}} + \sum_{i\langle j} \left[\frac{1}{r_{ij}} + H^{int}_{jellium}(x_i, x_j; L, D?, \theta?, E?) \right]$$

Photoionization

Apply few cycle perturbative pulse. (e.g. 0.5fs, 10^{13} W/cm^2)

Analyze wave function after pulse (50fs):

$$\hat{F} = i[\hat{H}, \Theta]$$

Use a Fourier transform with flux operator
Also can project onto final cation states

Formally: flux operator F; Θ is 1 in ionization region, 0 elsewhere
→ math →

Antihermitian part of
ECS hamiltonian

$$f(E) = \int_0^\infty dt \int_0^\infty dt'\, e^{iE(t-t')} \left\langle \Psi(t') \left| i(\hat{H} - \hat{H}^\dagger) \right| \Psi(t) \right\rangle$$

Formalism of Heidelberg group (they use complex absorbing potentials, inappropriate for electrons)

Photoionization

Need matrix elements between nonorthogonal slater determinants at t, t'

$$f(E) = \int_0^\infty dt \int_0^\infty dt' \, e^{iE(t-t')} \left\langle \Psi(t') \left| i(\hat{H} - \hat{H}^\dagger) \right| \Psi(t) \right\rangle$$

Overlap and Hamiltonian matrix elements are FULL. Intractable.
Solution: transform orbitals $\phi_\alpha(t), \phi_\alpha(t')$ to biorthogonal basis

$$<\phi_\alpha(t)|\phi_\beta(t')> = s_{\alpha\beta} \qquad \varphi(t') = s^{-1}\phi(t') \qquad <\phi_\alpha(t)|\varphi_\beta(t')> = \delta_{\alpha\beta}$$

Must transform A-vector at time t' to leave wave fn unchanged

$$\Psi(t') = \sum_{\vec{n}} A_{\vec{n}} |\vec{n}\rangle = \sum_{\vec{m}} B_{\vec{m}} |\vec{m}\rangle \qquad \vec{A}(t') = \boldsymbol{S}(t')\vec{B}(t')$$
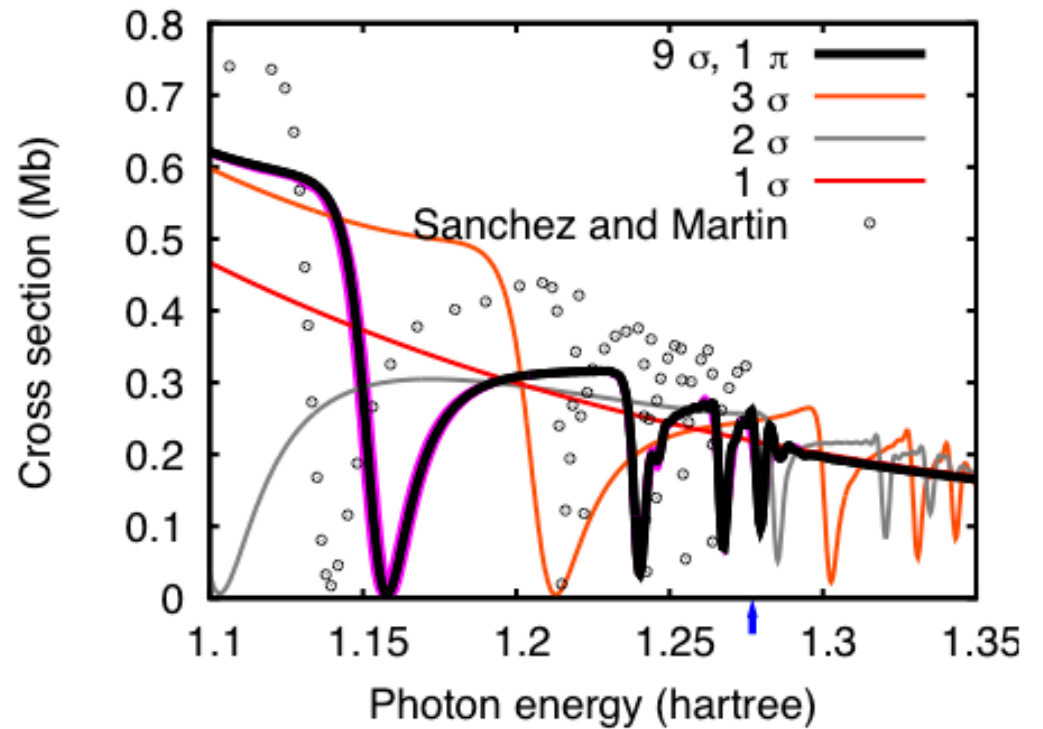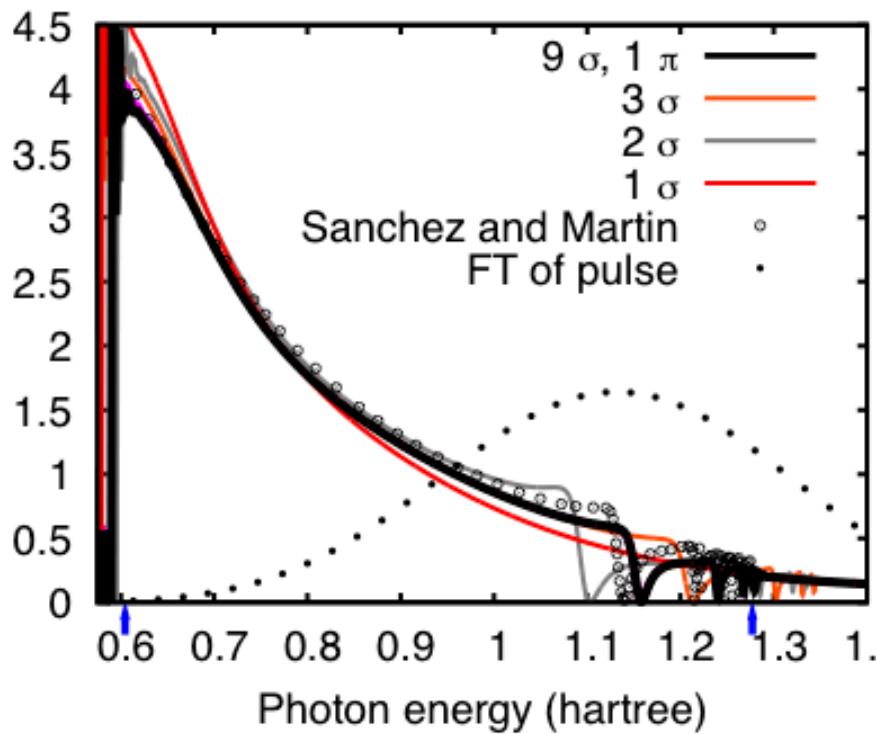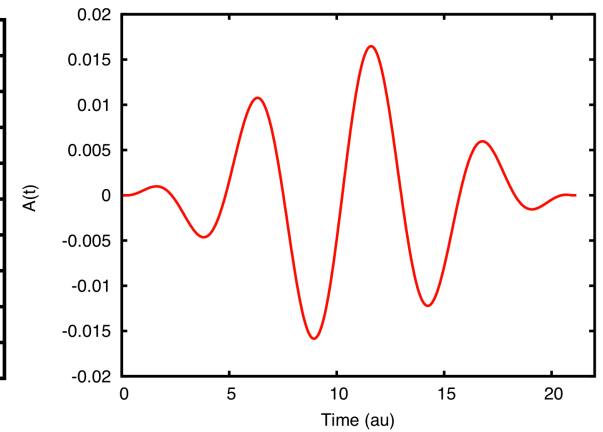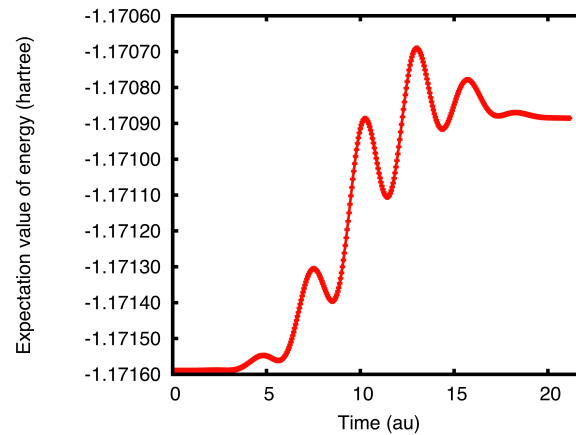$$\boldsymbol{S}_{\vec{n}\vec{m}} = \langle \vec{n}(t')|\vec{m}(t')\rangle \qquad \longrightarrow \vec{B} = \exp\left(-\ln \boldsymbol{S}\right)\vec{A} \; \boldsymbol{!}$$

Full

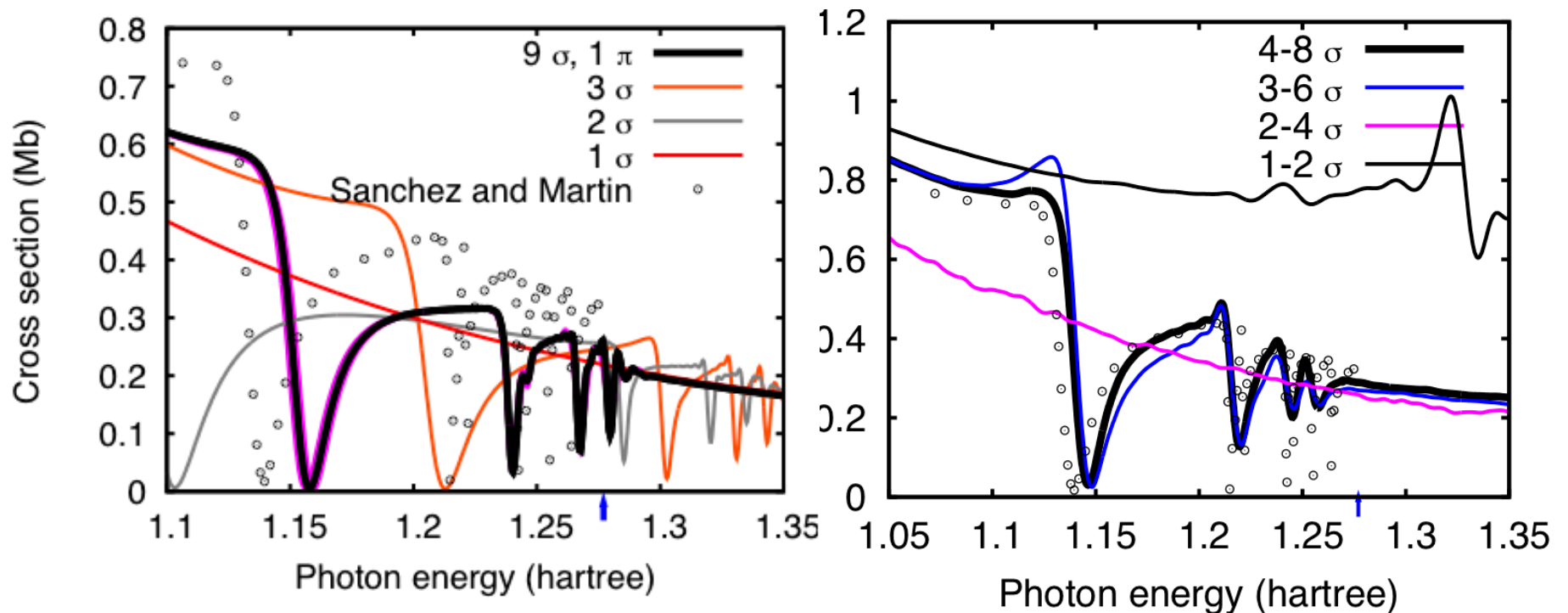Choose sparse branch

H$_2$ results wrt number of orbitals.

"Psi-prime" treatment is better for calculation of these perturbative results within MCTDHF.

Solve only for the change in the wave function due to the pulse.

$$\Psi(t) = e^{-iE_0 t}\Psi(0) + \Psi'(t)$$

$$i\frac{\partial}{\partial t}\Psi'(t) = H(t)\Psi'(t) + V(t)e^{-iE_0 t}\Psi(0)$$

TOEPLITZ

$$v_{i1,i2,i3}^{\alpha\beta} = \sum_{j1,j2,j3} \phi_{j1,j2,j3}^{\alpha} \phi_{j1,j2,j3}^{\beta} V_{i1,i2,i3;j1,j2,j3}$$

$$[\alpha\beta||\gamma\delta] = \sum_{j1,j2,j3} \phi_{j1,j2,j3}^{\alpha} \phi_{j1,j2,j3}^{\beta} v_{j1,j2,j3}^{\gamma\delta}$$

Hybrid grid/orbital project - SciDAC

J. R. Jones, K. Ibrahim, S. Williams, E. Vecharynski, F.-H. Rouet, X. Li, C. Yang, D. J. Haxton

Fascinating issues with Fast Fourier Transform for Toeplitz Matrices

Originally pointed out by Sherry Li

Much help on this from Sam, Khaled, and Thorsten Kurth of NSD

A toeplitz matrix-vector multiplication ("matvec") is performed using fast fourier transform by embedding the toeplitz matrix in a circulant matrix of twice the size.

The circulant matrix is diagonalized by the Fourier transform.

WHEN BRANT SAID, AFTER TALKING WITH SHERRY, "This works because polynomial multiplication is local in Fourier space," or something close to that, DJH REALIZED that what is true for a usual, single Toeplitz matrix, is probably also true for the TRIPLE TOEPLITZ MATRICES that represent any operator in the sinc DVR basis. Well known.

"TRIPLE TOEPLITZ" = "TRANSLATIONALLY INVARIANT IN 3D" meaning the grid is self-similar if it is translated by an integer multiple of the spacing – such translation is automorphism

$$T^{-1}_{\vec{i}\vec{j}} \equiv v(\vec{i}-\vec{j})$$

Matrix element is only a function of the difference between the bra and ket indices.

Hybrid grid/orbital project - SciDAC

J. R. Jones, K. Ibrahim, S. Williams, E. Vecharynski, F.-H. Rouet, X. Li, C. Yang, D. J. Haxton

Fascinating issues with Fast Fourier Transform for Toeplitz Matrices

So, to perform a triple toeplitz matvec
   with a triple toeplitz matrix of dimension (n1 x n2 x n3) rows and columns
   and a vector, same size of course, (n1 x n2 x n3)

Embed that matrix in a triply circulant matrix of size (8 x n1 x n2 x n3)
And pad the vector with zeroes to that size

Multiply circulant times vector with FFT.   See the links

http://web.eecs.utk.edu/~dongarra/etemplates/node384.html
http://www.eecis.udel.edu/~saunders/courses/621/99f/p17b/p17.txt

Which Brant sent to me on 11/19/14 after his conversation with Sherry.

"The first link is from A Brief Survey of Direct Linear Solvers that Sherry Li both co-authored and suggested I add to my numerical analysis repertoire." – Brant

 I have followed the first; the manipulations in the second seem different.

Hybrid grid/orbital project - SciDAC

J. R. Jones, K. Ibrahim, S. Williams, E. Vecharynski, F.-H. Rouet, X. Li, C. Yang, D. J. Haxton

Fascinating issues with Fast Fourier Transform for Toeplitz Matrices

BUT.

(THIS IS A DIVERSION. PROBABLY.)

IS IT POSSIBLE TO EMBED THE (n1 x n2 x n3) TRIPLE TOEPLITZ MATRIX

IN A **SINGLE not TRIPLE** CIRCULANT MATRIX OF SIZE (8 x n1 x n2 x n3) ????

IF SO – *TRIPLE TOEPLITZ MATVEC WITH 1D FFT NOT 3D FFT.*

FUNDAMENTAL DIFFERENCES IN MPI ALGORITHM.

BUT ALSO – Relevance to fundamental math? Discrete Fourier Transform is an active area of research. Octonions? Riemann Zeta function? E8? Probably!!!!!

Hybrid grid/orbital project - SciDAC

J. R. Jones, K. Ibrahim, S. Williams, E. Vecharynski, F.-H. Rouet, X. Li, C. Yang, D. J. Haxton

Fascinating issues with Fast Fourier Transform for Toeplitz Matrices

Slides sent Jan 16

MPI 3D FFT strong scaling?

Size of hydrogen atom problem (n^3)
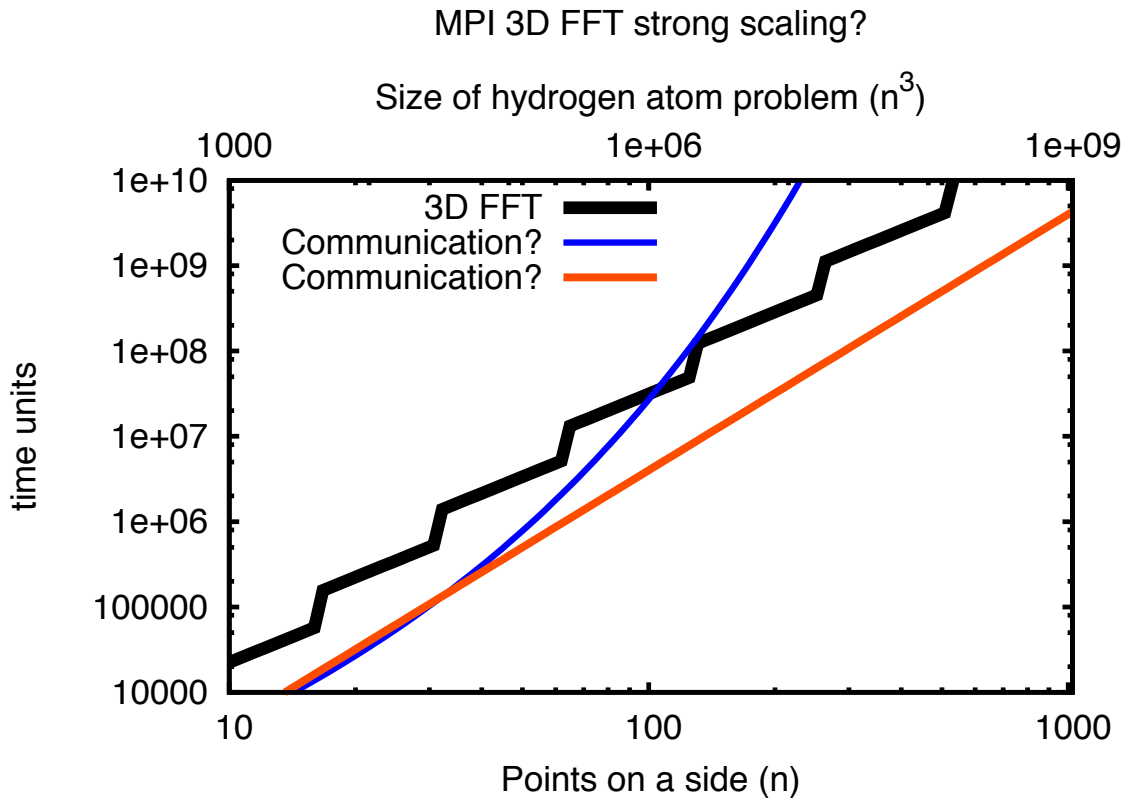
3D fast Fourier transform time as per Cooley-Tukey algorithm in black.

Answer from Khaled and Thorsten: BLUE IS CORRECT. NO STRONG SCALING.

Hybrid grid/orbital project - SciDAC

J. R. Jones, K. Ibrahim, S. Williams, E. Vecharynski, F.-H. Rouet, X. Li, C. Yang, D. J. Haxton

Fascinating issues with Fast Fourier Transform for Toeplitz Matrices
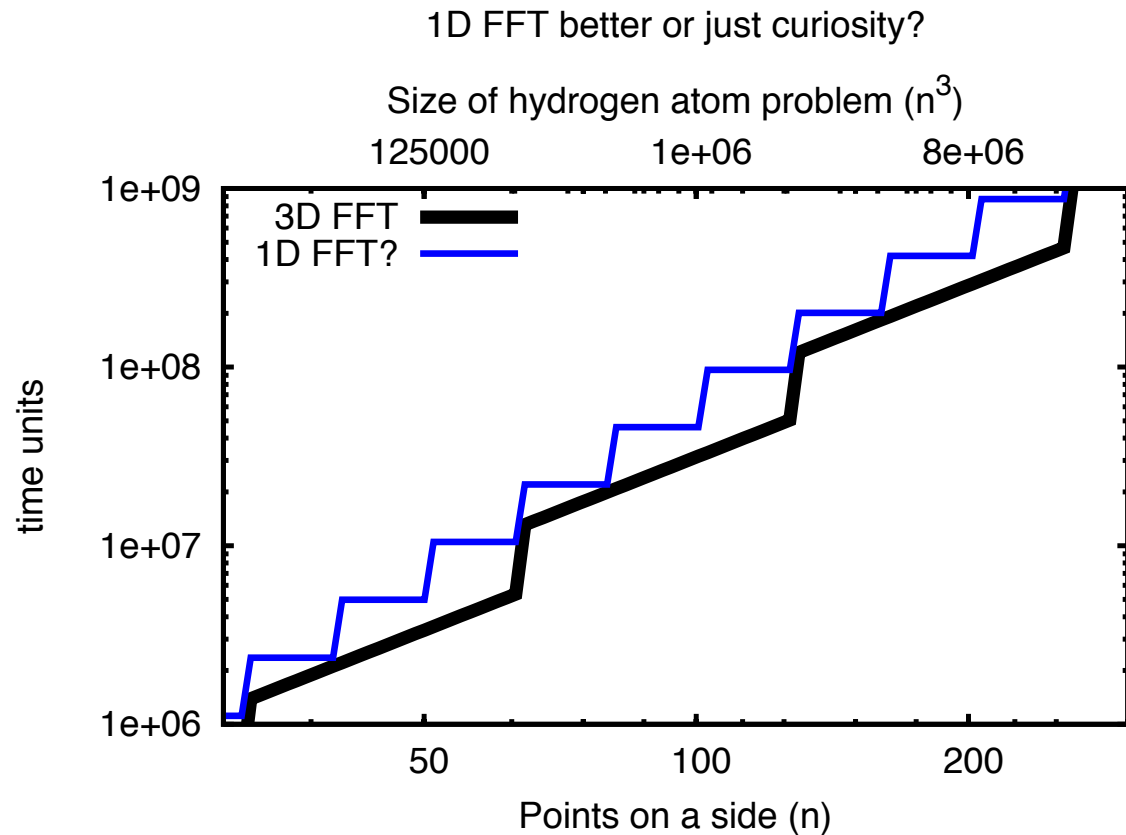
Slides sent Jan 16
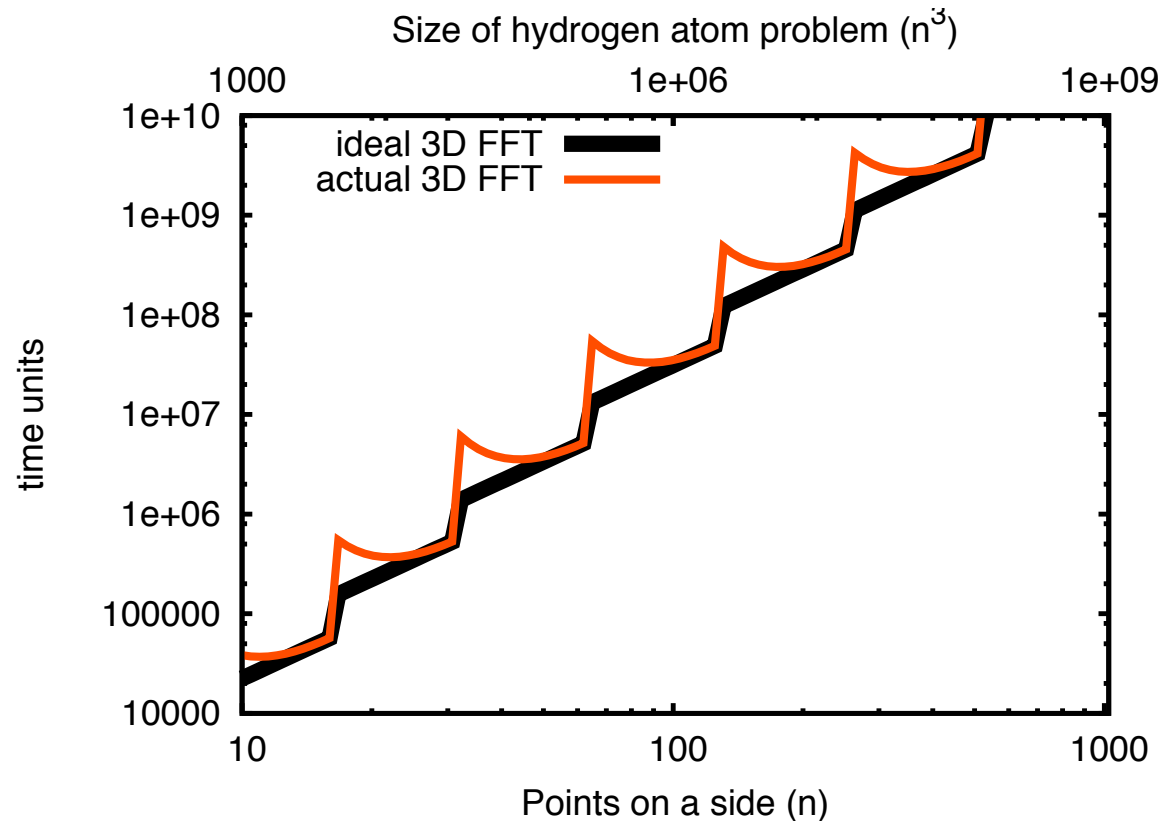
(3D fast Fourier transform time as actually observed, per DJH experience and conversation with Thorsten Kurth.)

Hybrid grid/orbital project - SciDAC

J. R. Jones, K. Ibrahim, S. Williams, E. Vecharynski, F.-H. Rouet, X. Li, C. Yang, D. J. Haxton

Fascinating issues with Fast Fourier Transform for Toeplitz Matrices

Slides sent Jan 16

1D FFT better or just curiosity?

Even if triple toeplitz matvec can be performed with 1D FFT not 3D FFT, and if DJH did math correctly, 1D does not confer any advantage as far as computation time is concerned, and in fact is generally slightly disadvantageous versus 3D

Hybrid grid/orbital project - SciDAC

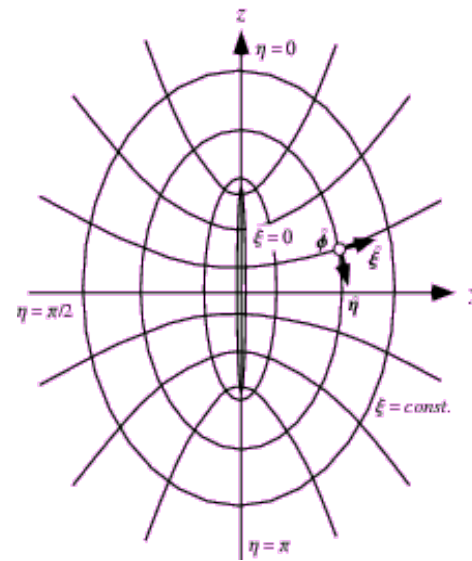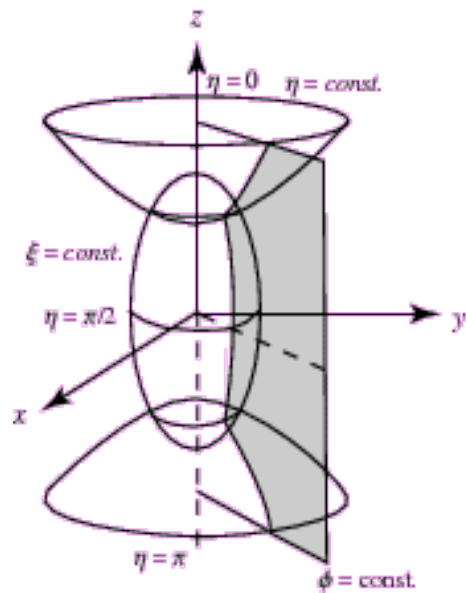J. R. Jones, K. Ibrahim, S. Williams, E. Vecharynski, F.-H. Rouet, X. Li, C. Yang, D. J. Haxton

Fascinating issues with Fast Fourier Transform for Toeplitz Matrices

Slides sent Jan 16

MPI 1D FFT strong scaling?
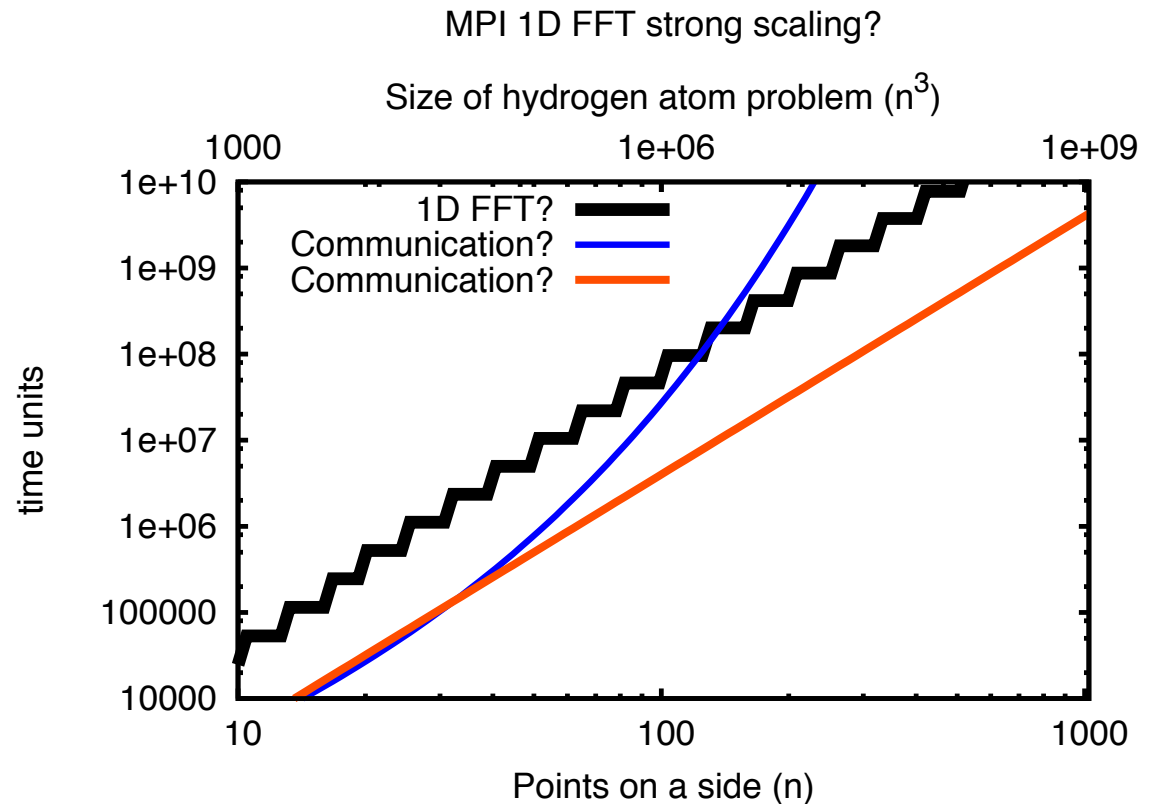
But is there a better scaling 1D MPI FFT algorithm than the 3D FFT algorithm described by Khaled and Thorsten? The one involving all-to-all and explicit transposes?

PROLATE EQS

Primitive Basis: Discrete Variable Representation

We employ a DVR (Dickinson and Certain, JCP 49, 4209 (1968), etc.) which is essentially a product basis in the prolate spheroidal coordinates ξ, η, φ, R. It is based on interpolating polynomials based on Gauss-Radau, Gauss-Lobatto, and Gauss-Legendre quadrature, with the proper behavior at singular points tacked on post-hoc. The basis is a generalized DVR.

$$\varphi_{ia}^{\Lambda} = \begin{cases} \sqrt{\dfrac{8}{\xi_a^2 - \eta_i^2}}\, \chi_i(\eta)\chi_a(\xi)\dfrac{e^{i\Lambda\phi}}{\sqrt{2\pi}} & \text{for even } \Lambda; \text{ for odd,} \\[3ex] \sqrt{\dfrac{8}{\xi_a^2 - \eta_i^2}}\sqrt{\dfrac{1-\eta^2}{1-\eta_i^2}}\chi_i(\eta)\sqrt{\dfrac{\xi^2-1}{\xi_a^2-1}}\chi_a(\xi)\dfrac{e^{i\Lambda\phi}}{\sqrt{2\pi}} \end{cases}$$

Two-electron matrix elements

The two-electron matrix elements are calculated using the Neumann expansion. The radial (ξ) part is done with a DVR poisson solve; the η part is done with the DVR approximation. Very sparse, near diagonal.

$$\frac{1}{r_{12}} = \frac{8\pi}{R} \sum_{lm} (-1)^m \frac{(l-m)!}{(l+m)!} P_{lm}(\xi_<) Q_{lm}(\xi_>) Y_{lm}(\eta_1, \phi_1) Y_{lm}(\eta_2, \phi_2)^*$$

$$\left\langle \chi_a \chi_b \left| (-1)^m \frac{2}{2l+1} \widetilde{P_{lm}}(\xi_<)\widetilde{Q_{lm}}(\xi_>) \right| \chi_c \chi_d \right\rangle = \delta_{ac}\delta_{bd} \left[\frac{(l-m)!}{(l+m)!} \frac{\Gamma\left(\frac{l+m+2}{2}\right)\Gamma\left(\frac{l+m+1}{2}\right)}{\Gamma\left(\frac{l-m+2}{2}\right)\Gamma\left(\frac{l-m+1}{2}\right)} \left(T_{lm}^{-1}\right)_{ab} w_a^{-1/2} w_b^{-1/2} \right.$$

$$\left. + (-1)^{m+1} \frac{2}{2l+1} \frac{\widetilde{P_{lm}}(\xi_a)\widetilde{P_{lm}}(\xi_b)\widetilde{Q_{lm}}(\xi_N)}{\widetilde{P_{lm}}(\xi_N)} \right]$$

Hamiltonian, with KE cross terms

In general, if the orbitals follow the nuclei, there will be cross terms in the KE.

$$H = -\frac{1}{2\mu_{AB}}\left[\left(\frac{\partial}{\partial R}\right)_{\xi\eta\phi} - \frac{1}{R}\hat{Y}\right]^2 + \frac{\mathbf{J}^2 - 2J_z^2 + \mathbf{l}^2 - l_-J_+ - l_+J_-}{2\mu_{AB}R^2} - \frac{1}{2\mu_e}\nabla_r^2 + V$$

$$\nabla^2 = \frac{1}{a^2(\xi^2 - \eta^2)}\left[\frac{\partial}{\partial\xi}(\xi^2 - 1)\frac{\partial}{\partial\xi} + \frac{\partial}{\partial\eta}(1 - \eta^2)\frac{\partial}{\partial\eta}\right] + \frac{1}{a^2(\xi^2 - 1)(1 - \eta^2)}\frac{\partial^2}{\partial\phi^2}$$

MCTDHF working equations

are now more complicated, with R
matrices and terms from Y

$$\mathscr{R}_{\alpha\beta}^{(-2)} = \sum_{i\ ms} \rho_{i\ \alpha\ ms\ i\ \beta\ ms}^{(1)} \frac{1}{R_i^2}$$

$$(\mathscr{D}_{\mathscr{R}})_{\alpha\beta} = \sum_{i\ j\ ms} \rho_{i\ \alpha\ ms\ j\ \beta\ ms}^{(1)} [D_R]_{ij}$$

$$\forall_\alpha \quad \frac{\partial}{\partial t}\vec{c_\alpha} = \sum_\beta (1-\mathbf{p})\rho_{\alpha\beta}^{-1} \sum_\gamma \left[\mathscr{R}_{\beta\gamma}^{(-2)}\mathbf{D_{el}^{(2)}} + (\mathscr{D}_{\mathscr{R}})_{\beta\gamma}\ \mathbf{D_{el}} + \sum_{\beta'\gamma'} \mathscr{R}_{\beta\gamma\beta'\gamma'}^{(-1)}\ \bar{\mathbf{W}}_{\beta'\gamma'} \right] \vec{c_\gamma} + \sum_\beta \tau_{\alpha\beta}|\phi_\beta\rangle$$

$$i\frac{\partial}{\partial t}c(\vec{t}) = \left[\mathbf{g}(A(\vec{t}), c(\vec{t})) + (1 - [\mathbf{p}(c(\vec{t}))])\mathscr{U}(c(\vec{t}), A(\vec{t}))\right] c(\vec{t})$$

$$\frac{\partial}{\partial t}A(\vec{t}) = \left(\mathbf{H}(c(\vec{t})) + \boldsymbol{\tau}(A(\vec{t}), c(\vec{t}))\right) A(\vec{t})$$

$$i\frac{\partial}{\partial t}c(\vec{t}) = \left[\mathbf{g}(A(\vec{t}), c(\vec{t})) + (1 - [\mathbf{p}(c(\vec{t})])\mathscr{U}(c(\vec{t}), A(\vec{t}))\right] c(\vec{t})$$

$$\frac{\partial}{\partial t}A(\vec{t}) = \left(\mathbf{H}(c(\vec{t})) + \tau(A(\vec{t}), c(\vec{t}))\right) A(\vec{t})$$

$$\mathbf{H}(t) \approx \mathbf{H^P}(t) = \sum_{i=1...\text{numpoly}} \mathbf{H}(t_i)\, \varphi_i(t)$$
$$= \sum_{i=1...\text{numpoly}} \mathbf{H_i}\, t^{i-1}$$

$$U(t_1, t_2) \approx e^{-i \int_{t_1}^{t_2} dt'\, H(t')}$$

$$U(t_1, t_2) \approx e^{\int_{t_1}^{t_2} dt'\, -iH(t) + \frac{1}{2}\int_{t_1}^{t'} dt''\,[H(t''), H(t')]}$$

Stencils, e.g. S-vector leapfrog, A-vector predictor/corrector

A − vector			S − vector				A − vector		
$t =$	0	1	$t =$	−1	0	1	$t =$	0	1
	x	x		x		x		x	x
→o			→o				→o		o